Universidade de Aveiro Departamento de Química
2010

Sónia Andreia de Almeida Pinho

Indução e determinação de ROS e o seu efeito na dinâmica dos peroxissomas

Induction and determination of ROS and their effect on peroxisome dynamics

Universidade de Aveiro Departamento de Química
2010

Sónia Andreia de Almeida Pinho

Indução e determinação de ROS e seu efeito na dinâmica dos peroxissomas

Induction and determination of ROS and their effect on peroxisome dynamics

Dissertação apresentada à Universidade de Aveiro para cumprimento dos requisitos necessários à obtenção do grau de Mestre em Métodos Biomoleculares, realizada sob a orientação científica do Doutor Michael Schrader (equiparado a investigador principal com habilitação ou agregação), Centro de Biologia Celular & Departamento de Biologia da Universidade de Aveiro.

Apoio financeiro da FCT (FCT; PTDC/BIA-BCM/71932/2006), Centro de Biologia Celular & Departamento de Biologia da Universidade de Aveiro e Universidade de Aveiro.

Ao meu namorado

o júri

presidente

Professor António José Brito Fonseca Mendes Calado
Professor auxiliar do Departamento de Biologia da Universidade de Aveiro

Doutor Manuel António Botelho Pereira Pinto
Bolseiro Pós Doutoramento – IBMC – Universidade do Porto

Doutor Michael Schrader
Investigador Principal com habilitação no Departamento de Biologia da Universidade de Aveiro

agradecimentos

Quero agradecer a todas as pessoas que me apoiaram e que de alguma forma contribuíram para este trabalho.

Ao Doutor Michael Schrader pela excelente orientação deste trabalho, pela disponibilidade, valiosas sugestões e esclarecimentos científicos ao longo do trabalho.

Ao Doutor Joaquín Jordan, por me ter recebido no seu laboratório com tanta amabilidade e simpatia, bem como a todo o seu grupo de trabalho. Pela disponibilidade e auxílio na compreensão dos resultados de análise bioquímica.

A todos os colegas e amigos do laboratório, que sempre se disponibilizaram para me ajudar. Pelo carinho e amizade, por todo o apoio, ajuda, incentivo e motivação.

Por fim, agradeço à minha família e ao meu namorado por todo o apoio, compreensão e carinho.

palavras-chave

Peroxissomas, Mitocondria, Microtubulos, Dinâmica de Organelos, Stress Oxidativo, Quantificação de ROS, Glutationa, Antioxidantes.

resumo

Peroxissomas são organelos celulares de membrana simples, os quais têm importantes funções metabólicas, como por exemplo metabolismo de lípidos e ROS, sendo assim indispensáveis para a saúde e desenvolvimento humano. Os peroxissomas são organelos altamente flexíveis e dinâmicos que rapidamente se agregam, multiplicam e degradam em resposta a necessidades metabólicas. Em cultura celular, o stress oxidativo e outros estímulos externos (ex. factores de crescimento, ácidos gordos, despolimerização) têm mostrado induzir processos de crescimento (alongamento) e divisão de peroxissomas, os quais estão relacionados com a sua proliferação. Considerando que alguns dos componentes moleculares da maquinaria de crescimento e divisão têm sido identificados nos últimos anos, as vias de sinalização e regulação que medeiam a proliferação de peroxissomas são largamente desconhecidas.

O objectivo desta dissertação de mestrado foi examinar o efeito de diferentes estímulos externos promotores de ROS na indução do crescimento/proliferação do compartimento peroxisomal. Foi seleccionado um sistema de cultura de células de mamífero que apresentam um compartimento peroxisomal dinâmico. Análises baseadas em fluorescência para a detecção da produção de ROS e alterações nos níveis de GSH intracelular foram estabelecidos. Estes procedimentos foram usados primeiro para esclarecer se o alongamento de peroxissomas observado após despolimerização de microtubulos (pelo nocodazole) é mediado por ROS. O alongamento de peroxissomas e a despolimerização dos microtubulos após tratamento com nocodazole foi monitorizado e quantificado por microscopia de imunofluorescência. O Nocodazole induziu um aumento dos níveis de ROS intracelular e apesar do pré tratamento com antioxidantes ter baixado os níveis de ROS, não preveniu o alongamento peroxisomal. Estes resultados demonstram que as alterações morfológicas do compartimento peroxisomal induzidas pelo nocodazole são independentes da produção de ROS. Para além disso, foi examinado o efeito de alterações nos níveis de glutationa (GSH) celular no compartimento peroxisomal. Interessantemente, a redução dos níveis de GSH intracelular pelo BSO, um inibidor da enzima *γ-glutamylcystein synthetase (γ-GCS)*, resultou num aumento acentuado de crescimento/proliferação de peroxissomas. Os níveis de ROS e GSH foram determinados por análises baseadas em fluorescência. Pré tratamento com antioxidante preveniu o alongamento de peroxissomas indicando que a alteração no estado redox celular (citoplasmatico) levou à proliferação de peroxissomas a qual exerce, supostamente, uma função protectora para a célula. Finalmente, foi investigado se a inibição da cadeia respiratória mitocondrial e com isso, se ROS provenientes das mitocondrias foi capaz de induzir crescimento e divisão dos peroxissomas. Entre os inibidores analisados, apenas a rotenona, inibidor do complexo I, teve um efeito proeminente na elongação de peroxissomas. Todavia, foi demontrado que o seu efeito é devido à acção que a rotenona tem na despolimerização dos microtubulos. Assim, apesar da relação de proximidade entre mitocondria e peroxissomas, as ROS provenientes das mitocondrias não são prováveis de induzir alterações no compartimento peroxisomal. Os nossos resultados também indicam que estudos *in vivo* usando a rotenona têm de ser interpretados com muito cuidado. Além disso, os resultados mostram que as ROS podem alterar a dinâmica do compartimento peroxissomal, mas têm de vir de locais específicos dentro da célula (por exemplo, do citosol).

keywords

Peroxisomes, Mitochondria, Microtubules, Organelle Dymamics, Oxidative Stress, ROS measurement, Glutathione, Antioxidants

abstract

Peroxisomes are single membrane bound subcellular organelles, which fulfill important metabolic functions, for example in lipid and ROS metabolism, and are thus indispensable for human health and development. Peroxisomes are highly flexible organelles that rapidly assemble, multiply and degrade in response to metabolic needs. In cultured cells, oxidative stress and other external stimuli (e. g. growth factors, fatty acids, microtubule depolymerization) have been shown to induce processes of growth (elongation) and division of peroxisomes, which are related to peroxisome proliferation. Whereas some of the molecular components of the growth and division machinery have been identified in the last years, the regulatory and signaling pathways mediating peroxisome proliferation are largely unknown.

The aim of this master thesis was to examine the effects of different ROS-producing external stimuli on the induction of growth/proliferation of the peroxisomal compartment. A suitable mammalian cell culture system with a dynamic peroxisomal compartment was selected and fluorescent-based assays for the detection of ROS production and changes in the intracellular GSH levels were established. The setup was first used to clarify if peroxisome elongation observed after depolymerization of microtubules (by nocodazole) is mediated by ROS. Peroxisome elongation and microtubule depolymerization after nocodazole treatment was monitored and quantified by immunofluorescence microscopy. Although nocodazole induced an increase in cellular ROS levels, a pre-treatment with antioxidants and lowering of intracellular ROS levels did not prevent peroxisome elongation. These findings demonstrate that the morphological changes of the peroxisomal compartment induced by nocodazole are independent of ROS production. Furthermore, I examined the effect of changes in the cellular redox state on the peroxisomal compartment. Interestingly, the reduction of intracellular GSH levels by BSO, an inhibitor of γ-glutamylcystein synthetase (γ-GCS), resulted in a prominent increase in peroxisomal growth/elongation. ROS and GSH levels were determined by fluorescent-based assays. Pre-treatment with antioxidants prevented peroxisome elongation indicating that changes in the cellular (cytoplasmic) redox state lead to peroxisome proliferation, which is supposed to have a protective function for the cell. Finally, I investigated whether inhibition of the mitochondrial respiratory chain and thus, mitochondria-derived ROS were capable of inducing peroxisomal growth and division. Among the inhibitors tested, only rotenone, a complex I inhibitor, had a prominent effect on peroxisome elongation. However, I demonstrated that this effect is due to a microtubule-depolymerizing activity of rotenone. Thus, despite the close peroxisome-mitochondria relationship, mitochondria-derived ROS are unlikely to induce changes of the peroxisomal compartment. Our findings also indicate that *in vivo* studies using rotenone have to be interpreted with great care. In addition, the results show that ROS can alter the dynamics of the peroxisomal compartment, but have to come from specific locations (e.g. the cytosol) within the cell.

TABLE OF CONTENTS

LIST OF ABREVIATIONS

6-OHDA	6-Hydroxydopamine
AA	Amino acid
ALDP	Adrenoleukodystrophy protein
ATPsyn	ATP synthetase
BSO	L-Buthionine-sulfoximine
CAT	Catalase
CO_2	Carbone dioxide
CONT	Control
CuZnSOD	Copper-zinc-superoxide
cyt *c*	Cytochrome *c*
DAB	Alkaline 3, 3'-diaminobenzidine
DCF	Dichlorofluorescein fluorescent
DLP1	Dynamin like protein
DMEM	Dulbecco's modified Eagle's medium
DMSO	Dimethyl sulfoxide
DRPs	Dynamin-related proteins
ER	Endoplasmic reticulum
ETC	Electron transfer chain
FCS	Fetal calf serum
GFP	Green fluorescent protein
GSH	Glutathione
GST	Glutathione S-transferase
H_2DCF	Dichlorofluorescein non fluorescent
H_2DCFDA -2', 7'	Dichlorodihydrofluorescein diacetate
H_2O_2	Hydrogen peroxide

$HO^{\bullet -}$	Hydroxyl radical
HOCl	Hypochlorous acid
IMF	Immunofluorescence
LCFA	Long chain fatty acids
LYS	Lysosomes
MAPs	Microtubule-associated proteins
mBCL	Monoclorobimane
MCFA	Medium chain fatty acids
Mff	Mitochondrial fission factor
MIM	Mitochondrial inner membrane
MITO	Mitochondria
MnSOD	Manganese superoxide dismutase
MOM	Mitochondrial outer membrane
MT	Microtubules
MTOC	Microtubule organization center
NAC	N-acetyl cysteine
NADH	Nicotinamide adenine dinucleotide
NOC	Nocodazole
NOS	Nitric oxide synthase
O_2	Molecular oxygen
$O_2^{\bullet -}$	Superoxide radical anion
$ONOO^-$	Peroxinitrite
PBDs	Peroxisomal biogenesis disorders
PBS	Phosphate buffer saline
PD	Parkinson's disease
PEDs	Peroxisomal enzyme deficiencies

Pex	Peroxins
pFA	para-formaldehyde
PMPs	Peroxisomal membrane proteins
PO	Peroxisomes
POM	Peroxisomal outer membrane
PPARs	Peroxisome proliferator activated receptors
PPREs	Peroxisome proliferator response elements
PTS1	Peroxisomal targeting signal 1
PUFAs	Polyunsaturated fatty acids
RC	Respiratory chain
RNS	Reactive nitrogen species
ROO•	Peroxyl radical
ROS	Reactive oxygen species
ROT	Rotenone
RXRs	Retinoid X receptors
sER	Smooth endoplasmic reticulum
SKL	Serine-lysine-leucine (amino acids)
SN	Substantia nigra
TCA	Tricarboxylic acid
VIT C	Vitamin C
VIT E	Vitamin E
VLCFA	Very long chain fatty acids
X-ALD	X-linked adrenoleukodystrophy
XOx	Xanthine oxidase
β-OX	Fatty acid beta-oxidation
γ-GCS	γ-glutamylcysteine synthetase

I. INTRODUCTION

I. INTRODUCTION

1. PEROXISOMES

1.1. GENERAL FEATURES

Peroxisomes (originally called microbodies) were discovered in 1954 using electron microscopy in mouse kidney (Rhodin, 1954). De Duve and Baudhuin (1966) were the first who isolated peroxisomes from rat liver, and their biochemical studies led to the discovery of the colocalization of several H_2O_2-producing oxidases as well as catalase, an H_2O_2-degrading enzyme, in the matrix of peroxisomes (see Chapter I. 1.2., Figure 2). On the basis of these findings, De Duve proposed the functional term "peroxisome", which gradually replaced the former morphological designation, "microbody", coined by Rhodin, (1954). A specific cytochemical staining for peroxisomes in light and electron microscopy became available with the introduction of the alkaline 3, 3'-diaminobenzidine (DAB) reaction for catalase (Fahimi, 1968; Novikoff and Goldfischer, 1969) (Figure 1). Subsequent morphological studies exploiting this cytochemical procedure revealed that peroxisomes, such as mitochondria, are ubiquitous eukaryotic organelles (Hruban et al., 1972).

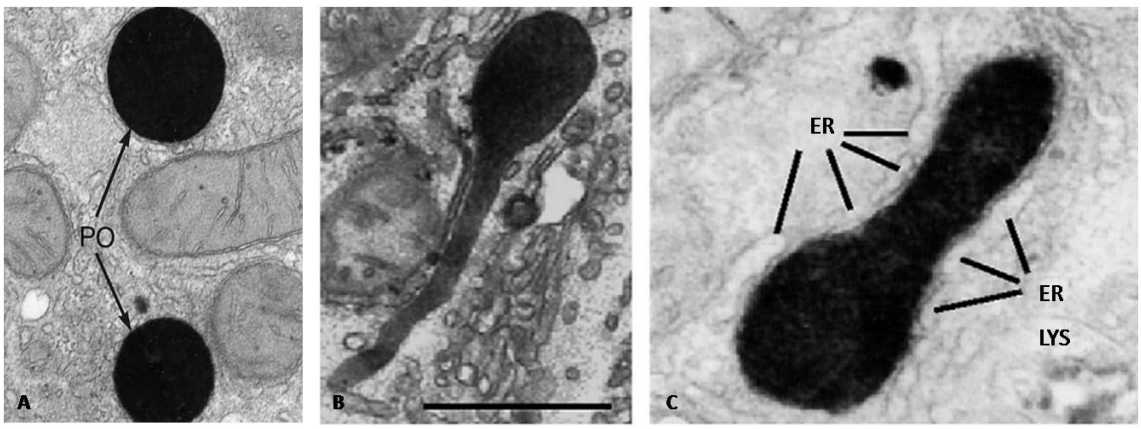

Figure 1. (A) Cytochemical localization of catalase in rat hepatic peroxisomes stained with the alkaline diamine-benzidine technique (Fahimi, 1969). Note the uniform staining of the peroxisome matrix. Magnification, x 28,600 (from Schrader and Fahimi, 2008). Electron micrographs of peroxisomes from regenerating rat liver. (B-C) Sections were stained cytochemically for localization of catalase (Fahimi, 1969). (B) A peroxisome with an elongated tail-like extension. Magnification, x 65,000. (C) A tubular peroxisome next to a lysosome (LYS) and in close association with endoplasmic reticulum (ER), Magnification, x 85,000 (Schrader and Fahimi, 2006a).

Peroxisomes are morphologically characterized by a single limiting membrane surrounding a fine granular matrix, which may contain crystalline inclusions of matrix

enzymes, with a range in size from 0.1-1 µm in diameter. Peroxisomes display some variability in morphology, enzyme content and metabolic function. Thus, they are designated as “multi-purpose organelles”. Peroxisomes are adjusted according to cellular needs (Opperdoes, 1988) and vary among different species, developmental stages and organs, even within the same organisms (Schrader and Fahimi, 2006a). They show a pronounced morphological plasticity, with highly dynamic structures exhibiting rapid changes of their shape, number and intracellular distribution. This plasticity is dependent on the organism, cell type and prevailing environmental conditions (Platta and Erdmann, 2007b; Schrader et al., 1998a).

Since peroxisomes are devoid of DNA, all peroxisomal proteins are encoded by the nuclear genome and have to be imported post-translationally into peroxisomes. More than 60 yeast and 80 human genes encoding peroxisomal proteins have been identified. Many of them are metabolic enzymes, necessary for their crucial role in cellular metabolism, such as β-oxidation of fatty acids and H_2O_2 detoxification (see Chapter I. 1.2.). Another group of peroxisomal proteins, called peroxins, is required for the biogenesis and maintenance of functional peroxisomes (see Chapter I. 2.) (reviewed in Schrader and Fahimi, 2008).

1.2. PEROXISOMAL FUNCTIONS

Notwithstanding the simplicity of peroxisome morphology, these organelles show a broad functional diversity.

The β-oxidation of fatty acids and the detoxification of the hydrogen peroxide produced are the central functions of peroxisomes. In fungi and plants the fatty acid degradation pathway is exclusively localized in the peroxisomal compartment, whereas in mammalian cells the breakdown of different types of fatty acids is distributed between peroxisomes and mitochondria (Platta and Erdmann, 2007a; Schrader and Yoon, 2007) (see Chapter I. 4.2.).

The massive proliferation of peroxisomes in the livers of rats treated with the hypolipidemic drug clofibrate (see Chapter I. 6.1.) (Hess et al., 1965) was the first indication of the possible involvement of peroxisomes in lipid metabolism and led eventually to the discovery of fatty acid β-oxidation in animal cells (Lazarow and De Duve, 1976). Other functions of peroxisomes include the biosynthesis of cholesterol, bile acids

and ether lipids (e.g. plasmalogens) which comprise more than 80% of the phospholipid content of white matter in the brain (Wanders and Waterham, 2006b; Platta and Erdmann, 2007a), catabolism of amino acids, polyamines and purines, detoxification of xenobiotics, glyoxylate, and last but not least reactive oxygen species (ROS) (see Chapter I. 5.) (Schrader and Fahimi, 2008; Delille et al., 2006). The metabolic pathways of peroxisomes are illustrated in Figure 2.

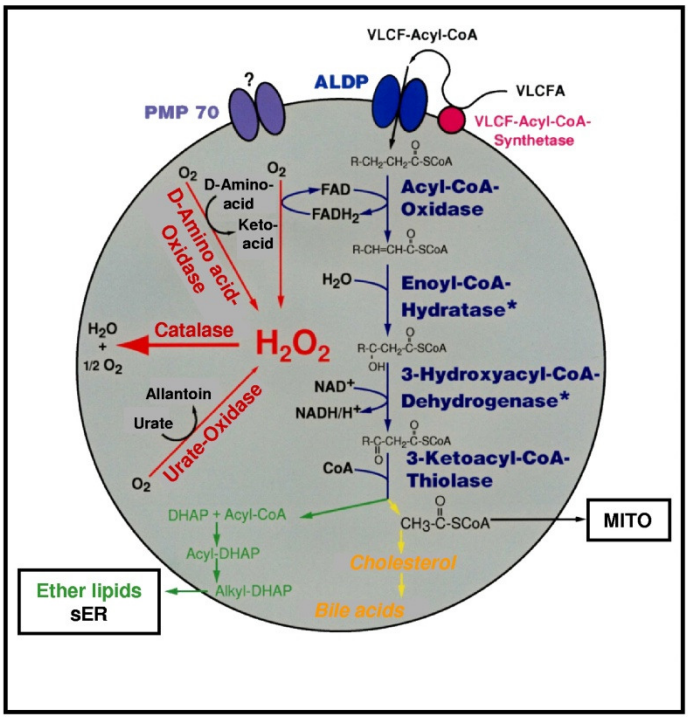

Figure 2. The major metabolic pathways in peroxisomes of the mammalian liver. The very long chain fatty acids (VLCFA) are transported by membrane proteins (e.g., the ABC transporter proteins PMP70 or ALDP) into the matrix, where they are oxidized by the lipid β-oxidation enzymes. The products of the β-oxidation can either serve as substrates for the biosynthesis of ether glycerolipids, cholesterol and bile acids or may exit the peroxisome for further oxidation in mitochondria (MITO). Peroxisomal β-oxidation and the activity of other peroxisomal oxidases result in the production of hydrogen peroxide, which is decomposed by catalase. *Asterisks,* there are separate enzymes for bile acid intermediates, *sER* smooth endoplasmic reticulum, *ALDP* adrenoleukodystrophy protein (Schrader and Fahimi, 2008).

1.3. IMPORTANCE OF PEROXISOMES

The critical role of peroxisomes in a variety of metabolic processes, especially in lipid metabolism, renders them essential for human health and development (Delille et al., 2006). Furthermore, their importance is also emphasized by the existence of inherited disorders that are caused by peroxisomal dysfunction (Wanders and Waterham, 2005; Steinberg et al., 2006).

As peroxisomes are central eukaryotic organelles, disturbances of their function can lead to severe multisystem pathologies, often associated with neurological and developmental defects. Inherited peroxisomal disorders can be divided into two main subgroups: the peroxisomal biogenesis disorders (PBDs) and the more frequent peroxisomal (single) enzyme deficiencies (PEDs) (see Chapter I. 5.3.) (Wanders and Waterham, 2006a).

2. BIOGENESIS OF PEROXISOMES

Peroxisomes are devoid of DNA or a protein translation machinery, and all of their proteins are encoded by nuclear genes. Most of the peroxisomal proteins (peroxisomal membrane and matrix proteins) are synthesized on free polyribosomes in the cytoplasm and are then post-translationally directed to the organelle (Lazarow and Fujiki, 1985).

The biogenesis of peroxisomes is thought to begin with the formation of the peroxisomal membrane – which involves both recruitment of lipids as well as the targeting and insertion of membrane proteins into the lipid bilayer – and is followed by targeting and import of peroxisomal matrix proteins to form a metabolically functional organelle. Subsequently, peroxisomes can grow and proliferate until the organelle is finally degraded (Lazarow and Fujiki, 1985).

2.1. IMPORT OF PEROXISOMAL MATRIX PROTEINS

Sorting of peroxisomal matrix proteins is achieved by cytosolic receptors (Pex5p for PTS1 and Pex7p for PTS2) that recognize two well-characterized classes of peroxisomal targeting signals (PTS1 and PTS2). The PTS1 comprises a C-terminal tripeptide (SKL), whereas the PTS2 is located near the N-terminus (Ma and Subramani, 2009). Most of the identified peroxins are involved in matrix protein import and contribute to the formation

of the docking and translocation machinery at the peroxisomal membrane. It is assumed that the receptors accompany their cargo inside the peroxisomes and recycle back to the cytosol (Platta and Erdmann, 2007a). In contrast to proteins imported into mitochondria or endoplasmic reticulum (ER), peroxisomal proteins pass through the intact peroxisomal membrane in a folded or even oligomeric state. For a review on peroxisomal import see Gould and Collins, 2002; Eckert and Erdmann, 2003; Ma and Subramani, 2009.

2.2. IMPORT OF PEROXISOMAL MEMBRANE PROTEINS

The insertion of peroxisomal membrane proteins (PMPs) requires the peroxins Pex19p, Pex3p and Pex16p. It is suggested that Pex19p functions as a cycling receptor/chaperone for PMPs, which is recruited to the peroxisomes by the membrane receptor Pex3p (Ma and Subramani, 2009). This is based on the finding that most PMPs contain conserved Pex19p-binding sites which almost always are also required for their peroxisomal localization and protein stability (Vizeacoumar et al., 2006; Rottensteiner et al., 2004). Most PMPs contain a peroxisomal membrane targeting signal (mPTS) that is recognized by the import receptor and chaperon Pex19p which directs its cargo to the peroxisomal membrane or alternatively to the ER during *de novo* formation of peroxisomes (see Chapter I. 3.1.) (Platta and Erdmann, 2007b).

3. PEROXISOME FORMATION

3.1. GROWTH AND DIVISION VS. ER MATURATION

Peroxisome formation, multiplication/proliferation and maintenance have been debated for a long time, and is still in discussion. According to the classical view, peroxisomes represent autonomous organelles, which form out of pre-existing peroxisomes by growth and division (Lazarow and Fujiki, 1985).

The “growth and division” model was supported by the discovery of the synthesis of peroxisomal proteins on free ribosomes, their post-translational transport into peroxisomes, and the observation of interconnections between peroxisomes. Furthermore, peroxisomes have been reported to divide, and recently proteins of the peroxisomal division machinery have been identified in yeast, mammalian and plant cells

(Fagarasanu et al., 2007; Schrader and Fahimi, 2006b). In contrast, the ER-maturation concept proposes that the ER contributes to peroxisome formation (Tabak et al., 2006). The degree of this contribution is, however, controversially discussed, whereas there is general agreement that the ER provides the lipids for the formation of the peroxisomal membrane. Its role in the delivery of peroxisomal membrane proteins (PMPs) is hotly debated (Delille et al., 2009).

The ER-maturation-model received strong support by the observation that a loss of the peroxins Pex3p, Pex16p, or Pex19p, which are required for peroxisomal membrane biogenesis and PMP targeting/insertion (Van Ael and Fransen, 2006) (see Chapter I. 2.2.) resulted in the absence of detectable peroxisomes/peroxisomal membranes, whereas their reintroduction led to a *de novo* formation of peroxisomes from the ER. The Pex3p and Pex19p have been observed to initially localize to the ER before maturing into import-competent peroxisomes (Ma and Subramani, 2009), indicating that the ER is the source of the newly synthesized membrane and organelle. However, recent findings in *S. cerevisiae* indicate that in wild-type cells, peroxisomes multiply by growth and division and do not form *de novo*. Only cells lacking peroxisomes as a result of a segregation defect were observed to form peroxisomes *de novo* out of the ER (Motley and Hettema, 2007; Nagotu et al., 2008b). Furthermore, evidence has been presented that Pex3p is directly transported to peroxisomes in a novel Pex19p- and Pex16p-dependent manner in mammalian cells (Matsuzaki and Fujiki, 2008). Thus, the physiological significance of the mechanism of *de novo* formation in comparison to the classical pathway of growth and division is debatable. The *de novo* formation of peroxisomes from the ER may represent a rescue mechanism that becomes functional in some organisms only in case peroxisomes are lost (e.g., due to failure in inheritance) (Delille et al., 2009).

3.2. GROWTH AND DIVISION OF PEROXISOMES

Morphological observations show that growth and division of peroxisomes in mammalian cells is a multistep process including peroxisome elongation (Chapter I. 5.), constriction, and final fission (reviewed in Schrader 2006; Schrader and Fahimi, 2008).

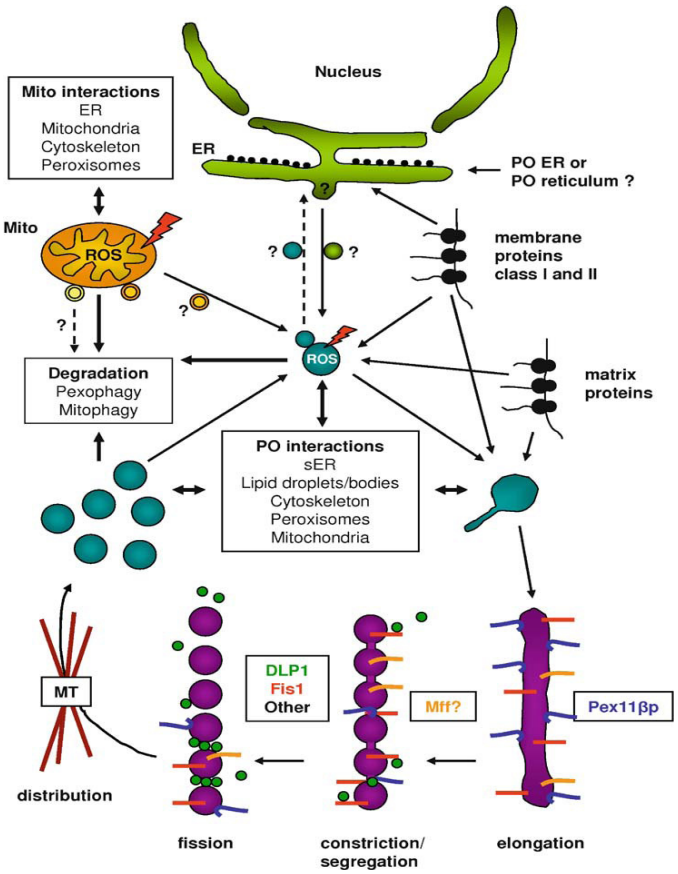

Figure 3. Schematic view of peroxisome dynamics and interactions in mammalian cells. Most peroxisomal (and mitochondrial) matrix and membrane proteins (class I PMPs) are synthesized on free polyribosomes in the cytosol and are posttranslationally imported into pre-existing organelles. Other membrane proteins (class II PMPs, early peroxins; e.g., Pex3p) are routed to peroxisomes via the ER or a pre-peroxisomal compartment, presumably by vesicular transport. A retrograde peroxisome-to-ER transport might also exist. A novel vesicular mitochondria-to-peroxisome trafficking route has been described recently (Neuspiel et al., 2008). A well defined sequence of morphological changes of peroxisomes, including elongation (growth), constriction, and final fission (division) contributes to peroxisome proliferation in mammalian cells. Pex11βp is involved in the elongation (tubulation) of peroxisomes, whereas DLP1 and Fis1 mediate peroxisomal (and mitochondrial) fission. Fis1 is supposed to recruit cytosolic DLP1 to the peroxisomal (mitochondrial) membrane. The involvement of other components (related to yeast Mdv1p/Caf4p) is likely. Mff, which localizes to mitochondria and peroxisomes, might be involved in constriction. Proper intracellular distribution of peroxisomes formed by fission requires microtubules (MT) and motor proteins. In yeast and plants peroxisomes are distributed via the actin cytoskeleton (Schrader and Fahimi, 2008). Organelle dynamics are supposed to be linked to degradation by autophagy (pexophagy, mitophagy) (from Camoes et al, 2009).

Pex11 proteins are implicated early in the elongation step of peroxisome division, whereas dynamin-related proteins (DRPs), and Fis1 catalyze the final fission event (Schrader and Fahimi, 2006a, 2008). In mammals, three Pex11p isoforms, designated Pex11α, Pex11β, and Pex11γ, have been identified. They are all integral PMPs and have both their amino and carboxyl termini exposed to the cytosol. A striking increase in elongated forms of peroxisomes upon expression of Pex11p has been observed in all organisms studied, indicating that tubule formation is an important aspect of peroxisome division (Schrader et al., 1996b, 1998b).

In mammals, the dynamin-related GTPase DLP1 (dynamin like protein) has been reported to be essential for peroxisome division presumably by forming ring-like structures around the membrane constrictions, thus regulating the final fission step in a nucleotide-dependent manner. Fis1, a protein targeted to both the peroxisomal and mitochondrial membrane, has been shown to function as a DLP1 adaptor protein (Koch et al., 2005). Recently, a second mammalian adaptor protein, mitochondrial fission factor (Mff) was reported to control mitochondrial and peroxisomal fission (Gandre-Babbe and van der Bliek, 2008; Delille et al., 2009). Interestingly, Fis1, Mff and DLP1 are also involved in mitochondrial fission and are shared by both organelles (see Chapter I. 4., Figure 5) (Schrader, 2006; Delille et al., 2009).

3.3. PEROXISOMES AND THE CYTOSKELETON

The cytoskeleton plays an essential role in intracellular translocation, distribution and determination of the shape of membrane-bounded organelles. The generation and maintenance of this organization is particularly dependent on the microtubular system. The importance of microtubular interactions has been demonstrated for numerous organelles including peroxisomes (Schrader et al., 2003; Thiemann et al., 2000).

Several studies with microtubule-active drugs, like nocodazole, colcemid and vinblastine - and also with the microtubule-stabilizing drug paclitaxel (taxol) - have been performed to investigate the interaction of the cytoskeleton and in particular the microtubule system with the peroxisomal compartment. Depolymerization of microtubules by nocodazole disrupted the intracellular organization and fast transport of the peroxisomal compartment (Wiemer et al., 1997; Schrader et al., 1996b; Schrader et al., 2003). Treatment with nocodazole resulted in the formation of large peroxisomal clusters indicating that microtubules are required for the proper distribution of peroxisomes throughout the cytoplasm (Schrader et al., 1996a; Wiemer et al., 1997).

Interestingly, microtubules are not essential for the formation, maintenance and dynamics of tubular or reticular peroxisomes (Schrader et al., 1996a; Schrader et al., 1998a; Schrader et al., 2000). Tubular peroxisomes can be formed in the complete absence of microtubules (Schrader et al., 1998a) and, surprisingly, tubule formation in HepG2 cells is induced by microtubule depolymerising agents (Schrader et al., 1996a).

This is quite different from other organelles with tubular or reticular shapes such as mitochondria (Johnson et al., 1980) or lysosomes (Swanson et al., 1987), which collapse or fragment after microtubule-depolymerisation. Furthermore, it seems unlikely that microtubules are involved in the formation of new peroxisomes by budding or fission out of a pre-existing compartment, e.g., during peroxisome proliferation, since the segmentation of tubular peroxisomes has been observed to be microtubule-independent (Schrader et al., 1996a; Schrader et al., 1998a).

4. THE PEROXISOME – MITOCHONDRIA CONNECTION

It has become more obvious over the last years that peroxisomes do not exist as single, isolated organelles, but that they co-operate extensively with other organelles, especially with mitochondria (Schrader and Yoon, 2007; Camoes et al., 2009).

Interestingly, several findings indicate that, despite obvious differences, mitochondria and peroxisomes share certain morphological and functional similarities (Figure 5). Both organelles can adopt a variety of different shapes in eukaryotic cells, ranging from small, spherical compartments to tubulo-reticular networks. Peroxisomes and mitochondria also share components of their division machinery (see Chapter I. 3.1. and I. 4.1., Table 1, Figure 4). Both organelles cooperate in the β-oxidation of fatty acids (see Chapter I. 4.2., Figure 5) and contribute to the metabolism of reactive oxygen species (see Chapter I. 5.4.). These observations indicate that peroxisomes and mitochondria exhibit a much closer interrelationship than previously assumed, which is supposed to have an impact on their cooperative functionality and contribution to diseases (Camoes et al., 2009).

4.1. SHARED COMPONENTS OF PEROXISOMAL AND MITOCHONDRIAL DIVISION

As already mentioned (see Chapter I. 3.1.), some of the fission factors (e.g. DLP1/Drp1, Fis1, Mff) are shared between mitochondria and peroxisomes (Table 1) (Camoes et al., 2009; Schrader, 2006). The targeting of Fis1 to peroxisomal and mitochondrial membranes seems to follow independent mechanisms, but there might be a competition between mitochondria and peroxisomes for DRP1 and its membrane anchor Fis1 (Table 1, Figure 4) (Delille and Schrader, 2008). Mff is another shared component of mitochondrial and peroxisomal fission in mammalian cells (Table 1, Figure 4) (Gandre-Babbe and van der Bliek, 2008; Delille et al., 2009). In yeast, the soluble adaptors Mdv1 and Caf4 are involved in recruiting Dnm1 to peroxisomes and mitochondria for fission (Motley et al., 2008; Nagotu et al., 2008a). Sharing components of the division machinery between peroxisomes and mitochondria appears to be an evolutionary conserved strategy across organisms (Table 1).

As the basic fission machinery is shared by mitochondria and peroxisomes (Schrader and Fahimi, 2006a, 2008), dysfunction of the components is likely to affect both organelles and to lead to combined diseases. The first case of a division defect in peroxisomes and mitochondria has been described recently (Waterham et al., 2007). Genetic analysis revealed a missense mutation in the central domain of DLP1 in a patient who died only few weeks after birth. Skin fibroblasts from the patient displayed elongated peroxisomes and mitochondria indicative for a block in DLP1-dependent organelle fission. The patient showed microcephaly, abnormal brain development, optic atrophy and hypoplasia. The important role of DLP1 in embryonic and brain development in mice has recently been demonstrated by the generation of DLP1 knock-out mice (Ishihara et al., 2009; Wakabayashi et al., 2009). Peroxisomes and mitochondria in these mice displayed an elongated or clustered morphology.

Table 1. Shared components of the peroxisomal and mitochondrial division machinery across organisms (from Delille et al., 2009).

Plants		Yeast		Mammals			
Peroxisomes	Mitochondria	Peroxisomes	Mitochondria	Peroxisomes	Mitochondria	Family	Function
Fis1a, b	Fis1a, b	Fis1	Fis1	hFis1	hFis1	TA protein TPR motif	Membrane adapter protein
		-	-	Mff	Mff	TA protein	Membrane adapter protein?
?	ELM[1]	Mdv1 Caf4[2]	Mdv1 Caf4[2]	?	?	WD protein other	Cytosolic linker protein
DRP3A, B	DRP3A, B DRP1C, E ADL2	Dnm1 Vps1[3]	Dnm1	Drp1/DLP1	Drp1/DLP1	large GTPase	Final scission
Pex11 (a-e)		Pex11	Mmm1, 2 Mdm (10, 12, 31-33)	Pex11 (α,β,γ)			Membrane tubulation

a) Identified in *A. thaliana* (Arimura et al., 2008); b) Only present in *S. cerevisae* and *C. glabrata*; c) Required in *S. cerevisae* but not in *H. polymorpha*.

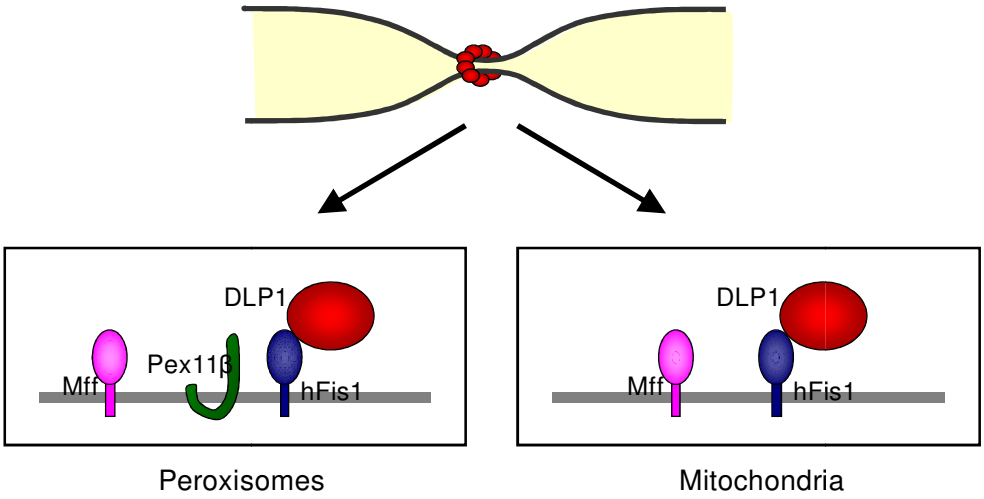

Figure 4. Organelle division in mammals. Peroxisomes and mitochondria are divided by similar machineries. *DLP1* is a GTPase performing the final scission of constricted membranes and is recruited from the cytosol by the tail-anchored protein *hFis1*, which might regulate organelle morphology and fission through self-interaction. hFis1 is supposed to interact with the peroxin Pex11β, which is known to regulate peroxisomal abundance and to tubulate membranes. *Mff* is a novel tail-anchored protein involved in peroxisomal and mitochondrial division. It is supposed to function in a complex different from *hFis1*. In yeast, additional linker proteins (Mdv1, Caf4) have been identified which are involved in mitochondrial and peroxisomal division (see Table 1) (from Delille et al., 2009).

4.2. PEROXISOMAL AND MITOCHONDRIAL METABOLISM AND CROSS-TALK

In animal cells, mitochondria and peroxisomes have separated β-oxidation systems which are distributed between the two organelles (Figure 5). Although peroxisomes and mitochondria contain their own sets of individual β-oxidation enzymes,

which differ in molecular and catalytic properties, the mechanism of β-oxidation is identical and involves the same reaction steps: (1) dehydrogenation, (2) hydration (of the double bond), (3) dehydrogenation, and (4) thiolytic cleavage (Wanders, 2004; Poirier et al., 2006).

Both peroxisomes and mitochondria have different substrate specificities and consequently different functions in their β-oxidation systems. Peroxisomes have a great importance for β-oxidation because they catabolize a variety of fatty acids and derivatives that cannot be handled by mitochondria and thus prevent the toxic effects caused by accumulation of these compounds (e.g. very long chain fatty acids, phytanic acid). However, peroxisomes are unable to oxidize fatty acids to completion, and the chain-shortened fatty acids are shuttled to the mitochondria for full oxidation (Figure 5) (Wanders, 2004; Schrader and Yoon, 2007). This requires a coordinated cross-talk and biogenesis of both organelles.

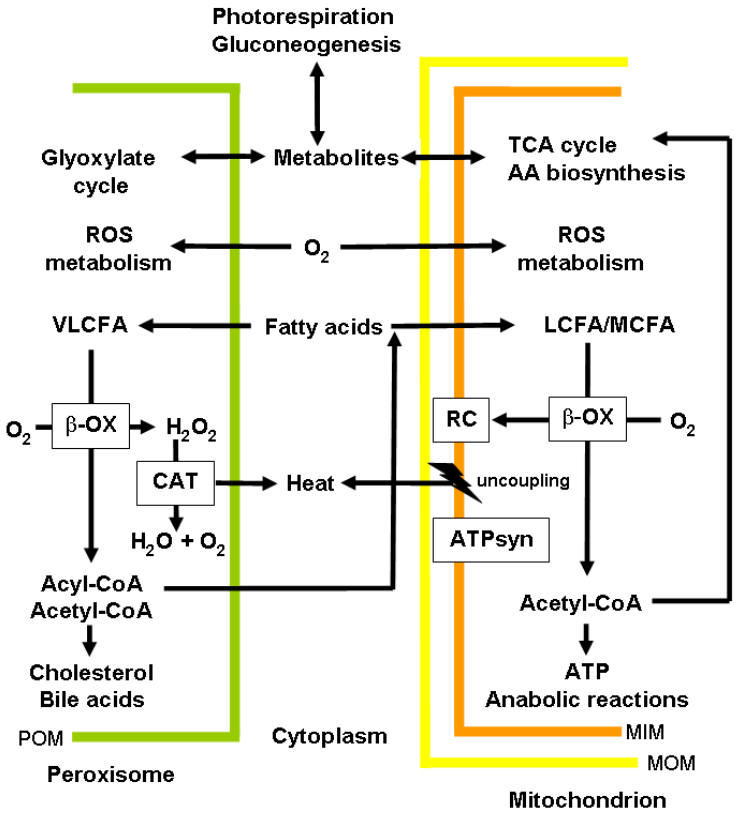

Figure 5. An overall representation of peroxisomal and mitochondrial cooperation and cross-talk. POM, peroxisomal outer membrane; MIM, mitochondrial inner membrane; MOM, mitochondrial outer membrane; TCA, tricarboxylic acid; AA, amino acid; ROS, reactive oxygen species; VLCFA, very long chain fatty acids; LCFA, long-chain fatty acids; MCFA, medium chain fatty acids; β-OX, fatty acid beta-oxidation; CAT, catalase; RC, respiratory chain; ATPsyn, ATP synthetase (from Schrader and Yoon, 2007).

Furthermore, both mitochondria and peroxisomes have a key role in both the production and scavenging of reactive oxygen species (ROS) (Schrader and Yoon, 2007), which will be discussed later (see Chapter I. 5.4.).

5. PEROXISOMES AND OXIDATIVE STRESS

5.1. OXIDATIVE STRESS

Reactive oxygen species (ROS) are formed and degraded by all aerobic organisms, leading to either physiological concentrations required for normal cell function, or excessive quantities, a state called oxidative stress (Nordberg and Arner, 2001). Oxidative stress takes place when the net flux of free radical production exceeds the antioxidant defenses of the cell (Bonekamp et al., 2009). Oxidative stress can be induced by various stressors like environmental toxins, ionizing and UV irradiation, heat shock or inflammation, all conditions in which the balance between generation and scavenging of ROS is disturbed. The resulting damage within the cells is based on the fact that the ROS increase leads on the one hand to a deregulation of redox sensitive pathways, and on the other hand to oxidative modification of all essential biomolecules (e.g. DNA, proteins, lipids) (Bonekamp et al., 2009). These hallmarks of oxidative stress are linked to many pathological conditions such as ischemia-reperfusion injury, atherosclerosis, hypertension, type-2 diabetes, cancer and neurodegenerative diseases (Schrader and Fahimi, 2006b). Besides their harmful role in pathological conditions, the importance of ROS and reactive nitrogen species (RNS) as mediators in various vital cellular processes and cell signaling pathways has became clear like their role in apoptosis, for example (Droge, 2003; Saran, 2003).

5.2. PEROXISOMES AND REACTIVE OXYGEN SPECIES

ROS include a number of chemically reactive molecules derived from oxygen, containing free (unpaired) electrons, such as the superoxide radical anion ($O_2^{\bullet -}$), the hydroxyl radical ($HO^{\bullet}$), and peroxyl radicals (ROO•), as well as nonradical derivatives of molecular oxygen (O_2), such as hydrogen peroxide (H_2O_2), hypochlorous acid (HOCl),

singlet oxygen O_2 and peroxynitrite ($ONOO^-$) (Fridovich, 1999; Betteridge, 2000; Jezek and Hlavata, 2005). Although H_2O_2 *per se* does not contain any unpaired electrons, it is ascribed to ROS, as it can be easily converted into more aggressive radical species, for example into HO• via Fenton-catalyzed reduction. Moreover, H_2O_2 is membrane permeable and diffusible, proving it suitable for intracellular signalling (Bonekamp et al., 2009).

Peroxisomes are one of the main sites in the cell where oxygen free radicals are both generated and scavenged. Initially, it was assumed that the main function of peroxisomes was the decomposition of H_2O_2 generated by different peroxisomal oxidases (mainly flavoproteins) via catalase, the classical peroxisomal marker enzyme (Figure 6). However, it is now clear that peroxisomes are involved in a variety of important cellular functions in almost all eukaryotic cells. The main metabolic processes contributing to the generation of H_2O_2 in peroxisomes are the β-oxidation of fatty acids, the enzymatic reactions of the flavin oxidases, the disproportion of superoxide radicals, and in plant peroxisomes, the photorespiratory glycolate oxidase reaction (Schrader and Fahimi, 2006b).

The oxidation of the various substrates is performed by $O_2^{\cdot-}$-consuming oxidases that produce H_2O_2 as a by-product which is then decomposed by catalase and other resident antioxidant enzymes (Figure 6). Moreover, RNS are also produced within peroxisomes, as the inducible form of nitric oxide synthase (NOS, Figure 6) which catalyses the oxidation of L-arginine to nitric oxide ($^{\bullet}NO$) has been detected at peroxisomes (Stolz et al., 2002). Oxidative stimuli appear to be linked to ‘‘growth and division’’-based peroxisome proliferation (see Chapter I. 3.1.), in which peroxisomes undergo a well-defined sequence of morphological changes, including elongation (growth), constriction and final fission (division) (see Chapters I. 3. and I. 6., Figure 3).

The extent to which peroxisomes are key players in oxidative metabolism is exemplified by the fact that they consume 20% of the total amount of oxygen consumed while producing 35% of all the cells H_2O_2 (Boveris et al., 1972). Thus, oxidative balance within peroxisomes needs to be tightly regulated - shifting this exact balance via endo- or exogenous factors, ageing or disease conditions leads to a deregulation of the system (Bonekamp et al., 2009).

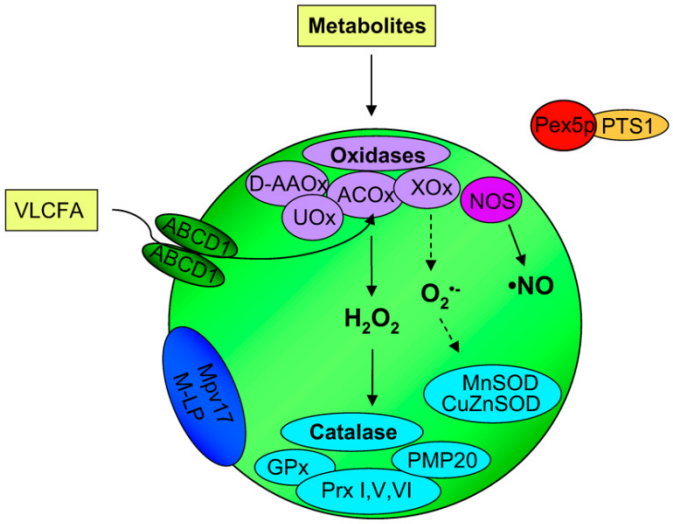

Figure 6. Schematic overview of peroxisomal ROS homeostasis. The various peroxisomal metabolites (e.g. VLCFA) are transported across the membrane via specific transporters (e.g. ABCD1), while most peroxisomal matrix proteins are imported in a PTS1/Pex5p-dependent manner. Substrates are then broken down by peroxisomal oxidases (light purple) which transfer the hydrogen extracted from the substrate directly to O_2. The generated H_2O_2 is subsequently converted to H_2O and O_2 by peroxisomal antioxidant enzymes (light blue), with catalase being the most prominent one. An additional by-product of xanthine oxidase (XOx) activity is $O^{\bullet-}_2$ which is scavenged by manganese superoxide dismutase (MnSOD) and copper-zinc-superoxide dismutase (CuZnSOD). Mpv17 and M-LP (dark blue) are implicated in the regulation of peroxisomal ROS metabolism, but their peroxisomal localization has been questioned. Nitric oxide synthase (NOS, dark purple) catalyses the oxidation of L-arginine to nitric oxide ($^{\bullet}$NO), which can react with $O^{\bullet-}_2$ radicals to form peroxynitrite ($ONOO^-$), a powerful oxidant. Both H_2O_2 and $^{\bullet}$NO can pass the peroxisomal membrane and act in cellular signalling. PTS1, peroxisomal targeting signal 1; VLCFA, very long chain fatty acids; D-AAOx, D-amino acid oxidase; UOx, urate oxidase; ACOx, acyl-CoA oxidase; XOx, xanthine oxidase; NOS, nitric oxide synthase; GPx, glutathione peroxidase; Prx: peroxiredoxin; M-LP, Mpv17-like protein (from Bonekamp et al., 2009).

To degrade the ROS, which are produced due to their metabolic activity, and to maintain the equilibrium between production and scavenging of ROS, peroxisomes harbor several powerful defense mechanisms and antioxidant enzymes in addition to catalase (Schrader and Fahimi, 2006b) (Figure 6 and Table 2). Although peroxisomes are considered a source of oxidative stress due to their oxidative metabolism, they respond to oxidative stress and ROS, which have been generated in other intra- or extracellular locations (e.g. in mitochondria, see Chapter I. 5.3.), most likely to protect the cell against an oxidative damage. Furthermore, certain peroxisome-generated ROS may act as mediators in intracellular signalling (Masters, 1996).

Table 2. Overview of ROS/RNS generated in mammalian peroxisomes (PO) (from Bonekamp et al., 2009)**.** NOHLA, Nx-hydroxy-L-arginine.

Type of ROS/RNS produced	Generating reaction	Produced in PO by	Scavenged in PO by
Hydrogen peroxide (H_2O_2)	$O_2^{\bullet-} + H^+ \rightarrow HO_2^{\bullet-}$, $2HO_2^{\bullet-} \rightarrow H_2O_2 + O_2$	Acyl-CoA oxidase (several types) Urate oxidase Xanthine oxidase D-amino acid oxidase D-aspartate oxidase Pipecolic acid oxidase Sarcosine oxidase L-alpha-hydroxy acid oxidase Polyamine oxidase	Catalase Glutathione Peroxidase Peroxiredoxin I PMP20
Superoxide anion ($O_2^{\bullet-}$)	$O_2 + e^- \rightarrow O_2^{\bullet-}$	Xanthine oxidase	MnSOD CuZnSOD
Nitric oxide ($^{\bullet}NO$)	L-Arg + NADPH + H^+ + O_2 → NOHLA + $NADP^+$ + H_2O, NOHLA + ½ NADPH + ½ H^+ + O_2 → L-citrulline + ½ $NADP^+$ + $^{\bullet}NO$ + H_2O	Nitric oxide synthase	

5.3. PEROXISOMAL DISORDERS AND ROS

Inherited peroxisomal disorders can be divided into two main subgroups: the peroxisomal biogenesis disorders (PBDs) and the more frequent peroxisomal (single) enzyme deficiencies (PEDs) (see Chapter I. 1.3.) (Wanders and Waterham, 2006a). One of the most prominent PEDs, the X-linked adrenoleukodystrophy (X-ALD), caused by mutations in the ABCD1 gene that encodes the transporter of VLCFA and/or its CoA-derivatives (Figure 7) (van Roermund et al., 2008), is a fatal neurodegenerative disorder (Wanders and Waterham, 2006a). It is characterized by an accumulation of VLCFAs, progressive demyelination/neurodegeration in the central nervous system and adrenal insufficiency. It was surmised that the accumulated VLCFAs could either incorporate into complex lipids and destabilize them (Moser et al., 2001) or that they could increase oxidative stress and lead to oxidative modification in nervous tissue (Schonfeld and Reiser, 2006), both possibilities inducing demyelination (Bonekamp et al., 2009).

Fourcade et al. (2008) have recently investigated the relation between oxidative lesions and neurodegeneration in an ABCD1 knock-out model, although the mouse model rather reproduces a milder AMN (adreno myelo neuropathy) phenotype of ALD. They also demonstrated that the VLCFA C26:0 accumulation could be a cause of oxidative stress via mild inhibition of the mitochondrial electron transfer chain (ETC), and also compromised

cellular GSH levels, thus combining to result in oxidative lesions that probably play a crucial role in neurodegeneration, as nervous tissue is very susceptible to oxidative damage (Arlt et al., 2002) (Figure 7 B, top). Another example of oxidative stress in peroxisomal disorders is observed in patients suffering from Zellweger syndrome as well as those with an enzyme defect in the bile acid synthesis pathway (Figure 7 B, bottom).

5.4. PEROXISOMES, MITOCHONDRIA AND ROS METABOLISM

Mitochondria and peroxisomes have a key role in both the production and scavenging of reactive oxygen species (ROS) (Schrader and Yoon, 2007). The mitochondrial electron transport chain is a major site of free radical generation. The major formation of superoxide radicals occurs at complex I (NADH-coQ reductase) and complex III (cytochrome bc1 complex) (Figure 9). In peroxisomes, the numerous oxidases along with cytochrome B_5, a cytochrome P-450-dependent hydroxylation system, produce ROS including hydrogen peroxide, superoxide radicals and hydroxyl radicals (Figure 6, 7; Table 2) (Schrader and Fahimi, 2006b).

Both peroxisomes and mitochondria contain antioxidant systems to minimize oxidative damage. Peroxisomes contain multiple antioxidant enzymes: catalase, Cu-Zn-SOD, glutathione peroxidase, MnSOD, epoxide hydrolase, PMP20 and peroxiredoxin (I, V, VI) (Figure 6). Mitochondria contain antioxidant molecules (glutathione, NADH, thioredoxin) and enzymes that degrade ROS (MnSOD, glutathione reductase, glutathione peroxidase) (Schrader and Yoon, 2007). Under conditions of oxidative stress, where the mitochondria generate more H_2O_2 than under normal conditions, the glutathione peroxidase/glutathione reductase system is often limited by the level of glutathione (and NADPH), and is inefficient in decomposing the increased H_2O_2. The H_2O_2 that escapes across the mitochondrial membrane might be degraded by catalase in the peroxisome (or in the cytosol) (Figure 5) (Schrader and Yoon, 2007). ROS accumulation, itself a consequence of defects in mitochondrial or peroxisomal function, will also affect mitochondrial morphology and function (see Chapter I. 4.). Another possibility is that retrograde signaling through transcriptional regulators might affect mitochondria and peroxisomes. Regulators such as PPARα (see Chapter I. 6.1.) might induce changes in mitochondria by feedback regulation if peroxisomes are defective (Thoms et al., 2009).

It is suggested that both mitochondrial and peroxisomal dysfunction and ROS generation contribute to ageing (Figure 7 A) neurodegeneration and carcinogenesis (Moldovan and Moldovan, 2004; Schrader and Fahimi, 2006b; Beal, 2005).

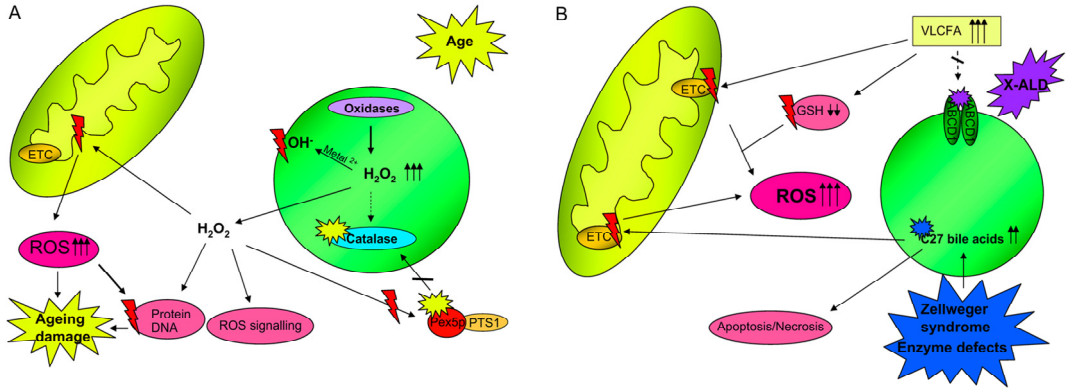

Figure 7. (A) Schematic overview of age-related alterations in peroxisomal ROS homeostasis and its putative consequences. With advancing age, the homeostatic balance of pro- and antioxidants is upset. Enzyme levels are altered and the fidelity of the PTS1/Pex5p-dependent import system is compromised. Catalase in particular is reduced or lost, leading to an accumulation of H_2O_2 in the organelle. H_2O_2 can subsequently be converted into the very reactive •OH radical by metal-ion catalyzed Fenton chemistry which then modifies peroxisomal proteins and lipids. Moreover, H_2O_2 can diffuse across the membrane into the cytoplasm where it perturbs regular ROS signalling, reacts into more damaging ROS and modifies essential biomolecules such as proteins and DNA, leading to cell damage. In addition, H_2O_2 also affects the PTS1/Pex5p import system, thereby further compromising catalase levels in peroxisomes, resulting in a negative feedback. Compromised catalase and the consequently elevated H_2O_2 also contributes to age-related mitochondrial dysfunction, as it decreases mitochondrial membrane potential and leads to the production of mitochondrial ROS, further elevating cellular ROS levels and oxidative damage. **(B) Schematic overview of the effects of certain peroxisomal diseases on ROS homeostasis**. (Top) In X-linked adrenoleukodystrophy, the function of the ABCD1 membrane transporter is compromised, leading to an accumulation of its substrates, VLCFA, in the cytoplasm. It was shown that the VLCFA C26:0 has a mild inhibitory effect on the mitochondrial electron transfer chain (ETC) while glutathione (GSH) levels are also compromised. Both factors combine, leading to ROS increase inside the cells and oxidative lesions. (Bottom) C27-bile acids accumulate under certain pathological conditions such as Zellweger syndrome or single enzyme deficiencies associated with bile acid synthesis. It was recently shown that they are potent inhibitors of the mitochondrial electron transfer chain, leading to an increase in ROS production that leads to harmful oxidative damage. Additionally, depending on their levels, C27 bile acids can either induce apoptosis or necrosis (from Bonekamp et al., 2009).

Additionally, impairment of normal peroxisomal function in for example, X-ALD or Zellweger syndrome leads to an accumulation of substrates (e.g. VLCFA, bile acids intermediates) that also directly have an effect on mitochondria and their redox balance by inhibiting the electron transfer chain (Figure 7 B). A pathophysiological link between the organelles can also be deduced from the fact that mitochondria in Pex5$^{-/-}$ mice show an extremely altered morphology with marked abnormalities in various tissues (Schrader and Fahimi, 2006b; Baumgart et al., 2001). Several authors described reduced oxidative

capacities of mitochondria in liver, brain and muscle tissue of PBD patients (Thoms et al., 2009).

Disturbance of mitochondrial β-oxidation leads to a shift in peroxisomal β-oxidation which results in an increase in ROS production due to higher activity of peroxisomal oxidases, inducing oxidative lesions in hepatic tissue. Mitochondrial dysfunction was further shown to exert an effect on peroxisome abundance in yeast. Screening for peroxisome-morphology mutants in *S. cerevisiae* revealed that many mutants in mitochondrial genes display increased peroxisome number compared to controls (Motley et al., 2008).

6. SIGNALLING AND PEROXISOME ELONGATION

6.1. PEROXISOME PROLIFERATION

The plasticity of peroxisomes to undergo proliferation in response to a variety of intrinsic and extrinsic stimuli has been quite well-known and used for the investigation of diverse questions such as the biogenesis of this organelle and its biochemical characterization (Fahimi et al., 1982). The list of compounds inducing proliferation of peroxisomes in rodent liver is very long comprising divergent drugs, industrial chemicals such as lubricants and plasticizers, as well as agrochemicals (Schrader and Fahimi, 2006a).

Peroxisome proliferation in mammals is regulated by nuclear transcription factors which belong to the superfamily of steroid/thyroid/retinoid receptors and were originally designated as peroxisome proliferator activated receptors (PPARs) (Issemann and Green, 1990). Three subtypes of PPARs were identified in different species: α, β and γ. The PPARs form heterodimers with retinoid X receptors (RXRs) and bind to specific DNA-sequences known as peroxisome proliferator response elements (PPREs) initiating the transcription of responsive genes (Figure 8). PPREs have been reported not only for all peroxisomal lipid β-oxidation enzymes but also for several microsomal cytochrome P-450 subtypes as well as for apolipoproteins type I and II (Schoonjans et al., 1996).

Peroxisome proliferation in mammalian cells appears to be initiated by extracellular signals, such as signals mimicked by peroxisome proliferators, which by activating intracellular signalling cascades, lead to the activation of the transcription factors PPARα and PPARγ. These have been shown to induce the transcription of

PEX11pα (Li et al., 2002). As activation of PPARα affects numerous metabolic pathways (Reddy and Hashimoto, 2001), and as metabolic activities have also been shown to affect the number of peroxisomes (Chang et al., 1999, Funato et al., 2005), this peroxisome proliferation pathway might be mediated through some kind of metabolic control. Although the activation of PEX11p is a common theme in the course of peroxisome proliferation, yeasts, plants and mammals have evolved distinct upstream mechanisms to actualize this process (Figure 8) (Kaur and Hu, 2009).

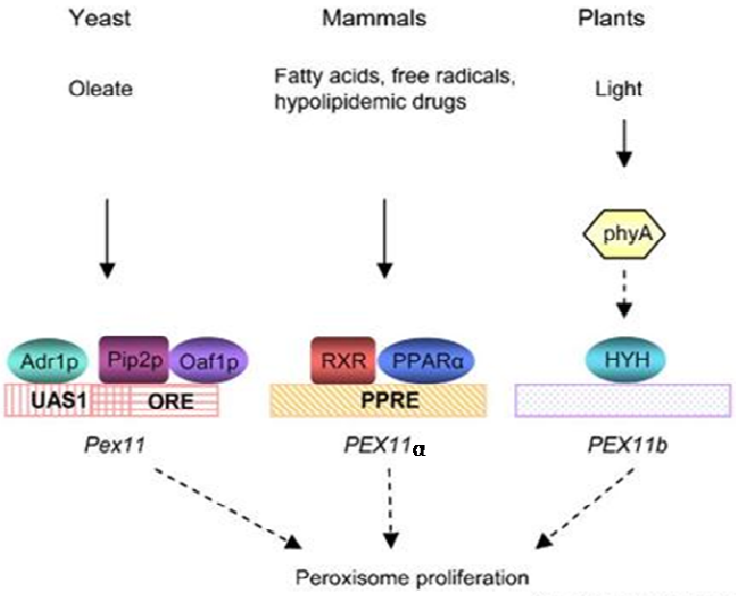

Figure 8. Comparative model for the activation of PEX11 genes in yeast, mammals and plants. This model is based on information garnered from *S. cerevisiae* (yeast), *H. sapiens* (mammals) and *A. thaliana* (plants). In yeast, in the presence of oleic acids, the zinc cluster transcription factors Oaf1p and Pip2p dimerize, and together with Adr1p bind to the partially overlapping oleate response element (ORE) and upstream activation sequence 1 (UAS1) in the promoter of the Pex11 gene to activate transcription. In mammals, peroxisome proliferator-activated receptor alpha (PPARα) and retinoid X receptor (RXR) coordinately bind to the PPAR response element (PPRE) to upregulate the expression of the PEX11α gene in response to hypolipidemic drugs, and fatty acids. In plants, light induces the expression of PEX11b via the action of the far-red light photoreceptor phyA and direct binding of the bZIP transcription factor HYH to the PEX11b promoter. In all cases, the induction of PEX11 further activates downstream events that culminate in peroxisome proliferation (adapted from Kaur and Hu, 2009).

6.2. PEROXISOME ELONGATION

Evidence has been presented in the last years that peroxisome elongation appears to be an important prerequisite of peroxisome division (see Chapter I. 3.1.), and that tubulation and fission of elongated peroxisomes represent processes of peroxisomal growth and division, which contribute to peroxisome proliferation (see Chapter I. 6.1.). A role for the peroxisomal membrane protein Pex11p family, the dynamin-like protein DLP1/Drp1, and Fis1, a putative membrane receptor/adaptor for DLP1/Drp1 at the peroxisomal membrane has been demonstrated (see Chapter I. 3.1.). Elongated/tubular peroxisomes can also be induced by partial hepatectomy (Yamamoto and Fahimi, 1987), stimulation of cultured cells with defined growth factors or polyunsaturated fatty acids (PUFAs), particularly arachidonic acid (Schrader et al., 1999), microtubule depolymerization (Schrader et al., 1996a) (see Chapter I. 3.), Pex11p overexpression (Schrader et al., 1998b ; Lingard and Trelease, 2006), or by inhibition of DLP1/Drp1 or hFis1 function (Koch et al., 2003; Tanaka et al., 2006). Whereas the latter manipulations

appear to act directly on the peroxisomal membrane, the other conditions require intracellular signalling to induce peroxisome elongation/growth (Schrader et al., 1998a). Arachidonic acid, for example, is a substrate for peroxisomal β-oxidation, but has also been shown to stimulate ROS production by cultured cells (Dymkowska et al., 2006). In plant cells (but also in mammals) it is suggested that diverse types of stress (e. g. wounding, pathogen attack, drought, osmotic stress, excess light) that generate H_2O_2 as a signalling molecule result in peroxisome proliferation via the up-regulation of PEX genes required for peroxisome biogenesis and import of proteins (del Rio et al., 2002; Lopez-Huertas et al., 2000; Desikan et al., 2001). A striking increase in elongated forms of peroxisomes upon expression of Pex11p has been observed in all organisms studied (Schrader et al., 1998b, Thoms and Erdmann, 2005).

In cultured cells, oxidative stress has been shown to induce morphological changes of the peroxisomal compartment. In mammalian and plant cells a pronounced elongation of peroxisomes is observed after UV irradiation, direct exposure to H_2O_2, or even during live cell imaging of GFP-PTS1 labeled peroxisomes by regular fluorescent microscopy (Schrader et al., 1999; Schrader and Fahimi, 2004, 2006b). Antioxidant treatment blocked the elongation of peroxisomes, thus supporting the role of ROS in UV-mediated peroxisomal growth (Schrader et al., 1999). Very recently, the rapid dynamic formation of peroxisomal tubular extensions in plant cells after exposure to H_2O_2 has been reported (Sinclair et al., 2009). Formation of these extensions was later on followed by peroxisome elongation and division, suggesting the existence of a rapid, transcription independent pathway and a transcription-dependent pathway in peroxisome response to H_2O_2 /oxidative stress.

However, most of the UV- or ROS-mediated signalling pathways and the gene responses leading to peroxisome elongation/proliferation are still largely unknown. Although information on the exact functions of elongated/tubular or complex peroxisomal structures is scarce, the evidence of ROS-mediated peroxisome elongation/proliferation and induction of peroxisomal genes supports an involvement in cellular rescue from ROS.

II. AIMS OF THE PRESENT STUDY

II. AIMS

Peroxisomes are crucial subcellular compartments for human life and health (Schrader and Fahimi, 2008). They orchestrate important functions during development, and peroxisome proliferation as well as dysfunctions are linked to tumor formation, neurodegeneration and aging. Previous work from our laboratory has demonstrated that different external stimuli (including UV-irradiation and ROS production) induce morphological alterations of the peroxisomal compartment, which are linked to peroxisome proliferation (Schrader et al., 1999, Schrader and Fahimi, 2004, 2006b). These alterations are supposed to exert a protective function, and are therefore important for the role of peroxisomes in health and disease. Furthermore, our group presented evidence that peroxisomes and mitochondria exhibit a much closer interrelationship than previously assumed (Camoes et al., 2009).

The general aim of the present study was to investigate if cellular manipulations which lead to the intracellular production of ROS (e.g. via mitochondrial respiration) are capable of inducing growth/proliferation of the peroxisomal compartment. As little is known about the ROS-mediated signalling pathways and the gene responses regulating peroxisomal biogenesis and disease, further insights are of great importance.

SPECIFIC AIMS

1. Selection and development of a mammalian cell culture system to examine peroxisomal growth/proliferation induced by different stressors.
2. Establishing fluorescent-based assays to measure and quantify ROS production and changes in the redox state of the cell.
3. Examination of the effect of different stressors on the induction of peroxisomal growth/proliferation in mammalian cells. Among them cytoskeleton-active drugs, inhibitors of the mitochondrial respiratory chain and compounds affecting the redox state of the cell were tested. Alterations of the peroxisomal compartment were visualized and quantified by immunofluorescence microscopy.
4. Involvement of ROS in peroxisomal growth/proliferation. ROS and GSH levels were measured and treatments with antioxidants were performed to verify the involvement of ROS.

III. MATERIAL AND METHODS

MATERIALS

1. ANTIBODIES

Table 3. List of antibodies used in this work

	Antigen	IMF	Species	Supplier	Reference
Primary antibodies	PMP70	1:100	Rabbit (polyclonal antibody)	kindly provided by A. Völkl, University of Heidelberg, Germany	Schrader et al., 1998b
	PEX14	1:200	Rabbit (polyclonal antibody)	kindly provided by D. Crane, Griffith University, Brisbane Australia	Nguyen et al., 2006
	α tubulin	1:100	Mouse (monoclonal antibody)	BD Biosciences Pharmingen, San Diego, CA, USA	Boll and Schrader, 2005
	TOM20	1:200	Mouse (monoclonal antibody)	BD Biosciences, USA	Wang et al., 2009
	α acetylated tubulin	1:100	Mouse (monoclonal antibody)	Sigma-Aldrich, Deisenhofen, Germany	Shim et al., 2008
Secondary antibodies	DαRb-Alexa 488	1:400	Donkey	Dianova (Hamburg, Germany)	Delille and Schrader, 2008
	DαM-TRITC	1:100	Donkey	Dianova (Hamburg, Germany)	Delille and Schrader, 2008

IMF: Indirect Immunofluorescence

2. CHEMICAL COMPOUNDS

Table 4. List of the chemical compounds used to treat the cells in this work

Drugs	Description	Supplier	References
Nocodazole	Microtubule depolymerizing drug	Sigma-Aldrich	Schrader et al., 1996a, 1998a, 2000
L-Buthionine - Sulfoximine	GSH depletion	kindly provided by J. Jordán (Centro Universidad de Castilla La Mancha, Albacete, Spain) Sigma-Aldrich	Jordan et al., 2002, Fernandez-Gomez et al., 2005, Neely et al., 2005
Rotenone	Complex I inhibitor of the mitochondrial respiratory chain	kindly provided by J. Jordán (Sigma-Aldrich)	Srivastava and Panda, 2007, Ren and Feng, 2007
Sodium Azide	Complex IV inhibitor of mitochondrial respiratory chain	Sigma-Aldrich	Gomez-Nino et al., 2009

Antioxidants	Description	Supplier	References
N-acetyl cysteine	Low molecular weight antioxidant, precursor of glutathione	Sigma-Aldrich	Schrader et al., 1999, Bowes and Gupta, 2005
Vitamin C	Low molecular weight antioxidant	Sigma-Aldrich	Gomez-Lazaro et al., 2008
Vitamin E	Low molecular weight antioxidant	Sigma-Aldrich	Jordan et al., 2000

3. LIST OF EQUIPMENT

- Vertical laminar flow hood – Heraeus, Germany
- CO_2 incubator – Sanyo, Japan
- Centrifuge – 5810R Eppendorf , Germany
- Inverted microscope – Leica DMIL, Leitz, Wetzlar, Germany
- Fluorescence microscope – Olympus IX81 microscope (Olympus Optical, Germany) equipped with a PlanApo 100X / 1.40 objective
- Nitrogen tank – Cryomed Forma Scientific, USA
- pH Meter, Sartorius, Germany
- Analytical balance, Sartorius BP 221S, Germany
- Thermal Cycler (mixing and incubation of samples) - Thermomixer 5436, Eppendorf, Germany
- Water bath – Memmert, Germany
- Electromagnetic agitator – Agimatic-N (JP Selecta), Vidrolab, Spain
- Multifunctional microplate reader TECAN i-control – infinite 200, Austria GmbH
- Spectophotometer – Perkin-Elmer fluorometer (luminescence-spectrophotometer LS50B), Perkin-Elmer, Wellesley, USA
- Autoclave – Uniclave 88, Portugal
- Sterilizing oven – Sanyo Drying Oven, Leicestershire, UK

4. LIST OF BUFFERS AND REAGENTS

Phosphate Buffered Saline (PBS) 10x, pH 7.4

1.37 M NaCl; 26.8 mM KCl; 78.1 mM Na_2HPO4 (2 H_2O_2); 14.7 mM KH_2PO_4

Krebs buffer, pH 7.4

140 mM NaCl; 5.9 mM KCl; 1.2 mM $MgCl_2$; 15 mM HEPES; 10 mM glucose; 2.5 mM $CaCl_2$

Trypsin/EDTA solution

Trypsin/EDTA 0.05% / 0.02% in Dulbecco's-PBS (PAA Laboratories GmbH, Pashing, Austria)

Cell Culture Medium

Dulbecco's modified Eagle's medium (DMEM) supplemented with 2 g/liter sodium bicarbonate, 2 mM glutamine, 100 U/ml penicillin, 100 g/ml streptomycin, and 10% fetal calf serum (FCS) (all from PAA Laboratories GmbH, Pashing, Austria)

Freezing medium (DMEM)

20% FCS and add 10% DMSO to preserve the cells. Filtrate to sterilize.

4% para-Formaldehyde (w/v), pH 7.4 for immunofluorescence

Weigh 4 g pFA, add 90 ml H_2O, 1N NaOH. Shake and heat no more than 60ºC, remove from heat. Then add 10 ml 1xPBS and adjust pH to 7.4, store at -20ºC

0.2% Triton-X-100 (v/v), pH 7.4 for immunofluorescence

0.5 ml Triton-X-100, adjust to 250 ml with 1x PBS

2% BSA (w/v) for immunofluorescence, pH 7.4

Weigh 1 g BSA and adjust to 50 ml with 1xPBS

n-propyl-Gallat for immunofluorescence

Weigh 0.625 g n-propyl-Gallate add 12 ml 1xPBS (adjust pH to 7.0) add 12.5 ml glycerol, stir overnight (in the dark). Store at 4ºC in a dark bottle

Mowiol (mounting solution for fluorescence microscopy)

Weigh 10 g Mowiol 4-88 add 40 ml 1xPBS (stir overnight) and 20 ml Glycerol (ultrapure) (stir overnight). Then centrifuge 1h, 1500 rpm (Centrifuge Eppendorf 5810R), take supernatant, add NaN_3 and store at 4ºC.

Use, 3 parts Mowiol (stock) + 1 part n-propyl-Gallate

Dimethyl Sulfoxide (DMSO) – 99. 9%

Oxidation-sensitive fluorescent dye 2',7'-dichlorodihydrofluorescein diacetate (DCFH-DA)

Stock solution prepared in DMSO at 10 mM, and used at 10 µM in 1x PBS

Monochlorobimane (mBCL) fluorescent

Stock solution prepared in DMSO at 80 mM, and used at 160 µM in Krebs buffer

METHODS

1. CELL CULTURE

1.1. CELL LINES

At the beginning of this study, different mammalian cell lines have been tested by immunofluorescence microscopy (see Methods, Chapter 3.) to select a cell culture model with an elaborate and dynamic peroxisomal compartment suitable to monitor peroxisome elongation and proliferation. In addition, serum-containing and serum-free culture conditions were tested to select optimal conditions for induction of ROS and stimulation of peroxisome elongation/proliferation (not shown).

The following cell lines have been tested:

HepG2 cells are well differentiated human hepatocellular carcinoma cells (hepatoblastoma). This cell line was obtained from the American Type Culture Collection (ATCC; Rockville, MD) (ATCC number: HB - 8065).

COS-7 cells are derived from kidney epithelial cells of the African green monkey. The line was derived from the CV-1 cell line (ATCC® CCL-70) by transformation with an origin defective mutant of SV40 which codes for wild type T antigen. SV40 is an abbreviation for Simian vacuolating virus 40 or *Simian virus 40*, a polyomavirus that is found in both monkeys and humans (http://www.lgcstandards-atcc.org). COS-7 cells were obtained from the American Type Culture Collection (ATCC; Rockville, MD) (ATCC number: CRL-1651).

COS-7-GFP-PTS1 cells are derived from COS-7 cells by stable transfection with a construct encoding for a fusion protein of green fluorescent protein (GFP) carrying a peroxisomal targeting signal 1 (PTS1). The three amino acids added (SKL; serine-lysine-leucine) represent a consensus peroxisomal targeting sequence (PTS1), which is sufficient to direct a polypeptide to peroxisomes *in vivo* in animals, plants, and yeasts.

Although HepG2 cells exhibit several morphologically distinct forms of peroxisomes, and COS-7-GFP-PTS1 cells have the advantage not to require antibody based staining of peroxisomes, we decided to use COS-7 cells for most of the experiments performed. COS-7 cells showed a prominent response to the stressors applied, as well as good cell viability and cell growth. In addition, morphological changes of the peroxisomal compartment (e.g. elongation; see IV, Figure 12 B.) were readily visible and easy to quantitate.

1.2. CELL CULTURE MAINTENANCE

The cells were routinely cultured in Dulbecco's modified Eagle's medium (DMEM) supplemented with 2 g/liter sodium bicarbonate, 2 mM glutamine, 100 U/ml penicillin, 100 g/ml streptomycin, and 10% FCS at 37ºC in a humidified atmosphere containing 5% CO_2. The medium was replaced twice weekly until cells reached confluence. Confluent cells were washed 1x with sterile 1x PBS, and were detached by incubating at 37ºC, 5% CO_2 with trypsin/EDTA solution. The cells were harvested with cell culture medium (DMEM, 10% FCS, 1x Penicillin/Streptomycin) and centrifuged at 1000 rpm for 3 min at room temperature (Centrifuge Eppendorf 5810R). The cell pellet was then resuspended in the appropriate medium and cells were plated in 10 cm diameter cell culture dishes at the appropriate density for maintenance or on glass coverslips for immunofluorescence.

1.3. CELL COUNTING

For the experiments the cells were seeded at a defined density ($1x10^5$ cells/ml) on glass coverslips in 12 well dishes and allowed to grow for 24h. Cell counting was performed in a Fuchs-Rosenthal chamber (Depth 0.200 mm and 0.0625 mm^2) and the following formula was used to calculate the amount of cells/ml:

$$\frac{1 \text{ big square x } 16 \text{ x } 1000}{3.2 \text{ µl}}$$

1.4. CELL STORAGE AND FREEZING

Cell stocks were made from dishes with confluent cells and low passages. After trypsinization and centrifugation the cell pellet was resuspended in freezing medium (DMEM with 20% FCS + 10% DMSO) and 1 ml aliquots were prepared in sterile cryotubes. Stocks ($3x10^6$cells/ml) were frozen at -80ºC overnight and afterwards stored in liquid nitrogen.

In contrast to the gradual process of freezing, all stocks were de-frozen quickly in a 37ºC waterbath, resuspended in pre-warmed medium and placed in the incubator. The culture medium was replaced to allow attachment after 12h.

2. DRUG TREATMENT

2.1. INDUCTION OF PEROXISOME PROLIFERATION IN MAMMALIAN CELLS BY DIFFERENT STRESSORS

To examine if different chemical stressors induce the growth/proliferation of the peroxisomal compartment, microtubule depolymerizing drugs (see Methods, Chapter 2.1.1.), inhibitors of the mitochondrial respiratory chain (which lead to the production of intracellular ROS) (see Methods, Chapter 2.1.3. and Figure 9) as well as modifiers of intracellular GSH levels (see Methods, Chapter 2.1.2.) were applied. Twenty four hours after seeding, the cells were treated with different concentrations of the reagents. At different time intervals, cells were processed for immunofluorescence microscopy (see Methods, Chapter 3.) to monitor changes of the peroxisomal compartment. Furthermore, fluorescence-based assays were established which allowed the measurement of cellular ROS and GSH levels (see Methods 4.1. and 4.2.).

2.1.1. MICROTUBULE-DEPOLYMERIZATION BY NOCODAZOLE

Nocodazole (NOC), a benzimidazole derivative, was initially developed as a potential anticancer drug. It is still widely used to study microtubule-dependent processes because of its ability to rapidly depolymerize microtubules (MTs) (inhibiting tubulin

polymerization) *in vivo* and *in vitro* (Vasquez et al., 1997). It is also freely membrane-permeable, and the microtubule-depolymerization is reversible.

A nocodazole stock solution was made in DMSO at a final concentration of 33.2 mM and stored in DMSO at -20ºC. The stock solution was diluted in culture medium at a final concentration of 33.2 µM. The exposure time was 3, 6 and 24h. After each time point cells cultured on glass coverslips were prepared for double-immunofluorescence and peroxisomes, mitochondria or microtubules were labelled with the appropriate antibodies (see Materials, Chapter 1., Table 3).

2.1.2. DEPLETION OF GLUTATHIONE LEVELS BY L-BUTHIONINE SULFOXIMINE (BSO)

Glutathione (GSH), a ubiquitous tripeptide thiol (found in the cytoplasm, mitochondria and nucleus), is a critical component of the cellular antioxidant system. It is involved in many important cellular functions including the detoxification of xenobiotics, by the formation of less-toxic GSH-xenobiotic conjugates often requiring the catalytic activity of GSH S-transferases (GST) (Hayes et al., 2005) and the deactivation of ROS, either via direct GSH–ROS interaction or via the activity of GSH peroxidases (Dickinson and Forman, 2002). Thus, GSH is involved in both chemical detoxification and antioxidant defence (Green et al., 2006).

BSO induces oxidative stress in mammalian cells by irreversibly inhibiting γ-glutamylcysteine synthetase (γ-GCS), an essential enzyme for the synthesis of GSH. Administration of BSO leads to decreased GSH levels in virtually all tissues including developing embryos, and a marked GSH depletion is associated with tissue damage.

A BSO stock solution was made (always fresh) in culture medium at a final concentration of 100 mM, filtered before use and then diluted in culture medium at a final concentration of 100 µM. The time intervals of exposure were 3h, 6h, 9h, 12h and 24h. After each time interval the cells were processed for immunofluorescence (see Methods, Chapter 3.).

2.1.3. INHIBITORS OF MITOCHONDRIAL RESPIRATION

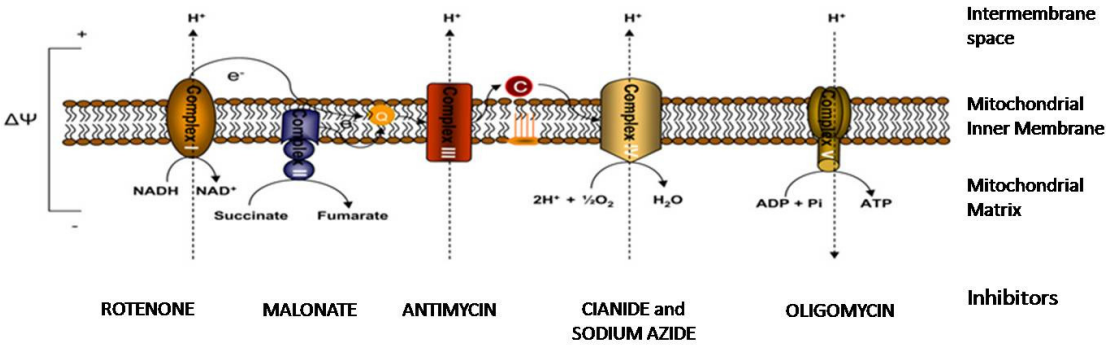

Figure 9. Electron transport chain (ETC) in the inner mitochondrial membrane. The ETC is composed of five multimeric complexes in the inner mitochondrial membrane. Complex I (NADH coenzyme Q reductase) accepts electrons from the Krebs cycle electron carrier nicotinamide adenine dinucleotide (NADH), and passes them to coenzyme Q (ubiquinine (UQ)), which also receives electrons from complex II (succinate dehydrogenase). UQ passes electrons to complex III (cytochrome bc_1 complex), which passes them to cytochrome *c* (cyt *c*). Cyt *c* passes electrons to complex IV (cytochrome *c* oxidase), which uses the electrons and hydrogen ions to reduce molecular oxygen to water. The major ROS production occurs at complex I and III. (adapted from http://ccforum.com/content/pdf/cc6779.pdf).

2.1.3.1. ROTENONE

Rotenone is a pesticide that was widely used as herbicide in private gardens and in several powders for delousing humans or animals (Srivastava and Panda, 2007). It is the most potent member of the rotenoids, a family of natural cytotoxic compounds extracted from various parts of *Leguminosa* plants and its toxicity is relevant. Due to its lipophilic structure it freely crosses cell membranes and accesses cytoplasm and mitochondria (Jin et al., 2007). Rotenone inhibits complex I (NADH CoQ1 reductase) (Figure 9) in the mitochondrial respiratory chain (Chance et al. 1963). Complex I inhibition has several potential functional consequences, including decreased ATP production, loss of proton gradient, bioenergetic defects and oxidative damage (Testa et al., 2005).

A rotenone stock solution was made in DMSO at a final concentration of 100 mM and stored in DMSO at -20ºC. The stock solution was diluted in culture medium at a final concentration of 100 nM, 500 nM, 1 µM, 10 µM and 100 µM and cells were incubated for 6 and 24h of exposure time.

2.1.3.2. SODIUM AZIDE

Sodium azide blocks cytochrome *c* oxidase (complex IV) (Figure 9) by binding between the heme a_3 iron and Cu_B in the oxygen reduction site (Yoshikawa et al., 1998; Fei et al., 2000). Many other heme proteins and other metalloenzymes are inhibited by azide binding to their metal centers. Azide also inhibits the ATP hydrolase activity of the mitochondrial F-ATPase. Cyanine and azide are extremely toxic because they bind tightly to the cell's cytochrome oxidase complexes to stop electron transport, thereby greatly reducing ATP production and then leading to ROS production.

A sodium azide, stock solution (fresh solution) was made in culture medium at a final concentration of 10 mM, was filtered (with sterile syringe filter 0.2 µm cellulose acetate membrane, VWR international) before use and was then diluted at a final concentration of 10 µM, 1 mM and 10 mM. Cells were incubated for 3h, 6h, 24h and 48h.

2.2. PRE-TREATMENT WITH ANTIOXIDANTS

A pre-treatment with antioxidants was performed to investigate the involvement of ROS in peroxisome proliferation. This pre-treatment was performed 1h before the addition of the drugs (see Methods, Chapter 2.1.) with N-acetyl-cysteine (NAC), Vitamin C (ascorbic acid) and Vitamin E (α-tocopherol). The antioxidants remained in the culture medium until fixation (see Methods, Chapter 3.1.).

2.2.1. N-acetyl cysteine

N-acetyl cysteine (NAC) is a well known antioxidant GSH precursor (Kelly, 1998), which can be rapidly converted into reduced glutathione (GSH). It provides cysteine for glutathione synthesis (Han and Park, 2009) after uptake by the cells, thus serving as an intracellular reducing agent (Meister, 1991).

A NAC stock solution, (100 mM; always fresh) was made in cell culture medium. The used concentration was 10 mM (after pH neutralization and sterilization of the stock solution by filtration).

2.2.2. Ascorbic acid

Ascorbic acid (vitamin C) is water-soluble and has been shown to be a major antioxidant in human plasma (May, 1999; Frei et al., 1990). It prevents mainly lipid hydroperoxide formation in plasma lipoproteins, e.g. LDL (low density lipoprotein) by reducing α-tocopherol (α-TOH) radicals formed upon reaction with lipid peroxyl radicals (Sies et al., 1992). Intracellularly, in the aqueous phase, vitamin C and GSH act to protect the cell from oxidative damage (Meister, 1995). A vitamin C stock solution, (0.1%; always fresh) was made in cell culture medium. After pH neutralization and sterilization (by filtration) it was added to the cells at a final concentration of 0.01%.

2.2.3. Vitamin E

Vitamin E is a lipid-soluble vitamin present in biological membranes. It contains a hydroxyl group by which it reacts with unpaired electrons reducing it, e.g. peroxyl radicals (Nordberg and Arner, 2001). Vitamin E stock solution (50 mM; fresh or maximum storage for 1 day) was made in DMSO and added to the cells at a final concentration of 50 µM.

3. MORPHOLOGICAL STUDIES

3.1. INDIRECT IMMUNOFLUORESCENCE

Cells grown on glass coverslips were washed twice with 1x PBS, fixed with pre-warmed 4% paraformaldehyde (pH 7.4) for 20 min at RT (room temperature) and then washed three times with 1x PBS. Next, cellular membranes were permeabilized by incubation with 0.2% Triton-X 100 for 10 min at RT and the samples were blocked with 2% BSA. After blocking, the cells were washed 1-2 times in 1x PBS, and then incubated for 1h at RT with primary antibodies diluted in 1x PBS. After extensive washing in 1x PBS, cells were incubated with fluorescently labeled secondary antibodies diluted in 1x PBS (DαRb-Alexa 488 or DαM-TRITC). For staining of the nucleus, cells were incubated with Höchst 33258 for 2 min. To prepare the slides, the coverslips were washed one time in distilled water and mounted (after removal of excess water) in Mowiol 4-88 containing n-propyl galate as an anti-fading (Schrader et al., 1998b).

For staining of microtubules, the cells were fixed and permeabilized with ice-cold methanol at -20ºC for 30 min. Then, samples were blocked with 2% BSA and treated as described above. The slides were stored at 4ºC in a proper box for immunofluorescence slides and kept in the dark.

3.2. FLUORESCENCE MICROSCOPY

Samples were examined using an Olympus IX81 microscope (Olympus Optical, Hamburg, Germany) equipped with a PlanApo 100x/1.40 oil objective. Fluorescence images were acquired with an F-view II CCD camera (Soft Imaging System GmbH, Münster, Germany) driven by Soft imaging software. Digital images were optimized for contrast and brightness using appropriate software (Micrografx Picture Publisher (version 8); Soft Imaging Viewer and PowerPoint). For quantitative analysis of peroxisomal morphology, 200–300 cells per coverslip were examined and categorized as cells with spherical (0.1–0.3 µm) or tubular (2–5 µm in length) peroxisomes as described previously (Schrader et al., 1996a). The counting was made blind and in different areas of the coverslip (see Methods, Chapter 6.).

4. BIOCHEMICAL ANALYSIS

4.1. MEASUREMENT AND QUANTIFICATION OF ROS PRODUCTION INDUCED BY DIFFERENT STRESSORS

In order to detect and quantify ROS production and oxidative stress, a fluorescent based assay was established and developed in our group.

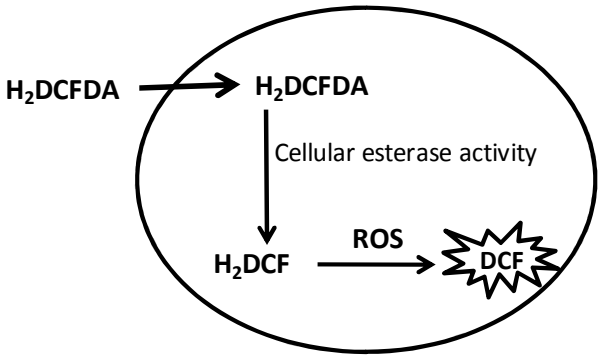

Figure 10. Oxidation of H_2DCFDA by ROS. H_2DCFDA, 2′, 7′-dichlorodihydrofluorescein diacetate; H_2DCF, dichlorofluorescein non fluorescent; DCF, dichlorofluorescein fluorescent (see Chapter I. 5.2.).

To establish this assay I cooperated with the group of Dr. Joaquín Jordan (Faculty of Medicine, University of Castilla-La Mancha, Albacete, Spain), and I spend some time in his laboratory. Furthermore, I was supported by Nina Bonekamp, a PhD student in our laboratory.

We used the sensitive fluorescent dye 2′, 7′-dichlorodihydrofluorescein diacetate (H_2DCFDA) to measure the production of reactive oxygen species (ROS), mainly hydrogen peroxide and hydroxyl radicals (Figure 10). H_2DCFDA freely enters the cell and is deacetylated by esterases to dichlorofluorescein (H_2DCF). This non-fluorescent product is then converted by ROS into the fluorescent DCF, which can easily be detected by measuring the fluorescence at 530 nm when excited at 485 nm (Figure 10) (Fernandez-Gomez et al., 2006; Perez-Ortiz et al., 2004).

During the establishment of the method in our laboratory, addition of H_2O_2 was used as a positive control for the presence of ROS. Thus, COS-7 cells were treated with increasing concentrations of H_2O_2 (100, 300, 500, 700 and 1000 µM). Furthermore, different concentrations of H_2DCFDA (5, 10 and 100 µM) and different incubation times (10, 20, 30 min) were tested as well as different cell culture plates. We were testing multiwell plates with black or transparent wells. All wells tested had a flat bottom,

transparent lid and were made of polystyrene. We finally selected 96-well culture plates with black wells which prevented fluorescence interference between neighboring wells. The following protocol for ROS measurement was determined:

Cells were seeded in 96-well culture plates (10^4 cells/well) and the day after were treated with the different stressors already tested by immunofluorescence (see Methods, Chapter 2.). At different time points, the medium was removed and the cells were washed one time with 1x PBS. The PBS was removed, the cells were incubated with H_2DCFDA (10 μM) and the fluorescence intensity was measured immediately during a period of 30 min (every 5 min) in a multifunctional microplate reader (TECAN i-control – infinite 200, Austria GmbH). An average of 4 to 6 wells per condition (untreated cells; cells incubated with the dye; a blank containing cell culture medium and dye; and H_2O_2 together with the dye as a positive control) was measured. A mean value for each condition was determined. A linear increase of fluorescence with time was plotted and used to calculate a linear regression. This was used to determine the average relative percentage of ROS production from at least 3 independent experiments. Results were expressed as mean ± S.D. values, and statistical analysis was performed as described (see Methods, Chapter 6.).

4.2. MEASUREMENT OF GLUTATHIONE (GSH) LEVELS

To verify the reduction of the levels of reduced GSH, another fluorescent based assay was established and developed in our group.

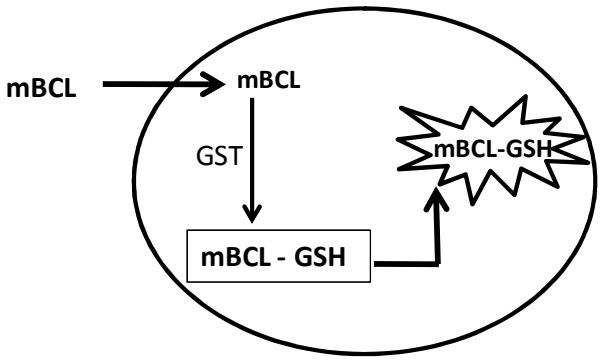

Figure 11. Determination of GSH levels using mBCL. mBCL, monoclorobimane; GST, glutathione-S-transferase; GSH, reduced glutathione.

This assay was developed in cooperation with the group of J. Jordan (Albacete, Spain). The intracellular levels of GSH were determined using monochlorobimane (mBCl) fluorescence. GSH is specifically conjugated to mBCl to form a fluorescent bimane-GSH adduct, in a reaction catalyzed by glutathione S-transferases (Figure 11). This conjugation reaction proceeds according to a first-order kinetic reaction and is followed by a second kinetic process that is many orders of magnitude slower and is thought to reflect the non-enzymatic reaction of mBCl with other intracellular thiols (Jordan et al., 2004; Fernandez-Gomez et al., 2006).

To establish this methodology in our group, a positive control for the depletion of GSH levels was made by treatment of the cells with increasing concentrations of BSO (50, 100, 500 and 1000 µM), a known GSH depletory drug, and also for different time periods of incubation (10, 20 and 30 min). A linear decrease of the GSH levels was expected with increasing concentrations of BSO and also with time. The following protocol for GSH quantification was determined:

Cells were seeded in 96-well culture plates (10^4 cells/well) and the day after were treated with the stressors described (see Methods, Chapter 2.). After different time points, the medium was removed and the cells were washed with 1x PBS and 100 µl of fresh Krebs buffer were added to each well. First a blank was measured (10 min) with Krebs buffer in a multifunctional microplate reader (TECAN i-control). After blank measurement the fresh Krebs buffer was removed and the cells were incubated with 100 µl of 160 µM mBCl. The fluorescence was immediately measured every 3 min during a period of 30 min (37ºC) at an excitation wavelength of 340 nm and emission wavelength of 460 nm. An average of 4 to 6 wells per condition (untreated cells; cells incubated with mBCL; no cells - just the cell culture medium and mBCL; and different concentrations of BSO with the dye) were measured. A mean value for each condition was determined. A decrease of fluorescence with time was plotted and used to calculate a linear regression. This was used to determine the average relative percentage of GSH from at least 3 independent experiments. Results were expressed as mean ± S.D. values, and statistical analysis was performed as described (see Methods, Chapter 6.).

5. CELL VIABILITY

In order to analyze the cell viability after drug treatment a cell viability assay was performed through a MTT assay using 3-[4, 5-dimethylthiazol-2-yl]-2, 5 diphenyltetrazolium bromide (MTT).

This assay is a colorimetric approach that assesses cell viability by measuring mitochondrial function. MTT is a yellow colored tetrazolium salt that is reduced to a purple formazan (by the active cells).

Twenty four hours after drug treatment 100 µl of 0.5 mg/ml of MTT stock solution were added to cells seeded in 96 well culture plates. The samples were incubated at 37ºC and the purple formazan crystals were allowed to develop for 45 min (Perez-Ortiz, 2004). The MTT-containing medium was removed and 100 µl of DMSO were added to each well to dissolve the formed crystals. The absorbance was measured in a spectrophotometer (luminescence-spectrophotometer LS50B; Perkin-Elmer, Wellesley, MA, USA) at excitation wavelength of 545 nm and an emission wavelength of 680 nm. Cell viability analysis was complemented by morphological studies and cell counting (data is not shown).

6. STATISTICAL ANALYSES

For the morphological studies (see Methods, Chapter 3.), usually two coverslips per preparation were analyzed and three to five independent experiments were performed. For biochemical analysis (see Methods, Chapter 4.), four wells in a 96-well cell culture dish per each condition (untreated and treated cells) and per time of measurement (3h, 6h, 9h and 24h) were analyzed and at least three independent experiments were performed.

Significant differences between experimental groups (both for morphological studies and biochemical analyses) were detected by analysis of variance for unpaired variables using Microsoft Excel software. Data are presented as means ± S.D., with an unpaired *t* test used to determine statistical differences. *p* values < 0.05 were considered as significant, and *p* values < 0.01 were considered as highly significant.

IV. RESULTS

IV. RESULTS

It is now well established that peroxisomes have a key role in both the production and scavenging of reactive oxygen species (ROS). They are generators of oxygen stress but also a source of ROS signal mediators. Previous work from our group has demonstrated that oxidative stress (by external stimuli) induces morphological alterations of the peroxisomal compartment, which are linked to peroxisome proliferation (see Chapter I. 6.).

To examine the effect of different ROS-producing stresses on peroxisomal dynamics, a suitable cell culture model had to be established. In the beginning three different cell lines (HepG2, COS-7-GFP-PTS1 and COS-7 cells) (see Methods, Chapter 1.1.) were analyzed by immunofluorescence microscopy to select a model with an elaborate and dynamic peroxisomal compartment suitable for induction of proliferation and the examination of peroxisomal dynamics. The cell culture model selected was the COS-7 cell line because these cells showed a good response to the stressors applied, as well as good viability and cell growth (based on morphological observations and cell viability measurements (see Methods, Chapter 5.)). Furthermore, morphological changes of the peroxisomal compartment could easily be visualized and quantitated due to the flatness of the cells and the very well defined peroxisome morphology. An example of spherical and tubular, elongated peroxisomes is presented in Figure 12.

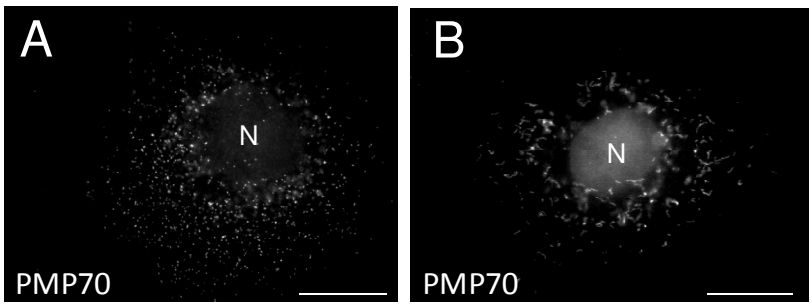

Figure 12. Peroxisome morphology in COS-7 cells shown by indirect immunofluorescence with an antibody to PMP70, a marker for the peroxisomal membrane, and DαRb-Alexa 488 as a secondary antibody. Peroxisomes are highly dynamic organelles with large plasticity, and spherical (A) as well as elongated-tubular (B) structures appear under normal cell culture conditions. N (Nucleus), Bars (20 µm).

The stimuli tested were a cytoskeleton-active drug (nocodazole), inhibitors of mitochondrial respiration (rotenone and sodium azide) and a GSH-depletory drug (L-Buthionine Sulfoximine). The morphological alterations of the peroxisomal compartment (as well as of mitochondria) were visualized and quantified by fluorescence microscopy.

Nocodazole is known to induce tubular peroxisomes (Schrader, 1996), therefore this drug was the first to be analyzed as a control for peroxisome elongation in COS-7 cells. A general workflow for the experiment with the different stressors is shown in Figure 13.

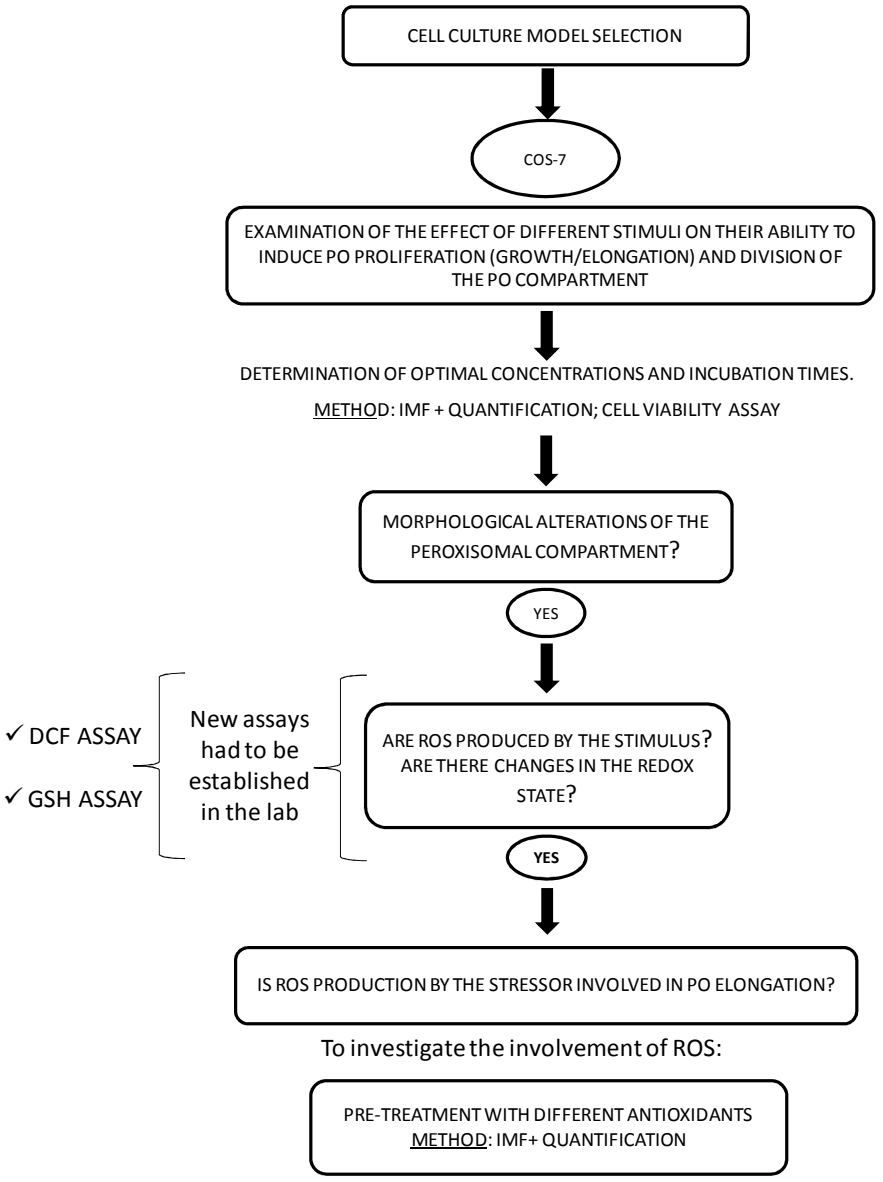

Figure 13. Experimental workflow. IMF, immunofluorescence

This approach required the development of new assays that were not established in our laboratory, which are fluorescent-based assays to quantify ROS production and GSH levels. To establish these assays I cooperated with the group of Dr. Joaquín Jordán (Faculty of Medicine, University of Castilla-La Mancha, Albacete, Spain) and spend some time in his laboratory. Furthermore, I cooperated with Nina Bonekamp, a PhD student in our laboratory (see Methods, Chapters 4.1. and 4.2.).

1. THE EFFECT OF NOCODAZOLE ON THE PEROXISOMAL COMPARTMENT

1.1. NOCODAZOLE INDUCES PEROXISOME ELONGATION AND CLUSTERING

COS-7 cells (see Methods, Chapter 1.1.) were seeded on coverslips and after 24h were treated with 33.2 µM of nocodazole for 3, 6 and 24h (see Methods, Chapter 2.1.1.). At each time point cells were fixed with 4% PFA and prepared for immunofluorescence by permeabilization with 0.2% Triton-X 100 (see Methods, Chapter 3.1.). Peroxisomes were labeled with an antibody to PMP70 (a peroxisomal ABC transporter in the membrane). Microtubules were stained with an antibody to α-tubulin, and mitochondria with an antibody to TOM20 (a protein from the mitochondrial outer membrane involved in protein transport) (see Materials, Chapter 1. Table 3).

By fluorescence microscopy, 200-300 cells per coverslip were categorized as cells with spherical (0.1–0.3 µm) or tubular (2–5 µm in length) peroxisomes in controls (containing DMSO) and in nocodazole treated cells (see Methods, Chapter 3.2.). Simultaneously to peroxisome labeling, microtubules and mitochondria were stained. Images showing the morphological alterations of peroxisomes, mitochondria and microtubules are shown in Figure 14.

In cells cultured under normal, untreated conditions, peroxisomes are mainly of spherical shape (with about 10 – 20% of the cells exhibiting tubular peroxisomes) (Figure 14 A and Figure 15). The mitochondrial compartment is composed out of filamentous and

bulbous structures in COS-7 cells (Figure 14 F). Microtubules form a radial array originating from the MTOC (Microtubule Organization Center) (Figure 14 D). After nocodazole treatment microtubules were completely depolymerized as expected, and a cytoplasmic staining was observed (Figure 14 E). Mitochondria in nocodazole treated cells appeared fragmented (Figure 14 G), and peroxisomes were largely elongated (Figure 14 B). In some cells also clustering of peroxisomes was observed (Figure 14 C).

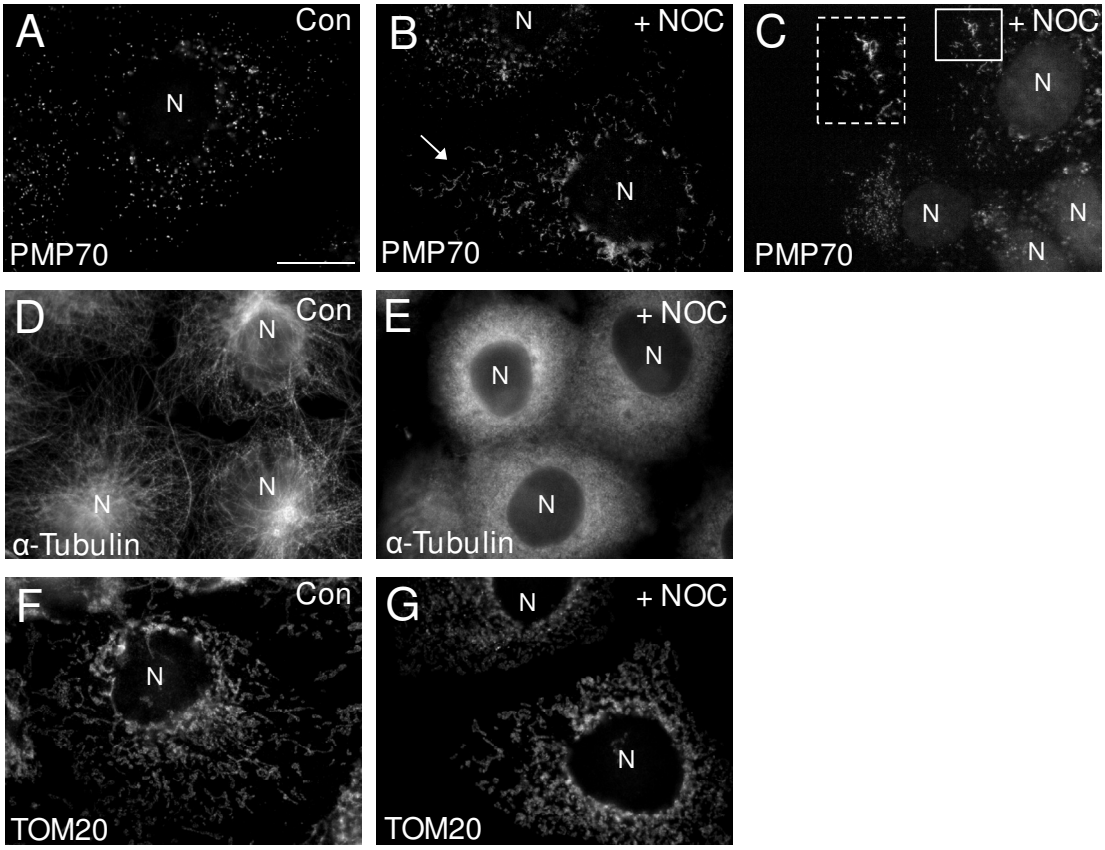

Figure 14. **Microtubule-depolymerization induces peroxisome elongation.** COS-7 cells were treated with the microtubule-depolymerizing drug nocodazole (+NOC) or solvent (Con) for 3, 6 and 24h (see Methods, Chapter 2.1.1) and processed for immunofluorescence microscopy using antibodies to PMP70 (A-C), a peroxisomal membrane protein, α-tubulin (D, E) or TOM20 (F, G), a mitochondrial outer membrane marker. Note the elongated, tubular peroxisomes in (B), arrow, and the clustered peroxisomes in (C) in contrast to the spherical ones in (A). Boxed regions in C show a higher magnification view. Nocodazole treatment results in complete depolymerization of microtubules (E) and in fragmentation of mitochondria (G). N (Nucleus). Bar (20 μm).

As shown in Figure 15, the most pronounced effect on peroxisome dynamics occurred after 6h of nocodazole treatment showing 70 ± 7.44% of tubular peroxisomes in cells treated in contrast to 20 ± 4.23% in controls. After 3 and 24h there were no statistically significant differences between the cells treated and the controls. However, this is explained by the fact that the elongated peroxisomes start to divide giving rise to

spherical organelles (Schrader et al., 1996a) (see Chapter I. 3.). In summary, these observations show that peroxisomes respond to microtubule depolymerization with an elongation/tubulation (growth and division) of the peroxisomal compartment. In contrast, mitochondria are observed to fragment in the absence of microtubules. These observations confirm earlier studies on the effect of microtubule-active drugs on peroxisomes (Schrader et al., 1996a). However, the physiological significance of peroxisome elongation after microtubule depolymerization and the signaling pathways involved are largely unknown.

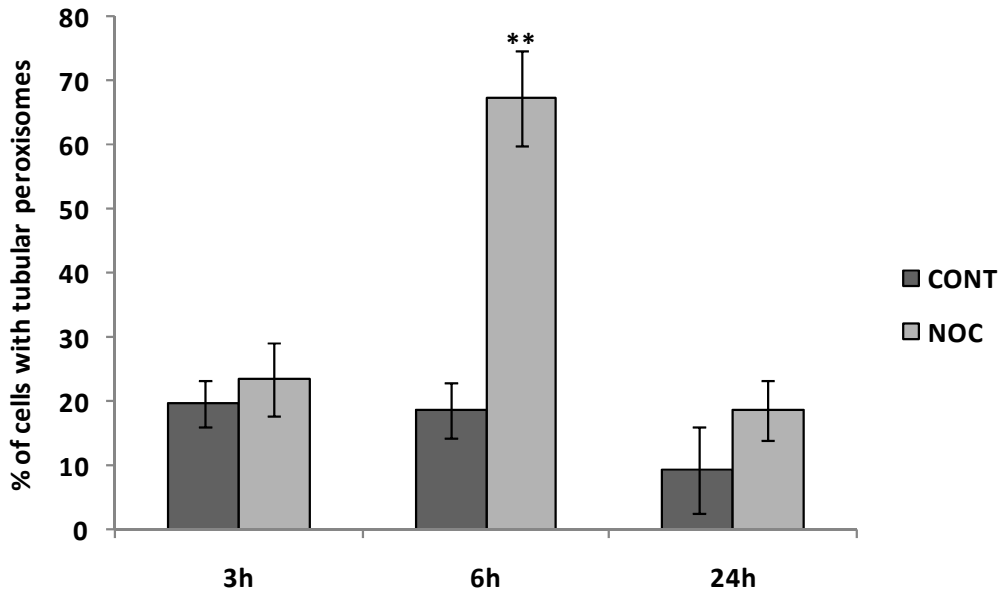

Figure 15. Influence of the microtubule-depolymerizing drug nocodazole on peroxisome morphology in COS-7 cells. Cells were treated for 3, 6 and 24h with 33.2 µM of nocodazole (NOC). Data are from 3 to 6 independent experiments and are expressed as mean ± S.D. ** $P < 0.01$ when compared to control.

1.2. TREATMENT WITH NOCODAZOLE INDUCES AN INCREASE IN INTRACELLULAR ROS LEVELS

To investigate if the elongation of the peroxisomal compartment after depolymerization of microtubules is related to ROS production, intracellular ROS levels were measured after treatment of COS-7 cells with nocodazole.

A fluorescent based assay was established for the quantification of ROS production (see Methods, Chapter 4.1. for details). In the developed assay, the properties of the fluorescent dye 2',7'-dichlorodihydrofluorescein diacetate (H_2DCFDA) were exploited (Figure 10). The sensitive fluorescent dye H_2DCFDA freely enters the cell and is deacetylated by esterases to dichlorofluorescein (H_2DCF). This non-fluorescent product is then converted by reactive oxygen species into the fluorescent DCF, which can easily be monitored by measuring the fluorescence emitted at 530 nm when excited at 485 nm (see Methods, Chapter 4.1.).

ROS production was quantified in controls (containing DMSO) and in cells treated with nocodazole (Figure 16). ROS were measured for each condition and time point with an average number of 4-6 wells. For data presentation, means and standard deviation of the values from each experiment were calculated and presented as percentage of control. Six hours after nocodazole treatment, there was a significant increase in ROS production.

To verify if antioxidants can block ROS production, an antioxidant pre-treatment was performed. The cells were pre-incubated with the antioxidant NAC, VIT E and VIT C one hour before nocodazole addition (Figure 16). All antioxidants applied significantly reduced ROS production when compared to controls (Figure 16).

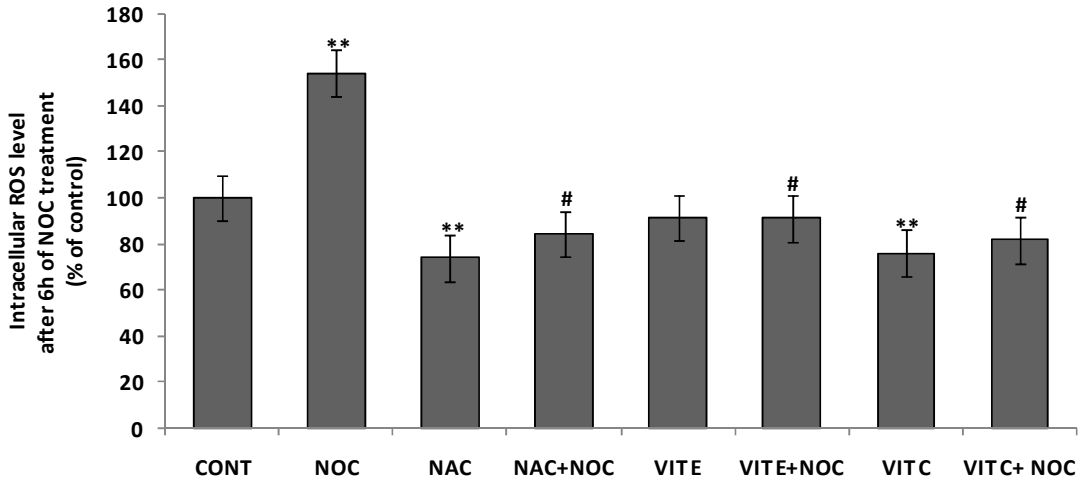

Figure 16. Intracellular ROS production induced by nocodazole in COS 7 cells. ROS levels were quantified in control cells (CONT), in cells treated with nocodazole (NOC) (33.2 μM), in cells treated with the antioxidant alone, and in cells pretreated (1h before addition of NOC) with the antioxidants N-Acetyl cystein (NAC) (10 mM), Vitamin E (VIT E) (50 μM) and Vitamin C (VIT C) (0.01 %). Levels were quantified 6h after nocodazole addition. Data are expressed as percentage of control (mean ± S.D.) and are from 3 independent experiments. ** highly significant to control ($P < 0.01$); # significant to NOC, ($P < 0.05$).

From the data above we can conclude that nocodazole treatment induces the production of ROS, and all antioxidants tested were able to reduce the increase in ROS production induced by nocodazole.

1.3. PEROXISOME ELONGATION INDUCED BY MICROTUBULE-DEPOLYMERIZATION IS NOT DEPENDENT ON ROS PRODUCTION

To elucidate if ROS are responsible for peroxisome elongation, an antioxidant pre-treatment was performed 1h before addition of nocodazole. The antioxidants used were NAC, VIT E and VIT C (see Methods, Chapter 2.2.). The analysis of the effect of the antioxidants was just performed 6h after nocodazole treatment since it was the time point with the maximum number of cells with tubular peroxisomes. Figure 17 shows the quantification of the effect of antioxidants on the tubulation of peroxisomes induced by nocodazole. Interestingly, none of the antioxidants tested was able to inhibit the elongation of the peroxisomal compartment in response to nocodazole (see above, Figure 15). There were no differences in peroxisome morphology between the cells treated with nocodazole and antioxidants or nocodazole alone. As shown by the statistical analysis

(Figure 17), antioxidants were not able to block the peroxisome elongation induced by nocodazole, indicating that the ROS increase was not the major cause for peroxisomal elongation induced by MT-depolymerization.

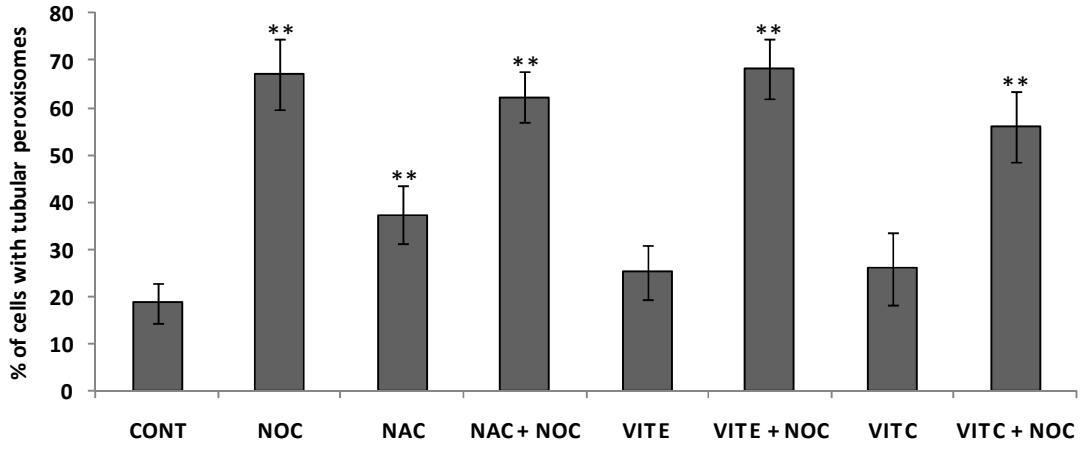

Figure 17. Effect of antioxidants on the elongation of peroxisomes induced by nocodazole. Antioxidants (NAC, 10 mM; VIT E, 50 µM; VIT C, 0.01%) were added or not to COS-7 cells 1h before nocodazole (NOC) treatment. Antioxidants were kept in the cell culture medium during nocodazole treatment. Cells were also treated with antioxidants alone for the same period of time. 6 hours after addition of nocodazole, cells were fixed and prepared for immunofluorescence. Data are from 3 to 6 independent experiments and are expressed as mean ± S.D. ** highly significant to control ($P < 0.01$). There are no differences when compared to cells treated with nocodazole.

Nocodazole treatment affected the morphology of both peroxisomes and mitochondria (Figure 14). Although nocodazole induced ROS production, which was inhibited by antioxidants (Figure 16), the antioxidants were not able to block peroxisome elongation (Figure 17). Furthermore, the antioxidants neither inhibited mitochondrial fragmentation nor microtubule depolymerization induced by nocodazole (data not shown).

1.4. NOCODAZOLE DOES NOT INDUCE ALTERATIONS OF THE GSH LEVEL

Depolymerization of microtubules produced an increase in ROS levels inside the cell which might also lead to cellular alteration in the redox state. To analyze the redox state in the cell, GSH levels were measured with a fluorescent-based assay using

monochlorobimane (mBCl). Once added to the cell culture medium, mBCL is able to penetrate the plasma membrane and inside the cell, GSH can specifically conjugate to mBCl to form a fluorescent bimane-GSH adduct in a reaction catalyzed by glutathione S-transferases (see Methods, Chapter 4.2., Figure 11). The GSH levels of control and nocodazole-treated cells were quantified after 3, 6, 9 and 24h. No statistically significant differences to control levels were found (Figure 18).

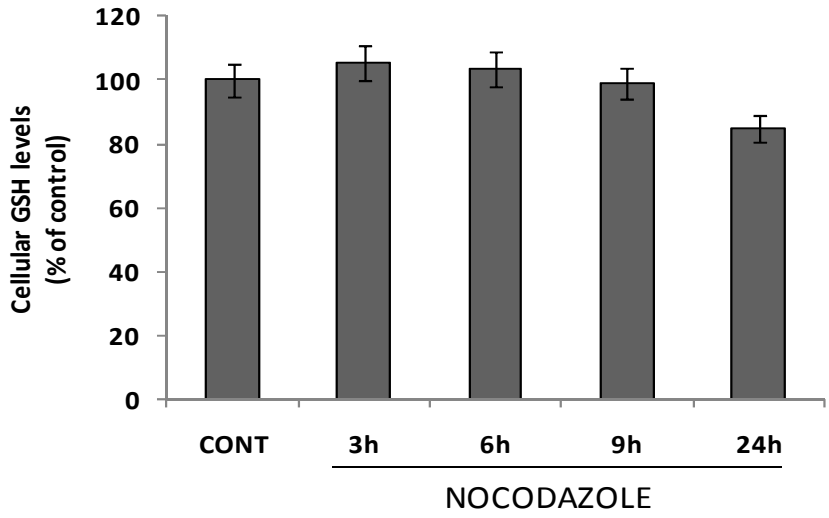

Figure 18. Effect of nocodazole on GSH levels in COS-7 cells. Quantification of cellular GSH levels was performed after 3, 6, 9 and 24h of NOC addition. Data are from 3 independent experiments and are expressed as mean ± S.D. There are no significant differences to the control.

Although nocodazole treatment induced ROS production, the GSH levels inside the cell were not grossly affected during the time intervals measured. This indicates that the redox state within the cells was not predominantly altered during treatment with nocodazole.

2. THE EFFECT OF BSO ON THE PEROXISOMAL COMPARTMENT

2.1. BSO INDUCES PEROXISOME ELONGATION

Next, the cellular effect of L-Buthionine Sulfoximine (BSO), a compound which changes the redox state in the cell irreversibly inhibiting the rate-limiting enzyme of GSH synthesis (γ-glutamylcysteine synthase) (Griffith and Meister, 1979) was analyzed in regard to its capacity to induce ROS production and the possible resulting effect on peroxisome elongation/proliferation.

For treatment with BSO, cells were seeded on coverslips and after 24h 100 µM of BSO were added. Then, the cells were incubated for 3, 6, 9, 12 and 24h (see Methods, Chapter 2.1.2.). After each time point, cells were fixed with 4% PFA and prepared for immunofluorescence (see Methods, Chapter 3.1.). Peroxisomes were labeled with an antibody to PMP70 and mitochondria with an antibody to TOM20 (see Materials, Chapter 1., Table 3). Afterwards, peroxisome morphology was evaluated by fluorescence microscopy, and for statistical evaluation, 200-300 cells per coverslip were categorized as cells with spherical (0.1-0.3 µm) or tubular peroxisomes (2-5 µm) in control and BSO-treated cells.

In comparison to control cells (Figure 19 A), where peroxisomes were mainly of spherical shape, BSO-treated cells displayed a primarily elongated morphology of peroxisomes with the induction of long tubular peroxisomes (Figure 19 C). On the other hand, mitochondria in control as well as treated cells appeared as filamentous structures (Figure 19 B-D), thus there was no effect of BSO on mitochondrial morphology.

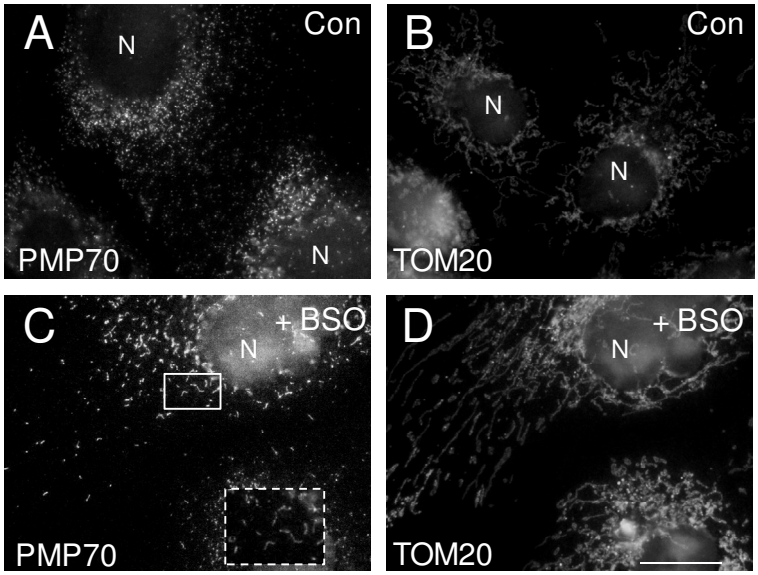

Figure 19. Depletion of cytosolic GSH levels induces peroxisome elongation. COS-7 cells were treated with 100 µM of BSO for 3, 6, 9, 12 and 24h (see Methods, Chapter 2.1.2.) and examined by immunofluorescence microscopy using a PMP70 antibody to peroxisomes (A, C) and TOM20 to mitochondria (B, D). 9h after BSO treatment peroxisomes presented an elongated morphology (C) in contrast to the spherical ones in untreated cells (A). Boxed regions in C show higher magnification view. GSH depletion does not cause morphological changes of mitochondria after BSO treatment (D) when compared with untreated cells (B). N (Nucleus). Bar (20 µm).

The statistical evaluation of tubular peroxisomes after BSO treatment is shown in Figure 20. The major effect on peroxisome elongation occurred after 9h of BSO exposure. After 3h to 9h of treatment, there was already an increase in tubular peroxisomes indicating that peroxisomes respond to this GSH-depletory drug; after 9h to 24h the number of cells with tubular peroxisomes decreased; most likely elongated peroxisomes start to divide giving rise to new, spherical organelles.

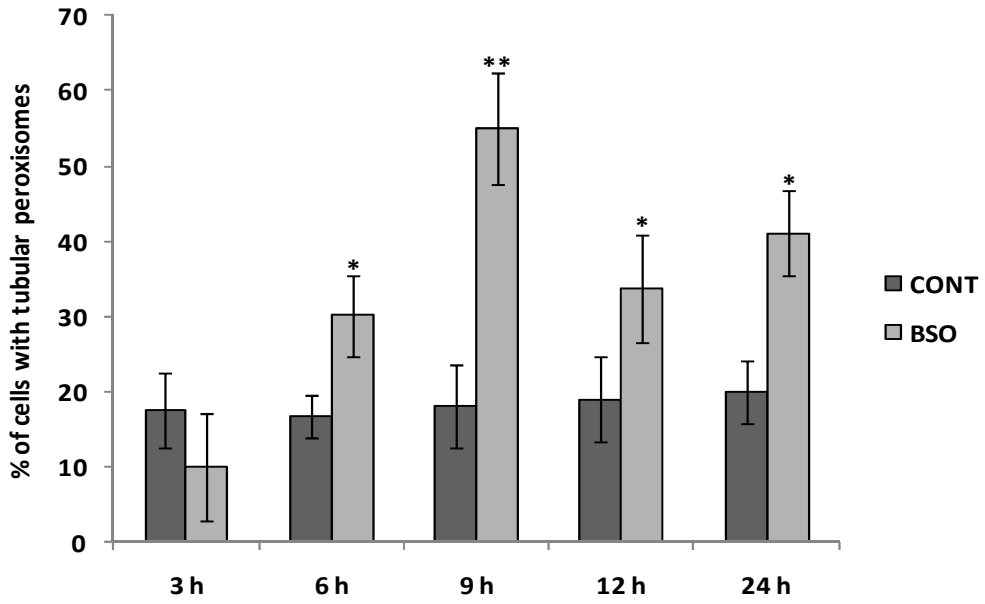

Figure 20. Influence of the GSH-depletory drug L-Buthionine Sulfoximine (BSO) on peroxisome morphology in COS-7 cells. Cells were treated for 3, 6, 9, 12 and 24h with 100 µM of BSO. Data are representative for 3 to 6 independent experiments and are expressed as mean ± S.D. ** highly significant ($P < 0.01$) and * significant ($P < 0.05$) to control.

2.2. BSO DEPLETES CELLULAR GSH LEVELS IN COS-7 CELLS

Glutathione (GSH) is a major component of the antioxidant defence system of mammalian cells being a critical component of the cellular antioxidant defense system and in the maintenance of the cellular redox potential (Jos et al., 2009). BSO is a well known GSH-depletory drug – acting by inhibition of γ-glutamyl cysteine synthase (γ-GCS) an essential enzyme of GSH synthesis, hence modulating the cellular redox state.

The cellular GSH levels were quantified by means of mBCL assay using a 96-well plate (see Methods, Chapter 4.2.) in untreated cells and cells treated with 100 µM of BSO, for 3, 6, 9 and 24h.

After BSO treatment, there was an early decline (3h) in cellular reduced glutathione levels that further decreased until 9h after BSO addition down to 33 ± 8.16%. Reduced GSH levels rose up again slightly after 24h of BSO addition (55 ± 6.93%) (Figure 21).

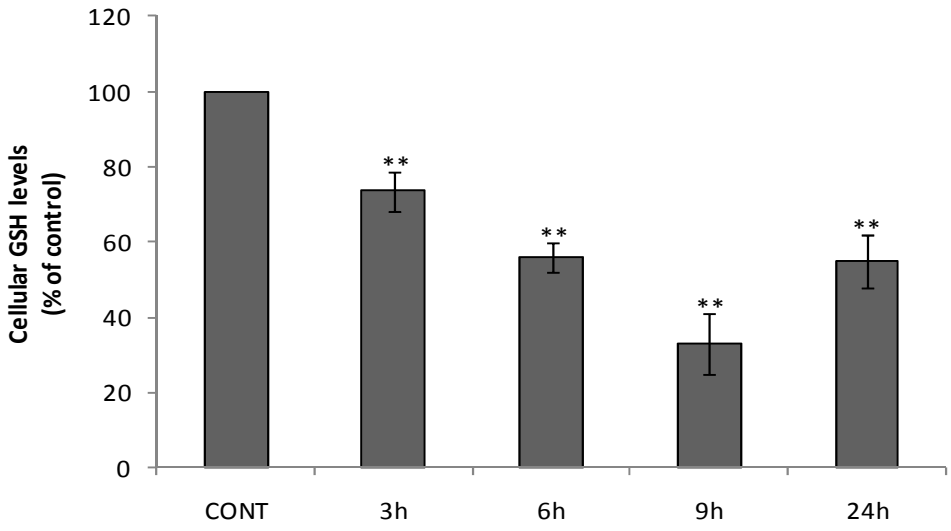

Figure 21. Effect of L-Buthione Sulfoximine (BSO) on GSH levels in COS-7 cells. Quantification of cellular GSH levels was performed after 3, 6, 9 and 24h of BSO addition. Data are from 3 independent experiments and are expressed as mean ± S.D. ** highly significant ($P < 0.01$) when compared to control.

2.3. DEPLETION OF GSH LEVELS BY BSO INDUCES ROS PRODUCTION

To examine if the elongation of the peroxisomal compartment after depletion of GSH is related to ROS production, intracellular ROS levels were measured after 9 and 24h of BSO treatment through the DCF assay (see Methods, Chapter 4.1.). ROS were measured and quantified in 3 independent experiments, with measuring for each condition and time point an average number of 4-6 wells. For data presentation, means and standard deviation of the values from each experiment were calculated and related to the control and presented as percentage of control.

As shown in the Figure 22, BSO increases ROS production after 9 (195 ± 3.5%) and 24 hours (218 ± 7%).

An antioxidant pre-treatment was performed 1h before BSO addition to verify if the antioxidants N-acetyl cysteine (NAC), Vitamin E (VIT E) and Vitamin C (VIT C) were able to reduce ROS production (Figure 22). All the antioxidants were able to decrease the ROS produced by BSO, both after 9 and 24h.

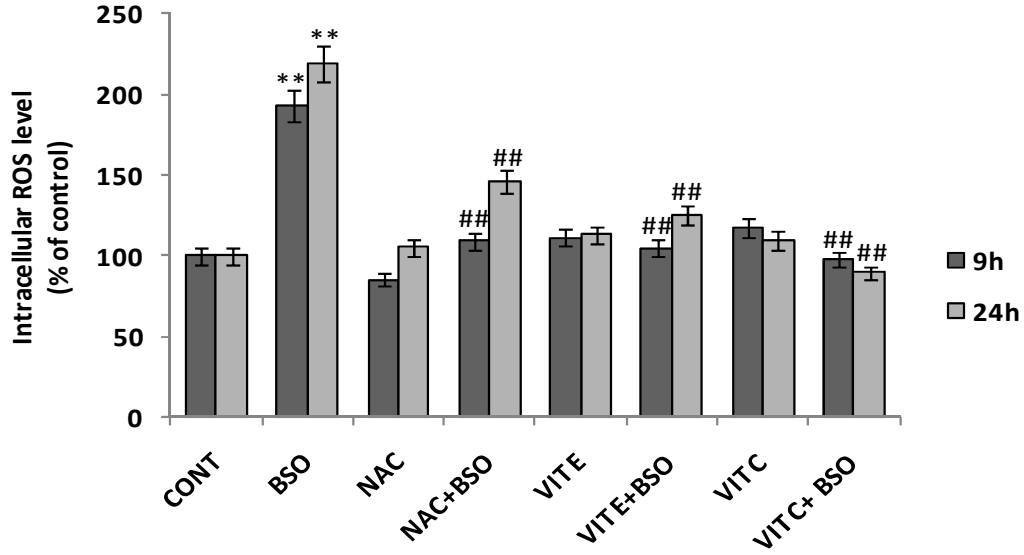

Figure 22. Intracellular ROS production induced by L-Buthionine Sulfoximine (BSO) in COS 7 cells. ROS levels were quantified in control cells (CONT), cells treated with BSO (100 µM), cells treated with the antioxidant alone, and also cells pretreated (1h before addition of BSO) with the antioxidants N-Acetyl cysteine (NAC) 10 mM), Vitamin E (VIT E) (50 µM) and Vitamin C (VIT C) (0.01%). Data are derived from 3 independent experiments and are expressed as percentage of control (mean ± S.D). ** highly significant to control ($P < 0.01$); ## highly significant to BSO ($P < 0.01$).

The decline in cellular glutathione (Figure 21) was followed by an increase in ROS production (Figure 22) which was reduced by NAC, VIT E and VIT C.

2.4. ANTIOXIDANT PRETREATMENT INHIBITS PEROXISOME ELONGATION INDUCED BY BSO

To clarify if ROS are responsible for peroxisome elongation in response to BSO, cells seeded on coverslips were treated with the antioxidants NAC and VIT E 1h before addition of BSO. The percentage of cells with tubular peroxisomes was quantified after 9 and 24h of BSO treatment (Figure 23). NAC is a well known antioxidant GSH precursor (Kelly, 1998), which can be rapidly converted into reduced glutathione (GSH) because it provides cysteine for glutathione synthesis. It thus serves as an intracellular reducing agent after uptake into the cell (Meister, 1991). However, metabolism of NAC to GSH requires glutamate-cysteine ligase [GCS; formally known as γ-glutamylcysteine synthetase (γ-GCS)], the enzyme that is inhibited by BSO. Thus, NAC is not able to block peroxisome elongation induced by BSO (Figure 23) (although it was able to reduce ROS production; maybe NAC is not so efficient in preventing morphological alterations of peroxisomes as the other antioxidants, at least in COS-7 cells). On the other hand, VIT E has a different mechanism of action, independent of the GSH mechanism, and was able to reduce peroxisome elongation. The effect of the antioxidants on peroxisome elongation is shown in Figure 23.

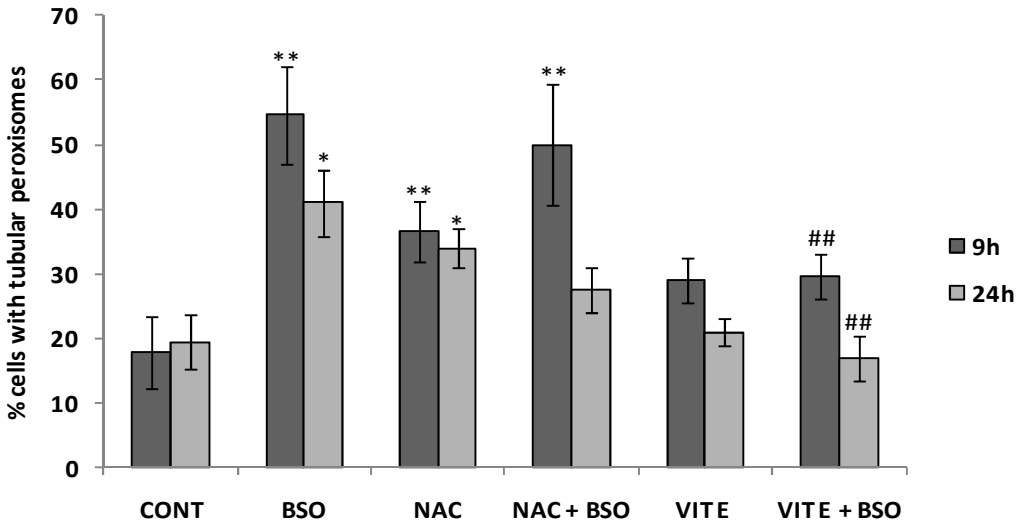

Figure 23. Effect of antioxidants on the elongation of peroxisomes induced by L-Buthionine Sulfoximine (BSO). Antioxidants (NAC, 10 mM; VIT E, 50 µM) were added or not to COS-7 cells 1h before BSO treatment. Antioxidants were kept in the cell culture medium during all the exposure time. Cells were also treated with antioxidants alone for the same period of time. 9 and 24h after BSO addition, cells were fixed and prepared for immunofluorescence microscopy. Data are from 3 to 6 independent experiments and are expressed as mean ± S.D. ** highly significant, $P < 0.01$; * significant, $P < 0.05$ when compared to controls. ## highly significant, $P < 0.01$ when compared to BSO.

3. EFFECTS OF INHIBITORS OF MITOCHONDRIAL RESPIRATION ON THE PEROXISOMAL COMPARTMENT

3.1. ROTENONE INDUCES PEROXISOME ELONGATION

Next I examined whether inhibitors of the mitochondrial respiratory chain known to produce ROS exhibit an effect on peroxisome elongation/proliferation. The first compound tested was rotenone, a well known inhibitor of complex I.

Rotenone treatment was performed 24h after seeding of the cells on coverslips. Different concentrations of rotenone (100 nM, 1 µM, 10 µM and 100 µM) were tested as well as two incubation times, 6 and 24h (see Methods, Chapter 2.1.3.). After 6 and 24h cells were fixed with 4% PFA and prepared for immunofluorescence (see Methods, Chapter 3.1.) Peroxisomes were labeled with an antibody to PMP70 and mitochondria with an antibody to TOM20 (see Materials, Chapter 1., Table 3). Afterwards cells were evaluated by fluorescence microscopy and for statistical evaluation 200-300 cells per coverslip were classified as cells with spherical (0.1-0.3 µm) or tubular (2-5 µm) peroxisomes in controls (containing DMSO) and in cells treated with rotenone.

Even at the lowest concentration (100 nM), rotenone induced morphological alterations in both peroxisomes and mitochondria (Figure 24). Whereas after rotenone treatment mitochondria appeared fragmented (Figure 24 E), peroxisomes appeared highly elongated (Figure 24 B). In samples treated with the highest concentration of rotenone (100 µM) a peroxisomal clustering was observed in some cells (Figure 24 C).

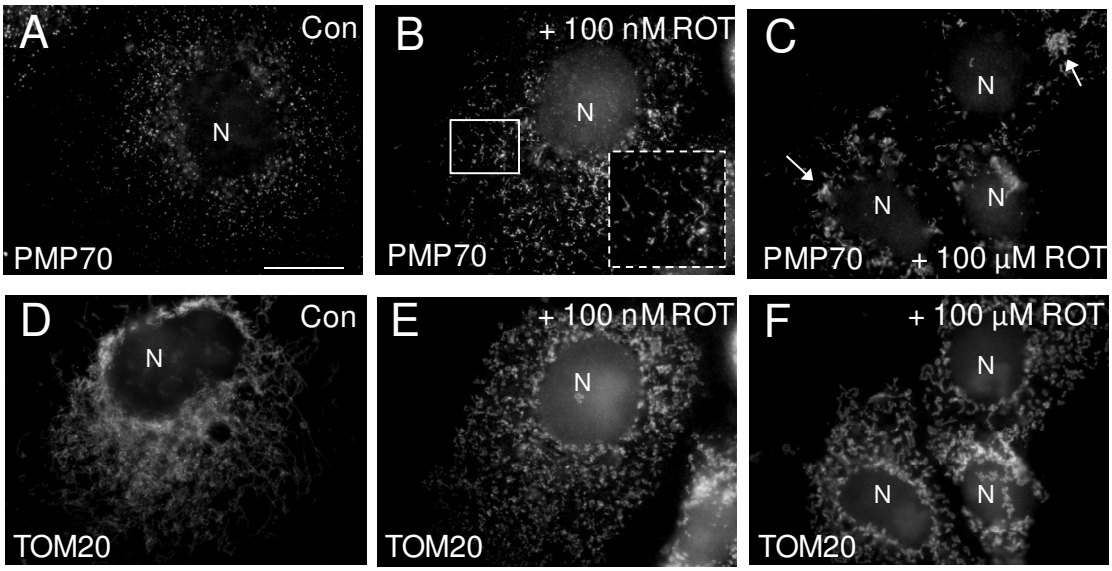

Figure 24. Rotenone induces peroxisome elongation and mitochondrial fragmentation. COS-7 cells were treated with rotenone (+ROT) for 6 and 24h (see Methods, Chapter 2.1.3.1.) and processed for immunofluorescence microscopy using antibodies directed to PMP70 (A-C) and to TOM20 (D-F). Note the elongated tubular peroxisomes in (B) and the clustering formation of peroxisomal clusters (arrows) in (C) in contrast to controls (A). Boxed regions in B show higher magnification view. Rotenone treatment results in a fragmentation of mitochondria (E, F). N (Nucleus), Bar (20 µm).

A statistical quantification of induction of tubular peroxisomes after rotenone treatment is displayed in Figure 25. The percentage of cells with tubular peroxisomes increased with rising rotenone concentrations, both after 6 and 24h.

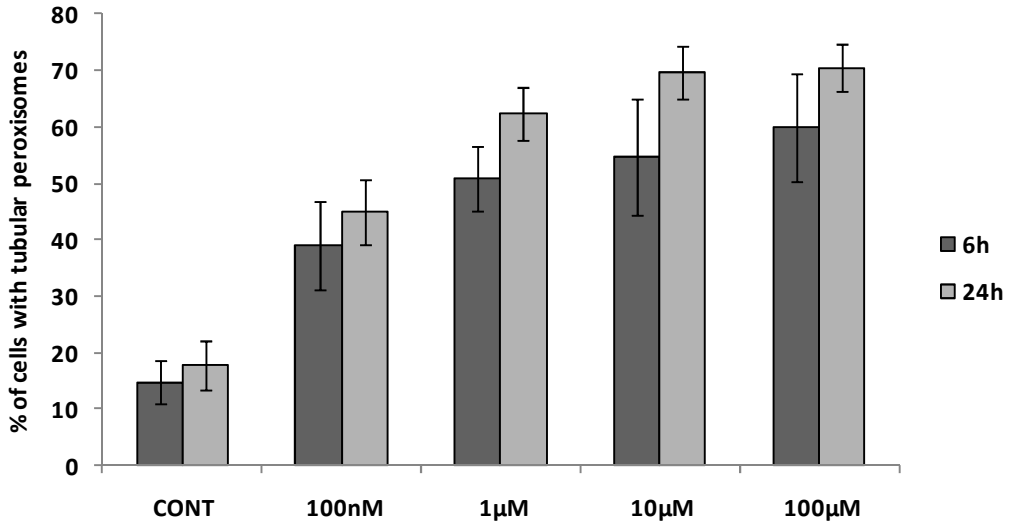

Figure 25. Effect of rotenone on peroxisome elongation. COS-7 cells were treated for 6 and 24h with different concentrations of rotenone. Data are from 3 to 6 independent experiments and are expressed as mean ± S.D. $P < 0.01$ for all groups.

3.2. ROS ARE PRODUCED IN COS-7 CELLS AFTER ROTENONE TREATMENT

Rotenone interferes with the mitochondrial electron transport chain, by inhibiting the transfer of electrons from iron-sulfur centers in complex I to ubiquinone (Figure 9). This prevents NADH from being converted into usable cellular energy (ATP) and consequently leads to ROS production. To examine if peroxisome elongation is the consequence of rotenone-dependent ROS production, intracellular ROS levels were quantified in cells under control conditions and after treatment with the lowest rotenone concentration (100 nM). ROS were measured by the DCF assay (see Methods, Chapter 4.1.) in 3 independent experiments with measuring for each condition and time point an average number of 4-6 wells. For data presentation, means and standard deviation of the values from each experiment were calculated and related with controls. Data are presented as percentage of control.

As displayed in Figure 26, rotenone increases ROS production in COS-7 cells after 6h (276 ± 6%) and 24h (414 ± 18%) when compared to control conditions.

An antioxidant pre-treatment was carried out 1h before rotenone addition in order to verify that the antioxidants were able to reduce ROS produced by rotenone. All antioxidants were able to reduce ROS produced by rotenone after 6 and 24h (Figure 26).

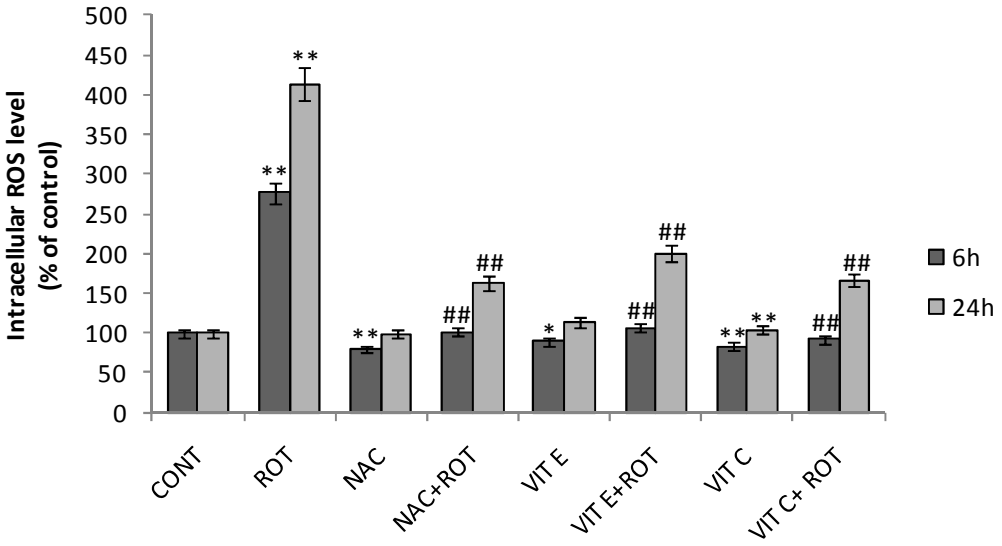

Figure 26. Intracellular ROS production induced by rotenone in COS 7 cells. ROS levels were quantified in control cells (CONT), cells treated with rotenone (ROT) (100 nM), cells treated with the antioxidant alone, and also cells pretreated (1h before addition of ROT) with the antioxidants N-Acetyl cysteine (NAC) (10 mM), Vitamin E (VIT E) (50 µM) and Vitamin C (VIT C) (0.01%). Data are expressed as percentage of control (mean ± S.D.) and are from 3 independent experiments ** highly significant to control ($P < 0.01$); * significant to control ($P < 0.05$); ## highly significant to ROT ($P < 0.01$).

3.3. ROS GENERATED BY MITOCHONDRIA ARE NOT INVOLVED IN PEROXISOME ELONGATION INDUCED BY ROTENONE

To elucidate if ROS produced by mitochondria are responsible for elongation of the peroxisomal compartment in response to rotenone, cells were treated 1h before rotenone addition with the antioxidants NAC and VIT E (see Methods, Chapter 2.2.). Different concentrations of rotenone (100 nM, 1 µM and 100 µM) were analyzed together with the antioxidant treatment after 6 and 24h (Figure 27). Interestingly, none of the antioxidants tested was able to block the peroxisome elongation induced by rotenone neither after 6 nor 24h, indicating that the increase in ROS levels was not the main cause for peroxisomal elongation induced by rotenone.

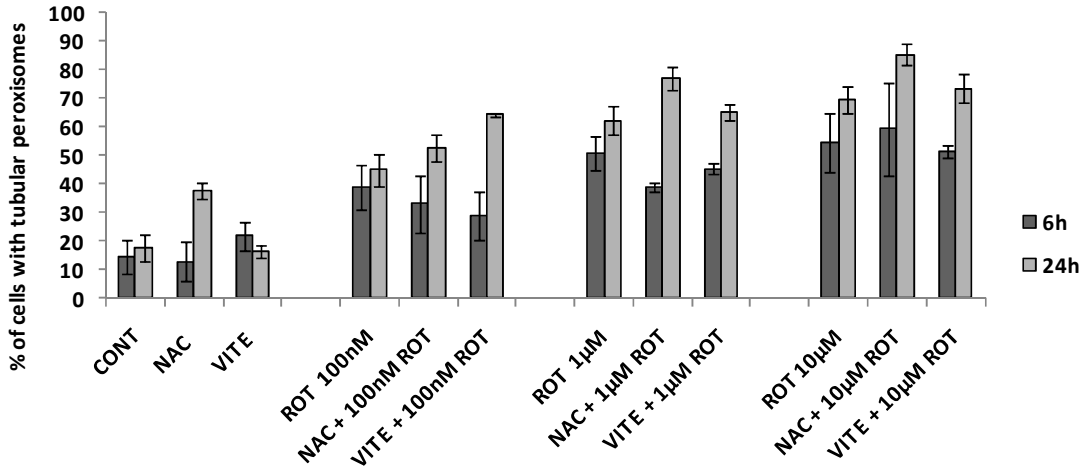

Figure 27. Effect of antioxidants on the elongation of peroxisomes induced by rotenone. Antioxidants (NAC, 10 mM and VIT E, 50 µM) were added or not to COS-7 cells 1h before rotenone (ROT) addition. We tested different concentrations of ROT (100 nM, 1 µM and 10 µM) together with antioxidants and also control cells (CONT). Antioxidants were kept in the cell culture medium during all the exposure times. Cells were also treated with antioxidants alone for the same period of time. 6 and 24h after ROT addition, cells were fixed and prepared for immunofluorescence. Data are from 3 to 6 independent experiments and are expressed as mean ± S.D. All groups are highly statistically significant to controls ($P < 0.01$) except for NAC (6h) and VIT E (24h).

Interestingly, the morphological alterations observed for mitochondria after rotenone treatment (Figure 24) were also not inhibited by antioxidants (data not shown).

3.4. ROTENONE DEPLETES INTRACELLULAR GSH LEVELS

Rats treated with rotenone *in vivo* have been used as a model to reproduce the neurochemical, neuropathological and behavioral features of Parkinson's disease (PD) and a decrease in glutathione levels has been implicated early on in PD (Chinta and Andersen, 2006).

Thus, we analyzed the redox state in COS-7 cells treated with rotenone through the mBCL assay (see Methods, Chapter 4.2.). In 3 independent experiments, an average number of 4-6 wells was used for measuring the GSH levels in each condition and time point. For data presentation, averages and standard deviations of the values from each experiment were calculated and related to the control as percentage of control.

After 6 and 24h GSH levels of control and rotenone-treated cells were quantified. After rotenone treatment (100 nM), GSH levels decreased to 86 ± 3.46% after 6h and to 59 ± 2.89% after 24h (Figure 28).

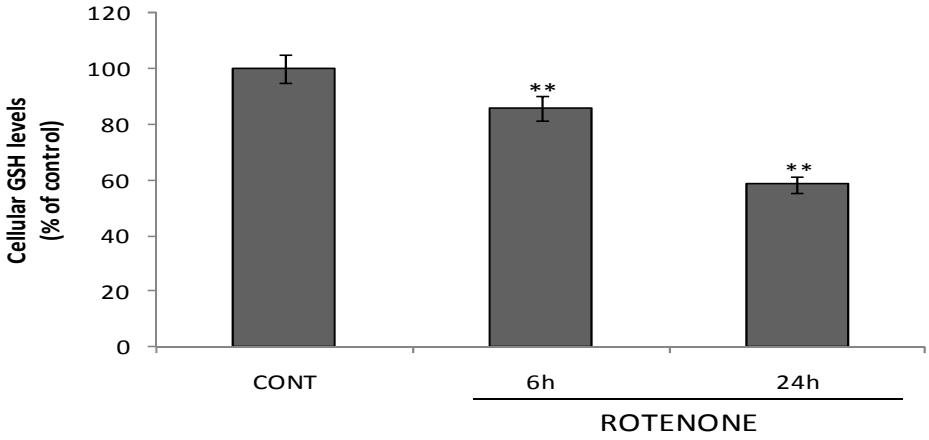

Figure 28. Effect of rotenone on GSH levels in COS-7 cells. Quantification of cellular GSH levels was performed after 6 and 24h of ROT (100 nM) treatment. Data are from 3 independent experiments and are expressed as mean ± S.D. ** highly significant ($P < 0.01$) when compared to control.

Thus, rotenone induced both ROS production and depletion of GSH levels. However, ROS produced by rotenone were not the main cause for peroxisome elongation (Figures 25 and 27).

3.5. PEROXISOME ELONGATION INDUCED BY ROTENONE IS DEPENDENT ON MICROTUBULE DEPOLYMERIZATION

Based on the observed clustering of peroxisomes in cells treated with the highest concentration of rotenone, we decided to stain the microtubules with an antibody to α-tubulin in cells treated with rotenone. Surprisingly, at the highest concentration, rotenone induced the complete depolymerization of microtubules (Figure 29). However, at the lowest concentration (100 nM) microtubules were still visible and appeared unaffected. As shown in Figure 29, at low rotenone concentrations (100 nM and 1 µM), microtubules form a radial array originating from the MTOC similar to control conditions, but at higher concentrations (10 µM and 100 µM) microtubules are completely depolymerized and peroxisomes are clustered.

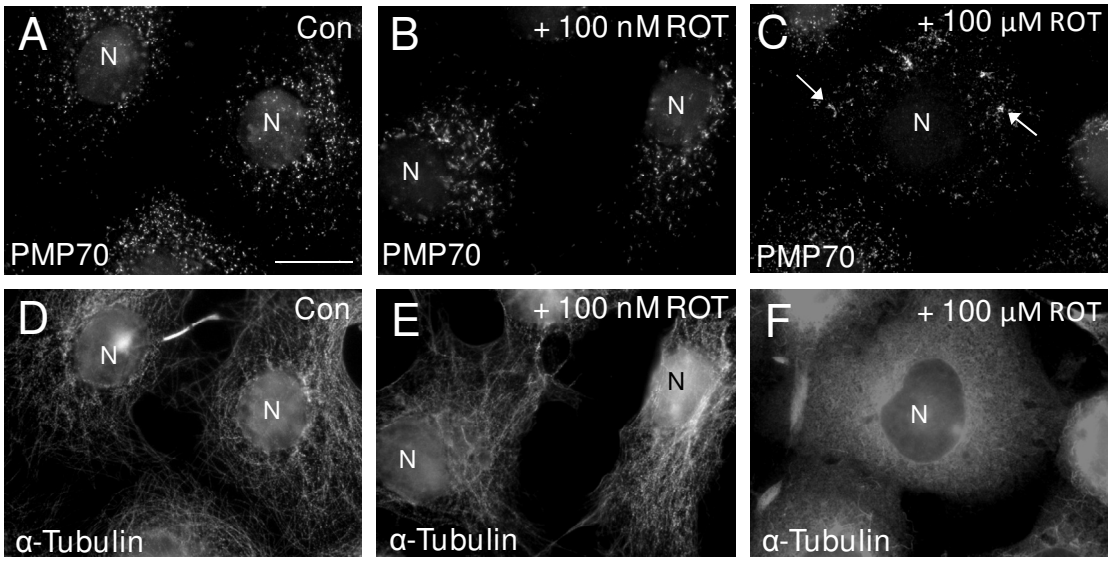

Figure 29. Rotenone induces microtubule depolymerization. COS-7 cells were treated with low (100 nM) and high concentrations (100 µM) of rotenone (ROT) for 6 and 24h (see Methods, Chapter 2.1.3.1.) and peroxisomes and microtubules were visualized by immunofluorescence microscopy using PMP70 antibodies to peroxisomes (A-C) and α-tubulin antibodies to microtubules (D-F). With the lowest concentration of ROT (100 nM) peroxisomes (B) are elongated (see Figure 24) and microtubules appear to be intact (E) compared with controls (D). However, with the highest concentration of rotenone (100 µM) microtubules are completely depolymerized (F) and the peroxisomes are elongated and clustered (C), arrows. N (Nucleus), Bar (20 µm).

To check for microtubule integrity at low rotenone concentrations, microtubules were stained with an antibody to acetylated α-tubulin. Acetylated α-tubulin is present in various microtubule structures and plays a role in the stabilization of microtubules.

Cells were treated with low concentrations of rotenone for 6, 24 and 48h. For visualization of microtubules, cells were fixed and permeabilized with methanol (see Methods, Chapter 3.1.). Microtubules were labeled with an antibody to α-acetylated tubulin (see Materials, Chapter 1., Table 3) (Figure 30). In control cells only a few microtubules were labeled per cell (Figure 30 A). Cells treated with 100 nM of rotenone were markedly different: the number of cells showing acetylation of tubulin was much higher than in controls. Furthermore, almost all microtubules in a given cell showed labeling for acetylation (Figure 30 B).

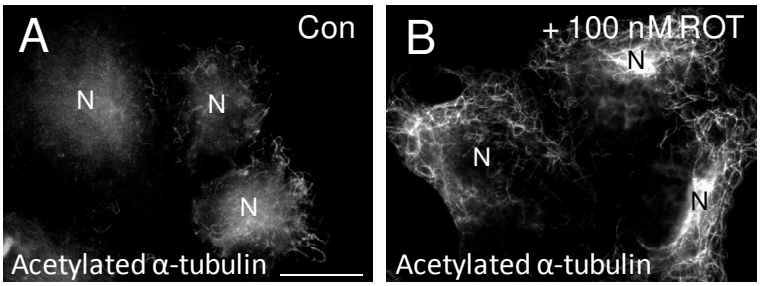

Figure 30. Rotenone induces microtubule acetylation. Microtubules after rotenone treatment were labeled with α-acetylated tubulin antibody. COS-7 cells were treated with 100 nM of rotenone (ROT) and fixed with methanol after 6, 24 and 48h. There is an increase in cells with acetylated microtubules after rotenone treatment indicating stabilization of microtubules. N (Nucleus), Bar (20 µm).

Figure 31 shows the quantification of the cells labeled for acetylated tubulin under normal culture conditions and in rotenone treated cells. In controls, cells showing acetylated tubulin were present in low frequency (49 ± 7.07% after 6h; 46 ± 3.36% after 24h and 23 ± 4.24% after 48h). A significant increase was visible in cells treated with 100 nM and 500 nM of rotenone after 6h to 48h. The concentration of 10 µM was not tested, since at this concentration microtubules were completely depolymerized.

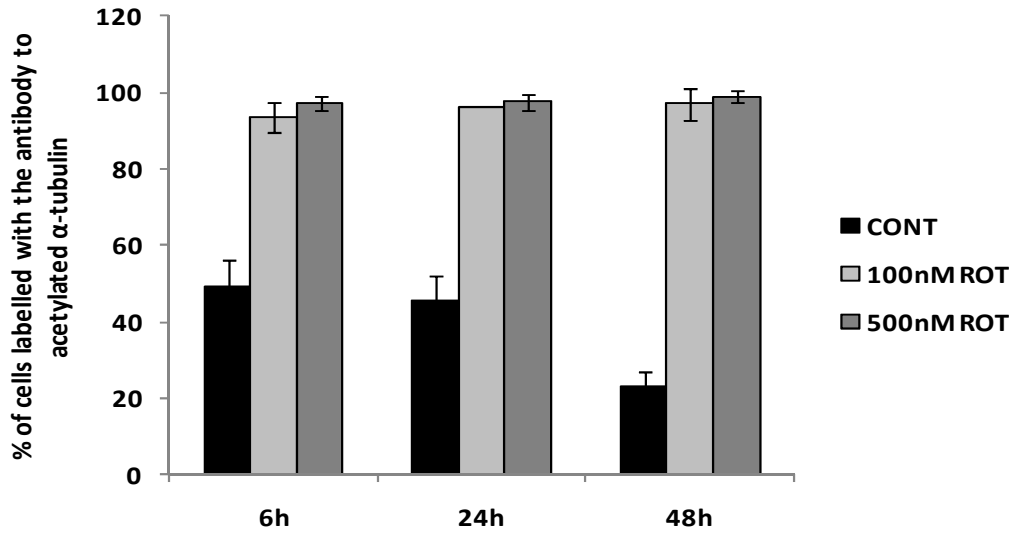

Figure 31. Labeling of microtubules with α-acetylated tubulin in cells treated with low concentrations of rotenone. Cells were treated with 100 nM, 500 nM of Rotenone (ROT) for 6, 24 and 48h. After each time point, cells were fixed and permeabilized with methanol and prepared for immunofluorescence (see Methods, Chapter 3.1.). Cells were counted as labeled or not labeled by the α-acetylated tubulin antibody. Data are derived from 3 independent experiments and are expressed as mean ± S.D. ($P < 0.01$ for all groups).

In summary, rotenone induced peroxisome elongation and also clustering at higher concentrations. Although ROS were generated in mitochondria after rotenone treatment, they are presumably not the main cause of peroxisome elongation induced by rotenone because the antioxidants were not able to block the peroxisome elongation. Rotenone is also responsible for alterations in the cellular redox state as well for modifications in the structure of the microtubule cytoskeleton. Thus, it is likely that microtubule depolymerization induced by rotenone is the main cause for peroxisome elongation.

3.6. THE COMPLEX IV INHIBITOR, SODIUM AZIDE, HAS A SLIGHT EFFECT ON THE PEROXISOMAL COMPARTMENT

Sodium azide (NaN_3) is known as an inhibitor of cytochrome *c* oxidase residing in the mitochondrial inner membrane and interferes with cellular respiration, particularly in the complex IV (Figure 9). NaN_3 was the next stimulus to be analyzed in its capacity to induce ROS production and its potential effect on peroxisome proliferation.

Sodium azide treatment was performed 24h after seeding the cells on coverslips. Different concentrations of sodium azide (10 µM, 1 mM and 10 mM) as well as three time periods of incubation (6, 24 and 48h) were tested (see Methods, Chapter 2.1.3.2.). After each time point, cells were prepared for immunofluorescence and then visualized and evaluated by fluorescence microscopy. For statistical evaluation, 200 – 300 cells per coverslip were categorized as cells with spherical or tubular peroxisomes in control and sodium azide-treated cells.

In COS-7 cells cultured under normal, untreated conditions peroxisomes were mainly of spherical shape (Figure 32 A) and mitochondria showed a normal tubular morphology (Figure 32 D). After drug treatment, morphological alterations of the peroxisomal compartment were not so pronounced comparing with the other stimuli already tested here (Figure 32 B). However, the mitochondrial compartment was dramatically affected (Figure 32 E). Mitochondria after sodium azide treatment displayed a fragmented morphology and showed swelling (more frequent at the higher concentration, 10 mM) (Figure 32 F).

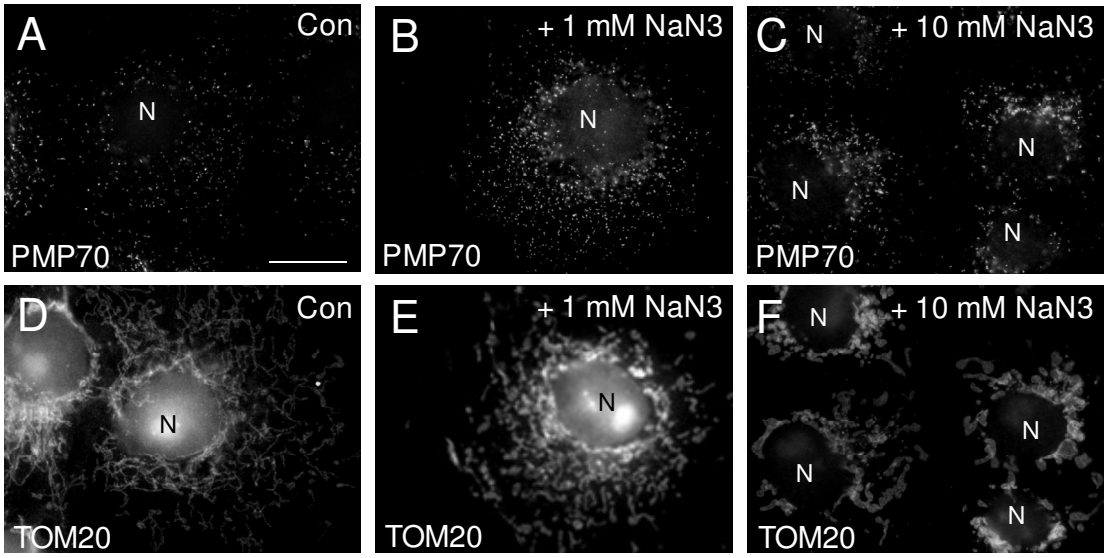

Figure 32. Sodium Azide (NaN_3) failed to induce changes in peroxisome morphology. COS-7 cells were treated with 10 µM, 1 mM and 10 mM for 6, 24 and 48h (see Methods, Chapter 2.1.3.2.) and prepared for imunofluorescence microscopy using PMP70 antibody to peroxisomes (A-C) and TOM20 antibody to mitochondria (D-F). Mitochondria showed a fragmented morphology (E, F) with swelling, whereas peroxisomes were not elongated (B, C). N (Nucleus), Bar (20 µm).

The quantification of induction of tubular peroxisomes after sodium azide treatment is shown in Figure 33. The first concentrations tested were 10 µM and 10 mM for 24 and 48h. As there was no effect on peroxisomes, another concentration (1 mM) and an earlier time point (6h) was tested. Only when high concentrations were applied (10 mM for 24h), a slight effect on peroxisome elongation was observed (30 ± 4.71%) when compared to controls (16 ± 5.61%). After 48h with 10 mM sodium azide a pronounced reduction occurred in the number of cells indicative for a toxic effect.

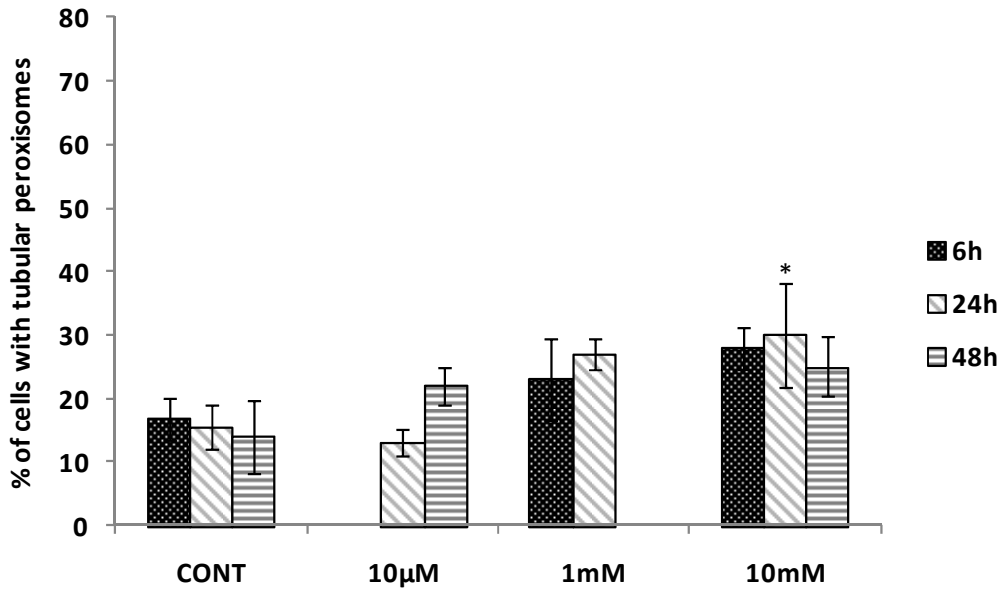

Figure 33. Effect of sodium azide, a complex IV inhibitor of mitochondrial respiration, on peroxisome morphology in COS-7 cells. Cells were treated for 6, 24 and 48h with different concentrations of NaN_3. Data are derived from 3 independent experiments and are expressed as mean ± S.D. * significant ($P < 0.05$) when compared to control.

As the effect on the morphology of the peroxisomal compartment was not so pronounced, despite a strong effect on mitochondrial morphology, a quantification of ROS production as well as a pre-treatment with antioxidants was not performed.

V. DISCUSSION AND CONCLUSIONS

V. DISCUSSION AND CONCLUSIONS

Mammalian cells contain hundreds of peroxisomes under normal growth conditions, suggesting that there are constitutive mechanisms for raising peroxisome abundance above one per cell. Peroxisome increase in response to extracellular stimuli is indicative for the existence of signal transduction pathways that exert additional control over peroxisome abundance.

In cultured cells, oxidative stress has been shown to induce morphological changes of the peroxisomal compartment, which are linked to peroxisome proliferation (Schrader and Fahimi, 2006b). In mammalian cells a pronounced elongation of peroxisomes is observed after UV irradiation, direct exposure to H_2O_2, or during live cell imaging of GFP-PTS1 labeled peroxisomes by regular fluorescent microscopy (Schrader et al., 1999; Schrader and Fahimi, 2004).

Evidence has been presented in the last years that peroxisome elongation appears to be an important prerequisite of peroxisome division, and that tubulation and fission of elongated peroxisomes represent processes of peroxisomal growth and division, which contribute to peroxisome proliferation (Schrader and Fahimi, 2006b). Because peroxisomes harbor most of the enzymes for catabolism of ROS, the tubulation and expansion of the peroxisomal compartment appears to be a logical response to the oxidative stress and could have a cell rescue function against the destructive effects of ROS (Schrader et al., 1999).

The general aim of this study was to investigate if different types of stresses applied to the cells will lead to intracellular ROS production and will be capable of inducing growth/proliferation of the peroxisomal compartment. Such an approach required the selection of a mammalian cell culture system suitable for the induction of peroxisome proliferation in addition to the examination of the effect of different stressors on the induction of peroxisomal growth/proliferation. Testing different types of stresses could help us to elucidate not only if ROS are involved in peroxisome elongation but also where the ROS responsible for this response come from.

1. Microtubule-depolymerization and peroxisomes: still a mysterious relationship

It has already been described that microtubule depolymerizing drugs (e.g. nocodazole) induce elongation of the peroxisomal compartment (Schrader et al., 1996a). However, it was not clear if this morphological alteration was ROS-dependent or if ROS-independent signalling events lead to peroxisomal elongation.

Here we observed that in COS-7 cells nocodazole induced peroxisome elongation and also clustering (Figure 14) as already described in HepG2 cells (Schrader et al., 1996a). In addition, it was observed that mitochondria fragmented upon nocodazole treatment. The microtubules were also depolymerized (Figure 14) as expected, since nocodazole is a well known microtubule-depolymerizing drug.

We demonstrated that microtubule depolymerization induced by nocodazole increased intracellular ROS production (Figure 16). Although antioxidants were capable to diminish the ROS produced, they were not able to inhibit peroxisome elongation (Figure 17) indicating that increased ROS levels were not involved in peroxisome elongation. Moreover, mitochondria were not able to recover their normal morphology by the antioxidant pre-treatment (data not shown).

Interestingly, after microtubule depolymerization most of the subcellular organelles fragment, for example mitochondria or the ER. In contrast, peroxisomes form elongated tubular structures, thus rising the question why peroxisomes behave differently, as they are also known to interact with microtubules (Thiemann et al., 2000; Schrader et al., 2003).

It has already been reported that the binding capacity of peroxisomes to microtubules can be affected by the addition or depletion of ATP (Schrader et al., 2003). While the addition of ATP or motor proteins such as kinesin and dynein were shown to increase the binding capacity of isolated peroxisomes to microtubules in vivo, ATP-depletion or the addition of microtubule-associated proteins (MAPs) decreased it. In addition, mitochondrial fragmentation induced by microtubule depolymerization can produce ROS and also decrease ATP production. This might affect the binding between

peroxisomes and microtubules and consequently lead to peroxisome elongation. Alternatively, peroxisome elongation is triggered by depolymerization of microtubules itself, most likely due to the mechanical link between peroxisomes and microtubules, as the microtubules are essential for proper peroxisome distribution and movement in the cell (Schrader et al., 2003).

Another possibility is that microtubule-depolymerization induced by nocodazole mimics entry in mitosis. Elongation of peroxisomes might be the first step of peroxisome proliferation to deliver a sufficient number of peroxisomes to the daughter cell before cytokinesis. However, the reason why peroxisomes elongate after microtubule depolymerization is still unclear and the relationship between peroxisomes and microtubules remains mysterious.

2. Peroxisome dynamics are sensitive to changes in intracellular redox state

Depletion of GSH has been shown to trigger oxidative stress (Reliene and Schiestl, 2006). L-Buthionine sulfoximine (BSO) is a well known specific agent for inhibiting GSH biosynthesis and thereby causing GSH depletion (Griffith, 1982). BSO has been used in a number of biochemical and pharmacological studies, enhancing the apoptotic effect of several chemotherapeutic agents (Lewis-Wambi et al., 2009).

In the present work we measured a significant depletion of cellular GSH after BSO treatment in COS-7 cells. Interestingly, the depletion of cellular GSH levels had a significant effect on the peroxisomal compartment inducing the formation of long tubular peroxisomes (Figure 19). The most pronounced effect occurred after 9h of BSO treatment (Figure 20) when GSH levels reached their minimum (Figure 21). In BSO treated cells, mitochondrial morphology was similar to untreated cells (Figure 19). Bowes and Gupta (2005) have shown that pharmacological depletion of GSH pools results in the formation of an elongated mitochondrial reticulum suggesting a link between GSH, redox status and organelle morphology.

We showed that BSO treatment increased the intracellular ROS levels more prominently after 9 and 24h (Figure 22) in parallel with the maximal peroxisome elongation (Figure 20) as well as with the minimal GSH levels (Figure 21).

To elucidate the involvement of ROS in peroxisome elongation induced by BSO, an antioxidant pre-treatment was performed with the antioxidants NAC and VIT E. Interestingly, VIT E, in addition to its ability to diminish ROS production and GSH depletion, also inhibited peroxisome elongation – indicating that ROS are involved in peroxisome elongation induced by BSO. A similar effect was shown by Schrader et al. (1999): in HepG2 cells elongation of peroxisomes was induced by UV irradiation but was blocked by antioxidant pre-treatment thus supporting the role of ROS in UV-mediated peroxisomal growth.

However, NAC was not able to block peroxisome elongation. One possible explanation is that the metabolism of NAC to produce GSH requires γ-GCS, which is the enzyme that is inhibited by BSO. In agreement with this, Reliene and Schiestl (2006) showed that NAC did not replenish GSH in NAC plus BSO treated mice. Although in another study, NAC rescued cells from toxic effects induced by dopamine and enhanced by BSO (Offen et al., 1996). Furthermore in the present study, NAC was able to reduce ROS production and to prevent the GSH depletion induced by BSO. This can be explained by the existence of a wide variety of antioxidant systems that scavenge ROS in a cell, or maybe a small amount of ROS that was not scavenged by NAC was sufficient to act on peroxisome morphology.

Vitamin E is the most important lipid soluble antioxidant and protects cell membranes from oxidation by reacting with lipid radicals. The inhibition of peroxisome elongation by vitamin E might indicate that BSO is acting on peroxisomal membranes.

From these data, we can conclude that peroxisomes (like mitochondria) are sensitive to changes in the intracellular redox state, and that ROS that are generated in the cytosol may induce peroxisome proliferation.

3. The peroxisome – mitochondria connection: looking at mitochondrial ROS production

There is growing evidence now that both, peroxisomes and mitochondria exhibit a closer interrelationship than previously thought. This connection includes metabolic cooperations and cross-talk (Schrader and Yoon, 2007), a novel putative mitochondria-to-peroxisome vesicular trafficking pathway (Neuspiel et al., 2008), as well as an overlap in key components of their fission machinery (Schrader and Fahimi, 2006a). Thus, peroxisomal alterations in metabolism, biogenesis, dynamics and proliferation can potentially influence mitochondrial functions, and vice versa (Camoes et al., 2009). The examination of inhibitors of the mitochondrial respiratory chain is therefore important to elucidate if ROS generated in mitochondria can induce morphological changes of the peroxisomal compartment.

The first mitochondrial inhibitor tested was rotenone. This drug is a well known complex I inhibitor of the mitochondrial respiratory chain and has been widely used to study Parkinson's disease (PD). In the present work, rotenone was used to induce ROS production via the mitochondrial compartment, and to examine the effect on peroxisome dynamics.

We showed that low concentrations of rotenone (100 nM) induced elongation of the peroxisomal compartment (Figure 24). Moreover, the mitochondrial morphology was also affected leading to a more fragmented phenotype (Figure 24).

We demonstrated in this work, that 100 nM of rotenone significantly increased ROS production in COS-7 cells (Figure 26) and, although all the antioxidants tested were capable to decrease the ROS levels produced (Figure 26), they were surprisingly not able to inhibit peroxisome elongation (Figure 27). These data reveal that ROS generated in mitochondria by rotenone are presumably not responsible for the elongation of peroxisomes.

We also showed that 100 nM of rotenone were able to deplete cellular GSH levels after up to 6 to 24 hours of treatment. Decreased levels of reduced glutathione, induced by rotenone, have been implicated in PD (Sian et al., 1994, Chinta and Andersen, 2006). Actually, glutathione depletion is the earliest reported biochemical change in the

dopaminergic neurons of the substantia nigra (SN) in PD (Perry et al., 1982). Decreases in glutathione availability in the brain promote morphological alterations of mitochondria, most likely via increased levels of oxidative or nitrosative stress in this organelle (Jain et al., 1991).

Thus, the elongation of the peroxisomal compartment might be related to the depletion of the cellular GSH pool and would indicate that peroxisomal dynamics are sensitive to changes in intracellular redox state.

However, this is still not completely clear because rotenone also exhibited an effect on microtubules. The cluster formation of peroxisomes induced by high rotenone concentrations (10 and 100 µM) was very surprising. When microtubules were labeled with an antibody to α-tubulin at low rotenone concentrations (100 nM and 1 µM) they showed a normal radial array originating from the MTOC (Figure 29 E). However, at higher concentrations (10 and 100 µM) they were completely depolymerized (Figure 29 F). Thus, at higher rotenone concentrations peroxisome elongation is presumably related to microtubule-depolymerization.

Acetylated α-tubulin is present in various microtubule structures and plays a role in stabilizing them. Using an antibody to acetylated tubulin we observed that at low rotenone concentrations (100 nM and 500 nM) microtubules were already modified. A pronounced staining for acetylated tubulin was found in cells treated with the lowest rotenone concentrations (100 nM and 500 nM) (Figure 30, 31) contrary to controls. Thus, rotenone is already affecting microtubule stability at low concentrations.

As rotenone interferes with mitochondrial respiration, redox state and microtubules, it is difficult to interpret its effect on peroxisome elongation. It is, however, likely that its microtubule-depolymerizing activity is responsible for alterations of the peroxisomal compartment.

The second mitochondrial inhibitor tested in this work was sodium azide, an inhibitor of cytochrome *c* oxidase (complex IV), which is located in the mitochondrial inner membrane. Sodium azide has been described to inhibit cellular respiration and consequently decreases ATP levels (Sato et al., 2008).

After treatment with sodium azide no significant morphological changes of the peroxisomal compartment (e.g. elongated peroxisomes) (Figure 32 B, 33) were observed. However, mitochondria were dramatically affected showing a completely fragmented morphology (Figure 32 E, F). Moreover, at the highest concentration (10 mM, 24h treatment) mitochondria appeared swollen.

Sodium azide is also known as a potent inhibitor of superoxide dismutase and catalase activities (Chang and Lamm, 2003; Richardson et al., 1983). Few studies have been devoted to analyzing the effects of chronically lowering the functional level of catalase within cells as well as how peroxisome morphology is affected after catalase inhibition. Catalase inhibition (by 3-amino-1,2,4-triazole (3-AT)) results in hydrogen peroxide accumulation (Koepke, 2008) and also reduces cell growth and induces peroxisome proliferation (Koepke, 2008; Terlecky, 2006). Peroxisome elongation occurs before peroxisome fission – steps that lead to peroxisome proliferation. This way catalase inhibition might be the reason for the slight effect in the elongation of peroxisomes observed.

Other data from our laboratory indicate that the drugs malonate and 3-NP (3-nitroprionate) which act on mitochondrial respiration do not have an effect on peroxisome morphology as well (unpublished data). Malonate and 3-NP are inhibitors of succinate dehydrogenase (complex II). This inhibition is capable of producing high amounts of superoxide and subsequent oxidative damage when applied to cells in culture or injected in animals (Gomez-Nino et al., 2009; Fernandez-Gomez et al., 2005).

6-Hydroxydopamine (6-OHDA), an oxidative metabolite of dopamine, is a neurotoxin which has been broadly used to generate experimental models of Parkinson's disease (PD) (Bove et al., 2005; Blum et al., 2001). Although there is a consensus in the ability of 6-OHDA to induce cytotoxicity in different cell types (Fernandez-Gomez et al., 2006; Galindo et al., 2003), the mechanism involved is still controversial (Blum et al., 2001). Among the mechanisms discussed, the generation of reactive oxygen species (ROS) is the most accepted (Galindo et al., 2003). 6-OHDA induced profound mitochondrial fragmentation in SH-SY5Y cells (human neuroblastoma from neuronal tissues), but failed to induce any changes in peroxisome morphology (Gomez-Lazaro et al., 2008).

Taking together all the results, it is not likely that ROS generated in mitochondria or manipulations of the respiratory chain complexes I, II, IV are a sufficient stimulus for peroxisome elongation/proliferation. However, changes in cellular redox state have the capacity to stimulate peroxisome elongation. It will be a challenge for future studies to unveil the signalling pathway(s) involved.

4. The rotenone problem

Rotenone has been used to induce PD-like symptoms (*in vivo*) or to study the mechanisms of toxicity in cells (*in vitro*). However, in some studies the strategy is not properly addressed. Some authors do not take into consideration that rotenone has two sites of action (complex I inhibition and microtubule depolymerization). In many *in vivo s*tudies the main reason for PD development is supposed to be the oxidative stress generated by inhibiting complex I (Verma and Nehru, 2009; Testa et al., 2005; Sherer et al., 2003; Chinta and Andersen, 2006). These data have to be interpreted with care. However, there are also studies where the authors address that microtubule depolymerization by rotenone might be one of the main causes of PD symptoms, e.g. by inhibiting organelle transport (Brinkley et al., 1974; Marshall and Himes, 1978; Srivastava and Panda, 2007).

Our data indicate that *in vivo* studies with rotenone have to be carefully interpreted. ROS production via complex I is not the only effect when dealing with cells or whole organisms. However, experiments with isolated mitochondria (*in vitro*) should not encounter side effects.

In this work we showed that together with the increased ROS production, depletion of GSH levels and microtubule depolymerization – aspects that have been reported in PD – rotenone also has an effect on peroxisome elongation/proliferation. This might indicate that the peroxisomal compartment is also important for Parkinson's disease. Peroxisomal elongation/proliferation might exert a protective function in PD, and is therefore important for the role of peroxisomes in health and disease.

5. FINAL CONCLUSIONS

Taking together all results we can conclude from this work that:

1. Peroxisome elongation induced by microtubule-depolymerization is not dependent on ROS production.
2. Peroxisome dynamics are sensitive to changes in intracellular redox state induced by BSO.
3. Despite the close peroxisome-mitochondria relationship, mitochondria-derived ROS are unlikely to induce changes of the peroxisomal compartment. Among the inhibitors tested, only rotenone had a prominent effect on peroxisome elongation, however, this effect is due to a microtubule-depolymerizing activity of rotenone.
4. The *in vivo* effects of rotenone have to be interpreted with care (e.g. in animal models of Parkinson's disease).
5. ROS can alter the dynamics of the peroxisomal compartment, but have to come from specific locations (e.g. the cytosol) within the cell.

Outlook

Future studies will include *in vivo* experiments (life cell imaging) using confocal microscopy with the purpose to examine and evaluate peroxisome motility along microtubules in cells treated with rotenone. Furthermore it will be interesting to examine if the stressors induce an up-regulation of Pex11 isoforms as Pex11 proteins are known to regulate peroxisome abundance.

VI. SCIENTIFIC PRESENTATIONS

VI. SCIENTIFIC PRESENTATIONS

The results of this work have been presented and discussed in laboratory seminars of the Centre for Cell Biology at the University of Aveiro.

Publications resulting from this work

Delille, H., N. Bonekamp, S. Pinho, M. Schrader: Hypertubulation of peroxisomes by multiple stimuli. 2009/10 (manuscript in preparation, experimental part finished)

Pinho, S., N. Bonekamp, M. G. Lazaro, J. Jordan, M. Schrader: Effect of Rotenone on peroxisome dynamics and motility. 2009/10 (manuscript in preparation, experiments ongoing; authors are subject of change)

VII. REFERENCES

VII. REFERENCES

Arimura, S., M. Fujimoto, Y. Doniwa, N. Kadoya, M. Nakazono, W. Sakamoto, and N. Tsutsumi. 2008. Arabidopsis ELONGATED MITOCHONDRIA1 is required for localization of DYNAMIN-RELATED PROTEIN3A to mitochondrial fission sites. *Plant Cell*. 20:1555-66.

Arlt, S., U. Beisiegel, and A. Kontush. 2002. Lipid peroxidation in neurodegeneration: new insights into Alzheimer's disease. *Curr Opin Lipidol*. 13:289-94.

Baumgart, E., I. Vanhorebeek, M. Grabenbauer, M. Borgers, P.E. Declercq, H.D. Fahimi, and M. Baes. 2001. Mitochondrial alterations caused by defective peroxisomal biogenesis in a mouse model for Zellweger syndrome (PEX5 knockout mouse). *Am J Pathol*. 159:1477-94.

Beal, M.F. 2005. Mitochondria take center stage in aging and neurodegeneration. *Ann Neurol*. 58:495-505.

Betteridge, D.J. 2000. What is oxidative stress? *Metabolism*. 49:3-8.

Blum, D., S. Torch, N. Lambeng, M. Nissou, A.L. Benabid, R. Sadoul, and J.M. Verna. 2001. Molecular pathways involved in the neurotoxicity of 6-OHDA, dopamine and MPTP: contribution to the apoptotic theory in Parkinson's disease. *Prog Neurobiol*. 65:135-72.

Boll, A., and M. Schrader. 2005. Elongation of peroxisomes as an indicator for efficient dynamin-like protein 1 knock down in mammalian cells. *J Histochem Cytochem.* 53:1037-40.

Bonekamp, N.A., A. Volkl, H.D. Fahimi, and M. Schrader. 2009. Reactive oxygen species and peroxisomes: struggling for balance. *Biofactors*. 35:346-55.

Bove, J., D. Prou, C. Perier, and S. Przedborski. 2005. Toxin-induced models of Parkinson's disease. *NeuroRx*. 2:484-94.

Boveris, A., N. Oshino, and B. Chance. 1972. The cellular production of hydrogen peroxide. *Biochem J*. 128:617-30.

Bowes, T.J., and R.S. Gupta. 2005. Induction of mitochondrial fusion by cysteine-alkylators ethacrynic acid and N-ethylmaleimide. *J Cell Physiol*. 202:796-804.

Brinkley, B.R., S.S. Barham, S.C. Barranco, and G.M. Fuller. 1974. Rotenone inhibition of spindle microtubule assembly in mammalian cells. *Exp Cell Res*. 85:41-6.

Camoes, F., N.A. Bonekamp, H.K. Delille, and M. Schrader. 2009. Organelle dynamics and dysfunction: A closer link between peroxisomes and mitochondria. *J Inherit Metab Dis*. 32:163-80.

Chang, C.C., S. South, D. Warren, J. Jones, A.B. Moser, H.W. Moser, and S.J. Gould. 1999. Metabolic control of peroxisome abundance. *J Cell Sci*. 112:1579-90.

Chang, S., and S.H. Lamm. 2003. Human health effects of sodium azide exposure: a literature review and analysis. *Int J Toxicol*. 22:175-86.

Chinta, S.J., and J.K. Andersen. 2006. Reversible inhibition of mitochondrial complex I activity following chronic dopaminergic glutathione depletion in vitro: implications for Parkinson's disease. *Free Radic Biol Med*. 41:1442-8.

del Rio, L.A., F.J. Corpas, L.M. Sandalio, J.M. Palma, M. Gomez, and J.B. Barroso. 2002. Reactive oxygen species, antioxidant systems and nitric oxide in peroxisomes. *J Exp Bot.* 53:1255-72.

Delille, H.K., R. Alves, and M. Schrader. 2009. Biogenesis of peroxisomes and mitochondria: linked by division. *Histochem Cell Biol*. 131:441-6.

Delille, H.K., N.A. Bonekamp, and M. Schrader. 2006. Peroxisomes and disease - an overview. *Int J Biomed Sci*. 2:308-314.

Delille, H.K., and M. Schrader. 2008. Targeting of hFis1 to peroxisomes is mediated by Pex19p. *J Biol Chem*. 283:31107-15.

Desikan, R., A.H.M. S, J.T. Hancock, and S.J. Neill. 2001. Regulation of the Arabidopsis transcriptome by oxidative stress. *Plant Physiol.* 127:159-72.

Dickinson, D.A., and H.J. Forman. 2002. Cellular glutathione and thiols metabolism. *Biochem Pharmacol*. 64:1019-26.

Droge, W. 2003. Oxidative stress and aging. *Adv Exp Med Biol.* 543:191-200.

Dymkowska, D., J. Szczepanowska, M.R. Wieckowski, and L. Wojtczak. 2006. Short-term and long-term effects of fatty acids in rat hepatoma AS-30D cells: the way to apoptosis. *Biochim Biophys Acta.* 1763:152-63.

Eckert, J.H., and R. Erdmann. 2003. Peroxisome biogenesis. *Rev Physiol Biochem Pharmacol*. 147:75-121.

Fagarasanu, A., M. Fagarasanu, and R.A. Rachubinski. 2007. Maintaining peroxisome populations: a story of division and inheritance. *Annu Rev Cell Dev Biol*. 23:321-44.

Fahimi, H.D. 1968. Cytochemical localization of peroxidase activity in rat hepatic microbodies (peroxisomes). *J Histochem Cytochem*. 16:547-50.

Fahimi, H.D. 1969. Cytochemical localization of peroxidatic activity of catalase in rat hepatic microbodies (peroxisomes). *J Cell Biol.* 43:275-88.

Fahimi, H.D., A. Reinicke, M. Sujatta, S. Yokota, M. Ozel, F. Hartig, and K. Stegmeier. 1982. The short- and long-term effects of bezafibrate in the rat. *Ann N Y Acad Sci*. 386:111-35.

Fei, M.J., E. Yamashita, N. Inoue, M. Yao, H. Yamaguchi, T. Tsukihara, K. Shinzawa-Itoh, R. Nakashima, and S. Yoshikawa. 2000. X-ray structure of azide-bound fully oxidized cytochrome c oxidase from bovine heart at 2.9 A resolution. *Acta Crystallogr D Biol Crystallogr*. 56:529-35.

Fernandez-Gomez, F.J., M.F. Galindo, M. Gomez-Lazaro, V.J. Yuste, J.X. Comella, N. Aguirre, and J. Jordan. 2005. Malonate induces cell death via mitochondrial potential collapse and delayed swelling through an ROS-dependent pathway. *Br J Pharmacol*. 144:528-37.

Fernandez-Gomez, F.J., M.D. Pastor, E.M. Garcia-Martinez, R. Melero-Fernandez de Mera, M. Gou-Fabregas, M. Gomez-Lazaro, S. Calvo, R.M. Soler, M.F. Galindo, and J. Jordan. 2006.

Pyruvate protects cerebellar granular cells from 6-hydroxydopamine-induced cytotoxicity by activating the Akt signaling pathway and increasing glutathione peroxidase expression. *Neurobiol Dis*. 24:296-307.

Frei, B., R. Stocker, L. England, and B.N. Ames. 1990. Ascorbate: the most effective antioxidant in human blood plasma. *Adv Exp Med Biol*. 264:155-63.

Fridovich, I. 1999. Fundamental aspects of reactive oxygen species, or what's the matter with oxygen? *Ann N Y Acad Sci*. 893:13-8.

Funato, M., N. Shimozawa, T. Nagase, Y. Takemoto, Y. Suzuki, Y. Imamura, T. Matsumoto, T. Tsukamoto, T. Kojidani, T. Osumi, T. Fukao, and N. Kondo. 2005. Aberrant peroxisome morphology in peroxisomal beta-oxidation enzyme deficiencies. *Brain Dev*. 20:20.

Galindo, M.F., J. Jordan, C. Gonzalez-Garcia, and V. Cena. 2003. Chromaffin cell death induced by 6-hydroxydopamine is independent of mitochondrial swelling and caspase activation. *J Neurochem*. 84:1066-73.

Gandre-Babbe, S., and A.M. van der Bliek. 2008. The Novel Tail-anchored Membrane Protein Mff Controls Mitochondrial and Peroxisomal Fission in Mammalian Cells. *Mol Biol Cell*. 19:2402-12.

Gomez-Lazaro, M., N.A. Bonekamp, M.F. Galindo, J. Jordan, and M. Schrader. 2008. 6-Hydroxydopamine (6-OHDA) induces Drp1-dependent mitochondrial fragmentation in SH-SY5Y cells. *Free Radic.Biol.Med.* 44(11): 1960-9.

Gomez-Nino, A., M.T. Agapito, A. Obeso, and C. Gonzalez. 2009. Effects of mitochondrial poisons on glutathione redox potential and carotid body chemoreceptor activity. *Respir Physiol Neurobiol*. 165:104-11.

Gould, S.J., and C.S. Collins. 2002. Opinion: peroxisomal-protein import: is it really that complex? *Nat Rev Mol Cell Biol*. 3:382-9.

Green, R.M., M. Graham, M.R. O'Donovan, J.K. Chipman, and N.J. Hodges. 2006. Subcellular compartmentalization of glutathione: correlations with parameters of oxidative stress related to genotoxicity. *Mutagenesis*. 21:383-90.

Griffith, O.W. 1982. Mechanism of action, metabolism, and toxicity of buthionine sulfoximine and its higher homologs, potent inhibitors of glutathione synthesis. *J Biol Chem*. 257:13704-12.

Griffith, O.W., and A. Meister. 1979. Potent and specific inhibition of glutathione synthesis by buthionine sulfoximine (S-n-butyl homocysteine sulfoximine). *J Biol Chem*. 254:7558-60.

Han, Y.H., and W.H. Park. 2009. The effects of N-acetyl cysteine, buthionine sulfoximine, diethyldithiocarbamate or 3-amino-1,2,4-triazole on antimycin A-treated Calu-6 lung cells in relation to cell growth, reactive oxygen species and glutathione. *Oncol Rep*. 22:385-91.

Hayes, J.D., J.U. Flanagan, and I.R. Jowsey. 2005. Glutathione transferases. *Annu Rev Pharmacol Toxicol*. 45:51-88.

Hess, R., W. Staubli, and W. Riess. 1965. Nature of the hepatomegalic effect produced by ethyl-chlorophenoxy-isobutyrate in the rat. *Nature.* 208:856-8.

Hruban, Z., E.L. Vigil, A. Slesers, and E. Hopkins. 1972. Microbodies: constituent organelles of animal cells. *Lab Invest*. 27:184-91.

Ishihara, N., M. Nomura, A. Jofuku, H. Kato, S.O. Suzuki, K. Masuda, H. Otera, Y. Nakanishi, I. Nonaka, Y. Goto, N. Taguchi, H. Morinaga, M. Maeda, R. Takayanagi, S. Yokota, and K. Mihara. 2009. Mitochondrial fission factor Drp1 is essential for embryonic development and synapse formation in mice. *Nat Cell Biol*. 11:958-66.

Issemann, I., and S. Green. 1990. Activation of a member of the steroid hormone receptor superfamily by peroxisome proliferators. *Nature.* 347:645-50.

Jain, A., J. Martensson, E. Stole, P.A. Auld, and A. Meister. 1991. Glutathione deficiency leads to mitochondrial damage in brain. *Proc Natl Acad Sci U S A*. 88:1913-7.

Jezek, P., and L. Hlavata. 2005. Mitochondria in homeostasis of reactive oxygen species in cell, tissues, and organism. *Int J Biochem Cell Biol*. 37:2478-503.

Jin, J., J. Davis, D. Zhu, D.T. Kashima, M. Leroueil, C. Pan, K.S. Montine, and J. Zhang. 2007. Identification of novel proteins affected by rotenone in mitochondria of dopaminergic cells. *BMC Neurosci*. 8:67-80

Johnson, L.V., M.L. Walsh, and L.B. Chen. 1980. Localization of mitochondria in living cells with rhodamine 123. *Proc Natl Acad Sci U S A*. 77:990-4.

Jordan, J., M.F. Galindo, S. Calvo, C. Gonzalez-Garcia, and V. Cena. 2000. Veratridine induces apoptotic death in bovine chromaffin cells through superoxide production. *Br J Pharmacol*. 130:1496-504.

Jordan, J., M.F. Galindo, D. Tornero, A. Benavides, C. Gonzalez, M.T. Agapito, C. Gonzalez-Garcia, and V. Cena. 2002. Superoxide anions mediate veratridine-induced cytochrome c release and caspase activity in bovine chromaffin cells. *Br J Pharmacol*. 137:993-1000.

Jordan, J., M.F. Galindo, D. Tornero, C. Gonzalez-Garcia, and V. Cena. 2004. Bcl-x L blocks mitochondrial multiple conductance channel activation and inhibits 6-OHDA-induced death in SH-SY5Y cells. *J Neurochem*. 89:124-33.

Jos, A., A.M. Camean, S. Pflugmacher, and H. Segner. 2009. The antioxidant glutathione in the fish cell lines EPC and BCF-2: response to model pro-oxidants as measured by three different fluorescent dyes. *Toxicol In Vitro*. 23:546-53.

Kaur, N., and J. Hu. 2009. Dynamics of peroxisome abundance: a tale of division and proliferation. *Curr Opin Plant Biol*. 12:781-8.

Kelly, G.S. 1998. Clinical applications of N-acetylcysteine. *Altern Med Rev*. 3:114-27.

Koch, A., M. Thiemann, M. Grabenbauer, Y. Yoon, M.A. McNiven, and M. Schrader. 2003. Dynamin-like protein 1 is involved in peroxisomal fission. *J Biol Chem*. 278:8597-605.

Koch, A., Y. Yoon, N.A. Bonekamp, M.A. McNiven, and M. Schrader. 2005. A role for fis1 in both mitochondrial and peroxisomal fission in Mammalian cells. *Mol Biol Cell*. 16:5077-86.

Lazarow, P.B., and C. De Duve. 1976. A fatty acyl-CoA oxidizing system in rat liver peroxisomes; enhancement by clofibrate, a hypolipidemic drug. *Proc Natl Acad Sci U S A*. 73:2043-6.

Lazarow, P.B., and Y. Fujiki. 1985. Biogenesis of peroxisomes. *Annu Rev Cell Biol*. 1:489-530.

Lewis-Wambi, J.S., R. Swaby, H. Kim, and V.C. Jordan. 2009. Potential of l-buthionine sulfoximine to enhance the apoptotic action of estradiol to reverse acquired antihormonal resistance in metastatic breast cancer. *J Steroid Biochem Mol Biol*. 114:33-9.

Li, X., E. Baumgart, G.X. Dong, J.C. Morrell, G. Jimenez-Sanchez, D. Valle, K.D. Smith, and S.J. Gould. 2002. PEX11alpha Is Required for Peroxisome Proliferation in Response to 4-Phenylbutyrate but Is Dispensable for Peroxisome Proliferator-Activated Receptor Alpha-Mediated Peroxisome Proliferation. *Mol Cell Biol*. 22:8226-8240.

Lingard, M.J., and R.N. Trelease. 2006. Five Arabidopsis peroxin 11 homologs individually promote peroxisome elongation, division without elongation, or aggregation. *J. Cell Sci.* 119:1961-1972.

Lopez-Huertas, E., W.L. Charlton, B. Johnson, I.A. Graham, and A. Baker. 2000. Stress induces peroxisome biogenesis genes. *Embo J*. 19:6770-7.

Ma, C., and S. Subramani. 2009. Peroxisome matrix and membrane protein biogenesis. *IUBMB Life*. 61:713-22.

Marshall, L.E., and R.H. Himes. 1978. Rotenone inhibition of tubulin self-assembly. *Biochim Biophys Acta*. 543:590-4.

Masters, C.J. 1996. Cellular signalling: the role of the peroxisome. *Cell Signal*. 8:197-208.

Matsuzaki, T., and Y. Fujiki. 2008. The peroxisomal membrane protein import receptor Pex3p is directly transported to peroxisomes by a novel Pex19p- and Pex16p-dependent pathway. *J Cell Biol*. 183:1275-86.

May, J.M. 1999. Is ascorbic acid an antioxidant for the plasma membrane? *FASEB J*. 13:995-1006.

Meister, A. 1991. Glutathione deficiency produced by inhibition of its synthesis, and its reversal; applications in research and therapy. *Pharmacol Ther*. 51:155-94.

Meister, A. 1995. Mitochondrial changes associated with glutathione deficiency. *Biochim Biophys Acta*. 1271:35-42.

Moldovan, L., and N.I. Moldovan. 2004. Oxygen free radicals and redox biology of organelles. *Histochem Cell Biol*. 122:395-412.

Moser, H., K.D. Smith, P.A. Watkins, J. Powers, and A.B. Moser. 2001. X-linked adrenoleukodystrophy. McGraw-Hill, New Jersey.

Motley, A.M., and E.H. Hettema. 2007. Yeast peroxisomes multiply by growth and division. *J Cell Biol*. 178:399-410.

Motley, A.M., G.P. Ward, and E.H. Hettema. 2008. Dnm1p-dependent peroxisome fission requires Caf4p, Mdv1p and Fis1p. *J Cell Sci*. 121:1633-40.

Nagotu, S., A.M. Krikken, M. Otzen, J.A. Kiel, M. Veenhuis, and I.J. van der Klei. 2008a. Peroxisome fission in Hansenula polymorpha requires Mdv1 and Fis1, two proteins also involved in mitochondrial fission. *Traffic*. 9:1471-84.

Nagotu, S., R. Saraya, M. Otzen, M. Veenhuis, and I.J. van der Klei. 2008b. Peroxisome proliferation in Hansenula polymorpha requires Dnm1p which mediates fission but not de novo formation. *Biochim Biophys Acta*. 1783:760-9.

Neely, M.D., A. Boutte, D. Milatovic, and T.J. Montine. 2005. Mechanisms of 4-hydroxynonenal-induced neuronal microtubule dysfunction. *Brain Res*. 1037:90-8.

Neuspiel, M., A.C. Schauss, E. Braschi, R. Zunino, P. Rippstein, R.A. Rachubinski, M.A. Andrade-Navarro, and H.M. McBride. 2008. Cargo-selected transport from the mitochondria to peroxisomes is mediated by vesicular carriers. *Current Biology*. 18:102-108.

Nguyen, T., J. Bjorkman, B.C. Paton, and D.I. Crane. 2006. Failure of microtubule-mediated peroxisome division and trafficking in disorders with reduced peroxisome abundance. *J Cell Sci.* 119:636-45.

Nordberg, J., and E.S. Arner. 2001. Reactive oxygen species, antioxidants, and the mammalian thioredoxin system. *Free Radic Biol Med*. 31:1287-312.

Novikoff, A.B., and S. Goldfischer. 1969. Visualization of peroxisomes (microbodies) and mitochondria with diaminobenzidine. *J Histochem Cytochem*. 17:675-80.

Offen, D., I. Ziv, H. Sternin, E. Melamed, and A. Hochman. 1996. Prevention of dopamine-induced cell death by thiol antioxidants: possible implications for treatment of Parkinson's disease. *Exp Neurol*. 141:32-9.

Opperdoes, F.R. 1988. Glycosomes may provide clues to the import of peroxisomal proteins. *Trends Biochem.Sci.* 13:255-260.

Perez-Ortiz, J.M., P. Tranque, C.F. Vaquero, B. Domingo, F. Molina, S. Calvo, J. Jordan, V. Cena, and J. Llopis. 2004. Glitazones differentially regulate primary astrocyte and glioma cell survival. Involvement of reactive oxygen species and peroxisome proliferator-activated receptor-gamma. *J Biol Chem*. 279:8976-85.

Perry, T.L., D.V. Godin, and S. Hansen. 1982. Parkinson's disease: a disorder due to nigral glutathione deficiency? *Neurosci Lett*. 33:305-10.

Platta, H.W., and R. Erdmann. 2007a. Peroxisomal dynamics. *Trends Cell Biol*. 17:474-84.

Platta, H.W., and R. Erdmann. 2007b. The peroxisomal protein import machinery. *FEBS Lett*. 581:2811-9.

Poirier, Y., V.D. Antonenkov, T. Glumoff, and J.K. Hiltunen. 2006. Peroxisomal beta-oxidation--a metabolic pathway with multiple functions. *Biochim Biophys Acta*. 1763:1413-26.

Reddy, J.K., and T. Hashimoto. 2001. Peroxisomal beta-oxidation and peroxisome proliferator-activated receptor alpha: an adaptive metabolic system. *Annu Rev Nutr.* 21:193-230.

Reliene, R., and R.H. Schiestl. 2006. Glutathione depletion by buthionine sulfoximine induces DNA deletions in mice. *Carcinogenesis*. 27:240-4.

Ren, Y., and J. Feng. 2007. Rotenone selectively kills serotonergic neurons through a microtubule-dependent mechanism. *J Neurochem*. 103:303-11.

Rhodin, J. 1954. Correlation of ultrastructural organization and function in normal experimentally changed convoluted tubule cells of the mouse kidney, Stockholm (PhD thesis).

Richardson, T.C., D.V. Chapman, and E. Heyderman. 1983. Immunoperoxidase techniques: the deleterious effect of sodium azide on the activity of peroxidase conjugates. *J Clin Pathol*. 36:411-4.

Rottensteiner, H., A. Kramer, S. Lorenzen, K. Stein, C. Landgraf, R. Volkmer-Engert, and R. Erdmann. 2004. Peroxisomal membrane proteins contain common Pex19p-binding sites that are an integral part of their targeting signals (mPTS). *Mol Biol Cell*. 15:3406-17.

Saran, M. 2003. To what end does nature produce superoxide? NADPH oxidase as an autocrine modifier of membrane phospholipids generating paracrine lipid messengers. *Free Radic Res.* 37:1045-59.

Sato, E., T. Suzuki, N. Hoshi, T. Sugino, and H. Hasegawa. 2008. Sodium azide induces necrotic cell death in rat squamous cell carcinoma SCC131. *Med Mol Morphol*. 41:211-20.

Schonfeld, P., and G. Reiser. 2006. Rotenone-like action of the branched-chain phytanic acid induces oxidative stress in mitochondria. *J Biol Chem*. 281:7136-42.

Schoonjans, K., B. Staels, and J. Auwerx. 1996. Role of the peroxisome proliferator-activated receptor (PPAR) in mediating the effects of fibrates and fatty acids on gene expression. *J Lipid Res.* 37:907-25.

Schrader, M. 2006. Shared components of mitochondrial and peroxisomal division. *Biochim Biophys Acta*. 1763:531-41.

Schrader, M., J.K. Burkhardt, E. Baumgart, G. Luers, H. Spring, A. Volkl, and H.D. Fahimi. 1996a. Interaction of microtubules with peroxisomes. Tubular and spherical peroxisomes in HepG2 cells and their alterations induced by microtubule-active drugs. *Eur J Cell Biol*. 69:24-35.

Schrader, M., J.K. Burkhardt, E. Baumgart, G. Luers, A. Volkl, and H.D. Fahimi. 1996b. The importance of microtubules in determination of shape and intracellular distribution of peroxisomes. *Ann N Y Acad Sci*. 804:669-71.

Schrader, M., and H.D. Fahimi. 2004. Mammalian peroxisomes and reactive oxygen species. *Histochem Cell Biol*. 122:383-393.

Schrader, M., and H.D. Fahimi. 2006a. Growth and division of peroxisomes. *Int Rev Cytol*. 255:237-90.

Schrader, M., and H.D. Fahimi. 2006b. Peroxisomes and oxidative stress. *Biochim Biophys Acta*. 1763:1755-66.

Schrader, M., and H.D. Fahimi. 2008. The peroxisome: still a mysterious organelle. *Histochem Cell Biol*. 129:421-40.

Schrader, M., S.J. King, T.A. Stroh, and T.A. Schroer. 2000. Real time imaging reveals a peroxisomal reticulum in living cells. *J Cell Sci*. 113:3663-71.

Schrader, M., K. Krieglstein, and H.D. Fahimi. 1998a. Tubular peroxisomes in HepG2 cells: selective induction by growth factors and arachidonic acid. *Eur J Cell Biol*. 75:87-96.

Schrader, M., B.E. Reuber, J.C. Morrell, G. Jimenez-Sanchez, C. Obie, T.A. Stroh, D. Valle, T.A. Schroer, and S.J. Gould. 1998b. Expression of PEX11beta mediates peroxisome proliferation in the absence of extracellular stimuli. *J Biol Chem*. 273:29607-14.

Schrader, M., M. Thiemann, and H.D. Fahimi. 2003. Peroxisomal motility and interaction with microtubules. *Microsc Res Tech*. 61:171-8.

Schrader, M., R. Wodopia, and H.D. Fahimi. 1999. Induction of tubular peroxisomes by UV irradiation and reactive oxygen species in HepG2 cells. *J Histochem Cytochem*. 47:1141-8.

Schrader, M., and Y. Yoon. 2007. Mitochondria and peroxisomes: Are the 'Big Brother' and the 'Little Sister' closer than assumed? *Bioessays*. 29:1105-14.

Sherer, T.B., R. Betarbet, C.M. Testa, B.B. Seo, J.R. Richardson, J.H. Kim, G.W. Miller, T. Yagi, A. Matsuno-Yagi, and J.T. Greenamyre. 2003. Mechanism of toxicity in rotenone models of Parkinson's disease. *J Neurosci*. 23:10756-64.

Shim, S.Y., B.A. Samuels, J. Wang, G. Neumayer, C. Belzil, R. Ayala, Y. Shi, L.H. Tsai, and M.D. Nguyen. 2008. Ndel1 controls the dynein-mediated transport of vimentin during neurite outgrowth. *J Biol Chem*. 283:12232-40.

Sian, J., D.T. Dexter, A.J. Lees, S. Daniel, Y. Agid, F. Javoy-Agid, P. Jenner, and C.D. Marsden. 1994. Alterations in glutathione levels in Parkinson's disease and other neurodegenerative disorders affecting basal ganglia. *Ann Neurol*. 36:348-55.

Sies, H., W. Stahl, and A.R. Sundquist. 1992. Antioxidant functions of vitamins. Vitamins E and C, beta-carotene, and other carotenoids. *Ann N Y Acad Sci*. 669:7-20.

Sinclair, A.M., C.P. Trobacher, N. Mathur, J.S. Greenwood, and J. Mathur. 2009. Peroxule extension over ER-defined paths constitutes a rapid subcellular response to hydroxyl stress. *Plant J*. 59:231-42.

Srivastava, P., and D. Panda. 2007. Rotenone inhibits mammalian cell proliferation by inhibiting microtubule assembly through tubulin binding. *FEBS J*. 274:4788-801.

Steinberg, S.J., G. Dodt, G.V. Raymond, N.E. Braverman, A.B. Moser, and H.W. Moser. 2006. Peroxisome biogenesis disorders. *Biochim Biophys Acta*. 1763:1733-48.

Stolz, D.B., R. Zamora, Y. Vodovotz, P.A. Loughran, T.R. Billiar, Y.M. Kim, R.L. Simmons, and S.C. Watkins. 2002. Peroxisomal localization of inducible nitric oxide synthase in hepatocytes. *Hepatology*. 36:81-93.

Swanson, J., A. Bushnell, and S.C. Silverstein. 1987. Tubular lysosome morphology and distribution within macrophages depend on the integrity of cytoplasmic microtubules. *Proc Natl Acad Sci U S A*. 84:1921-5.

Tabak, H.F., D. Hoepfner, A. Zand, H.J. Geuze, I. Braakman, and M.A. Huynen. 2006. Formation of peroxisomes: present and past. *Biochim Biophys Acta*. 1763:1647-54.

Tanaka, A., S. Kobayashi, and Y. Fujiki. 2006. Peroxisome division is impaired in a CHO cell mutant with an inactivating point-mutation in dynamin-like protein 1 gene. *Exp Cell Res*. 312:1671-84.

Testa, C.M., T.B. Sherer, and J.T. Greenamyre. 2005. Rotenone induces oxidative stress and dopaminergic neuron damage in organotypic substantia nigra cultures. *Brain Res Mol Brain Res*. 134:109-18.

Thiemann, M., M. Schrader, A. Volkl, E. Baumgart, and H.D. Fahimi. 2000. Interaction of peroxisomes with microtubules. In vitro studies using a novel peroxisome-microtubule binding assay. *Eur J Biochem*. 267:6264-75.

Thoms, S., and R. Erdmann. 2005. Dynamin-related proteins and Pex11 proteins in peroxisome division and proliferation. *Febs J*. 272:5169-81.

Thoms, S., S. Gronborg, and J. Gartner. 2009. Organelle interplay in peroxisomal disorders. *Trends Mol Med*. 15:293-302.

Van Ael, E., and M. Fransen. 2006. Targeting signals in peroxisomal membrane proteins. *Biochim Biophys Acta*. 1763:1629-38.

van Roermund, C.W., W.F. Visser, L. Ijlst, A. van Cruchten, M. Boek, W. Kulik, H.R. Waterham, and R.J. Wanders. 2008. The human peroxisomal ABC half transporter ALDP functions as a homodimer and accepts acyl-CoA esters. *FASEB J*. 22:4201-8.

Vasquez, R.J., B. Howell, A.M. Yvon, P. Wadsworth, and L. Cassimeris. 1997. Nanomolar concentrations of nocodazole alter microtubule dynamic instability in vivo and in vitro. *Mol Biol Cell*. 8:973-85.

Verma, R., and B. Nehru. 2009. Effect of centrophenoxine against rotenone-induced oxidative stress in an animal model of Parkinson's disease. *Neurochem Int*. 55:369-75.

Vizeacoumar, F.J., W.N. Vreden, J.D. Aitchison, and R.A. Rachubinski. 2006. Pex19p binds Pex30p and Pex32p at regions required for their peroxisomal localization but separate from their peroxisomal targeting signals. *J.Biol.Chem.* 281:14805-14812.

Wakabayashi, J., Z. Zhang, N. Wakabayashi, Y. Tamura, M. Fukaya, T.W. Kensler, M. Iijima, and H. Sesaki. 2009. The dynamin-related GTPase Drp1 is required for embryonic and brain development in mice. *J Cell Biol*. 186:805-16.

Wanders, R.J. 2004. Peroxisomes, lipid metabolism, and peroxisomal disorders. *Mol Genet Metab*. 83:16-27.

Wanders, R.J., and H.R. Waterham. 2005. Peroxisomal disorders I: biochemistry and genetics of peroxisome biogenesis disorders. *Clin Genet.* 67:107-33.

Wanders, R.J., and H.R. Waterham. 2006a. Peroxisomal disorders: the single peroxisomal enzyme deficiencies. *Biochim Biophys Acta*. 1763:1707-20.

Wanders, R.J.A., and H.R. Waterham. 2006b. Biochemistry of mammalian peroxisomes revisited. *Annu. Rev. Biochem.* 75:295-332.

Wang, H., P.J. Lim, M. Karbowski, and M.J. Monteiro. 2009. Effects of overexpression of huntingtin proteins on mitochondrial integrity. *Hum Mol Genet*. 18:737-52.

Waterham, H.R., J. Koster, C.W. van Roermund, P.A. Mooyer, R.J. Wanders, and J.V. Leonard. 2007. A lethal defect of mitochondrial and peroxisomal fission. *N Engl J Med*. 356:1736-41.

Wiemer, E.A., T. Wenzel, T.J. Deerinck, M.H. Ellisman, and S. Subramani. 1997. Visualization of the peroxisomal compartment in living mammalian cells: dynamic behavior and association with microtubules. *J Cell Biol*. 136:71-80.

Yamamoto, K., and H.D. Fahimi. 1987. Three-dimensional reconstruction of a peroxisomal reticulum in regenerating rat liver: evidence of interconnections between heterogeneous segments. *J Cell Biol*. 105:713-22.

Yoshikawa, S., K. Shinzawa-Itoh, R. Nakashima, R. Yaono, E. Yamashita, N. Inoue, M. Yao, M.J. Fei, C.P. Libeu, T. Mizushima, H. Yamaguchi, T. Tomizaki, and T. Tsukihara. 1998. Redox-coupled crystal structural changes in bovine heart cytochrome c oxidase. *Science*. 280:1723-9.